A study on the scale effects of propulsive characteristics of podded propulsors

Lane, S.

Publisher's version / Version de l'éditeur:
https://doi.org/10.4224/8895016
Student Report (National Research Council of Canada. Institute for Ocean Technology); no. SR-2006-18, 2006

DOCUMENTATION PAGE

REPORT NUMBER SR-2006-18	**NRC REPORT NUMBER**	**DATE** August 18, 2006

REPORT SECURITY CLASSIFICATION Unclassified	**DISTRIBUTION** Unlimited

TITLE
A STUDY ON THE SCALE EFFECTS OF PROPULSIVE CHARACTERISTICS OF PODDED PROPULSORS

AUTHOR(S)

Stephen Lane

CORPORATE AUTHOR(S)/PERFORMING AGENCY(S)

Institute for Ocean Technology, National Research Council, St. John’s, NL

PUBLICATION

N/A

SPONSORING AGENCY(S)

Institute for Ocean Technology, National Research Council, St. John’s, NL

IMD PROJECT NUMBER 42_2085_16	**NRC FILE NUMBER**

KEY WORDS Podded, Propeller, Propulsors, Azimuthing	**PAGES** v, 33, App. A-H	**FIGS.** 24	**TABLES** 22

SUMMARY

The following is a report detailing the procedure, analysis, and results of seven sets of tests conducted on podded propellers. The tests were conducted on either a single pod or dual pods running along side one another. Two sets of tests were conducted on a propeller of 270mm while the remainder were on a prop of 200mm. Two of the cases were numerical.

Not much is known about the performance characteristics of podded propellers to this date. This is reason behind the current study. With the data already collected along with future tests planned researchers will gain valuable knowledge about podded propellers and will be able to engineer future pods more efficiently and effectively.

ADDRESS

National Research Council
Institute for Ocean Technology
Arctic Avenue, P. O. Box 12093
St. John's, NL A1B 3T5
Tel.: (709) 772-5185, Fax: (709) 772-2462

National Research Council Canada
Conseil national de recherches Canada

Institute for Ocean Technology
Institut des technologies océaniques

A STUDY ON THE SCALE EFFECTS OF PROPULSIVE CHARACTERISTICS OF PODDED PROPULSORS

SR-2006-18

Stephen Lane

August 2006

TABLE OF CONTENTS

LIST OF TABLES

LIST OF FIGURES

LIST OF ABBREVIATIONS

D	Diameter (Propeller)
DAS	Data Acquisition System
deg	Degree(s)
EAR	Expanded Area Ratio
Hz	Hertz
ITTC	International Towing tank Conference
IOT	Institute for Ocean Technology
J	Advance Coefficient
K_Q	Torque Coefficient
K_T	Thrust Coefficient
m	Metre(s)
mm	Millimetre(s)
m/s(ec)	Metres per Second
n	Shaft Rotational Speed
NRC	National Research Council Canada
NSERC	Natural Sciences and Engineering Research Council of Canada
MUN	Memorial University of Newfoundland
P/D	Pitch-Diameter Ratio
Q	Torque
R_n	Reynolds Number
RPS	Revolutions per Second
T	Thrust
V	Speed (of advance)
η	Open Water Efficiency
ν	Kinematic Viscosity
ρ	Density (water)

1.0 INTRODUCTION

Podded propellers were introduced to the marine industry just over a decade ago and have since become a popular main propulsion system for ships. This is due to their better hydrodynamic characteristics than conventional propeller-rudder systems.

A podded propeller consists of a motor inside of a pod and a propeller(s) connected to the drive shaft at one or both end(s) of the shaft. The unit is connected to the vessel via a strut, which allows the whole system to rotate 360 degrees around the vertical, or z-axis. This allows for the thrust to be directed anywhere in a 360 degree compass, which gives far superior manoeuvring capabilities. The rapid adoption of podded propellers by the industry has outpaced the understanding of their performance. This lack of knowledge has translated into problems in practice, including propeller and bearing damage as well as vibration during manoeuvring.

The purpose of this study is to increase the understanding of podded propeller performance. NRC could also use these tests as a solid base on which further testing could be completed.

2.0 DESCRIPTION OF THE MUN-NRC-NSERC POD MODEL

The experiments conducted were on either a single podded propeller or two podded propellers operating simultaneously. Two of the cases used a propeller of 270mm diameter, while the remainder used a propeller of 200mm diameter. The arrangement and diameter of propellers are given in the section *DESCRIPTION OF CASES* for each particular case. All cases used a propeller that was four bladed, had a pitch-diameter ratio (P/D) of 1.0, and an expanded area ration (EAR) of 0.6. The geometric particulars of the pod are given below in *Table 1*. The values for the model propulsor were selected to provide an average representation of in-service, full-scale single screw podded propulsor. The geometric particulars of the pod-strut model were defined using the parameters depicted in *Figure 1*.[1]

Experimental Dimensions of Model Pods	**Pod** ***mm***
Propeller Diameter, D_{Prop}	270 or 200
Pod Diameter, D_{Pod}	139
Pod Length, L_{Pod}	410
Strut Height, S_{Height}	300
Strut Chord Length	225
Strut Distance, S_{Dist}	100
Strut Width	60
Fore Taper Length	85
Fore Taper Angle	15^o
Aft Taper Length	110
Aft Taper Angle	25^o

Table 1: Geometric particulars of the pod-strut model

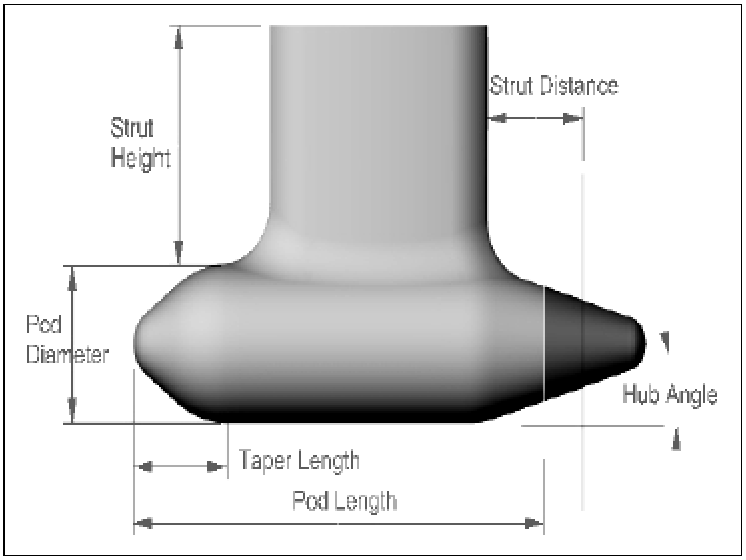

Figure 1: Geometric Parameters

3.0 DESCRIPTION OF FACILITIES

Several of the test cases took place at the NRC-IOT Ice Tank, while one of the test cases studied took place at the MUN Towing Tank. The flowing sub-sections describe the two Tanks that the tests were performed in.

3.1 NRC-IOT Ice Tank

The NRC-IOT ice tank is 90m long, 12m wide and 3m deep. The ice tank is equipped with a towing carriage that is capable of velocities from 0.1 – 4.0m/s. The control room is thermally insulated and houses the computer equipment for the drive control and the instrumentation racks for the model test transducers. The tank can accommodate models from 2-12m in length; and is equipped with force measurement, strain gauge load cells, model motions, accelerometer arrays, along with other instrumentation; all of which allow for various types of tests to be completed in the tank.[2]

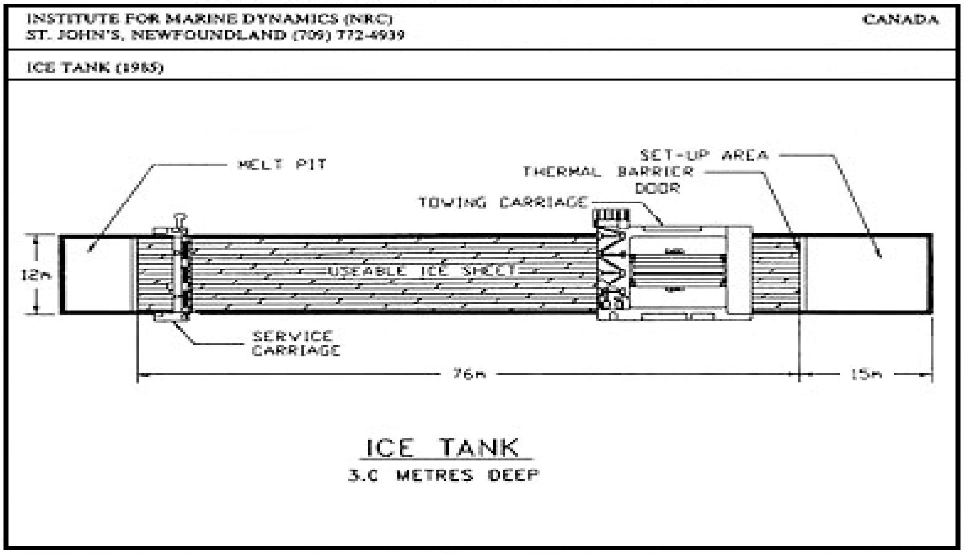

Figure 2: NRC-IOT Ice Tank schematic

3.2 MUN Towing tank

The towing tank facility at MUN has a length of 58m, is 4.5m wide, and a water depth of 2.2m. The tank is equipped with a towing carriage with a maximum towing speed of 5.0m/sec. The tank is equipped with a hydraulically operated wave maker, vertical mesh beaches, precision dynamometer, a 16 channel data acquisition system, along with other instrumentation; all of which allows for various types of testing to be competed at the facility.[3]

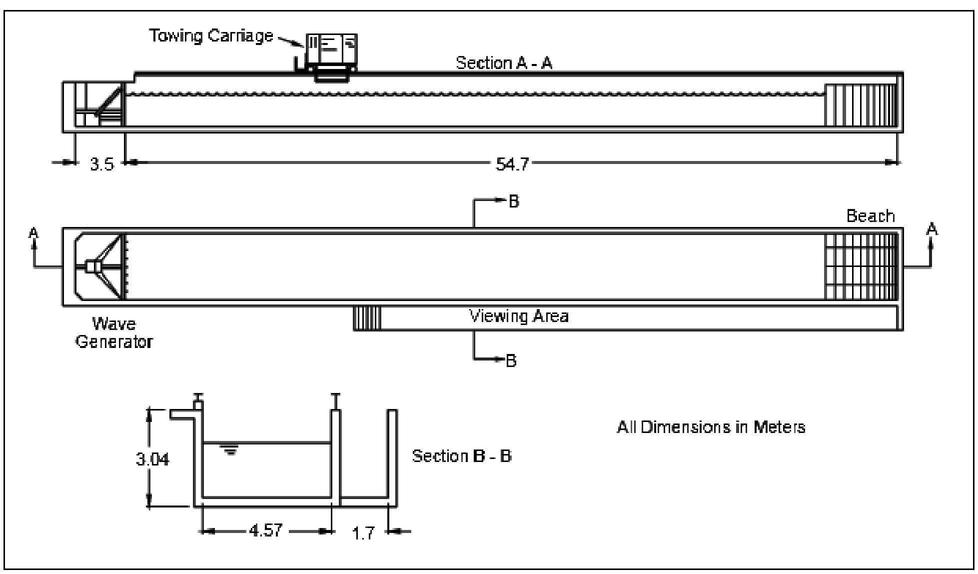

Figure 3: MUN Towing Tank schematic

4.0 DESCRIPTION OF INSTRUMENTATION

4.1 Experimental Apparatus

As in the previous section, this section will also contain a description of the experimental apparatus used at the NRC-IOT Ice Tank as well as the MUN Towing Tank.

4.1.1 NRC-IOT dynamometer

The set-up shown below in *Figure 3* was used for this set of experiments. The system has the ability to measure the propeller and pods forces and moments. It was used to measure unit thrust (T_{unit}), propeller thrust at hub end (T_{prop}), propeller thrust at pod end (T_{pod}), propeller torque (Q), as well as forces in the three coordinate directions.[3] The unit thrust is of particular interest, as it used for powering predictions for podded propellers. The unit thrust is the net available thrust available for propelling the ship. It not only includes the thrust of the propeller, but also the drag and other hydrodynamic forces acting on the pod-strut body.

The design includes an instrumented propeller hub, a custom mitre gearbox, an azimuth drive system, propeller drive system, a hull mounting and seal assembly, and a 6-component balance for measuring global loads on the pod.[4]

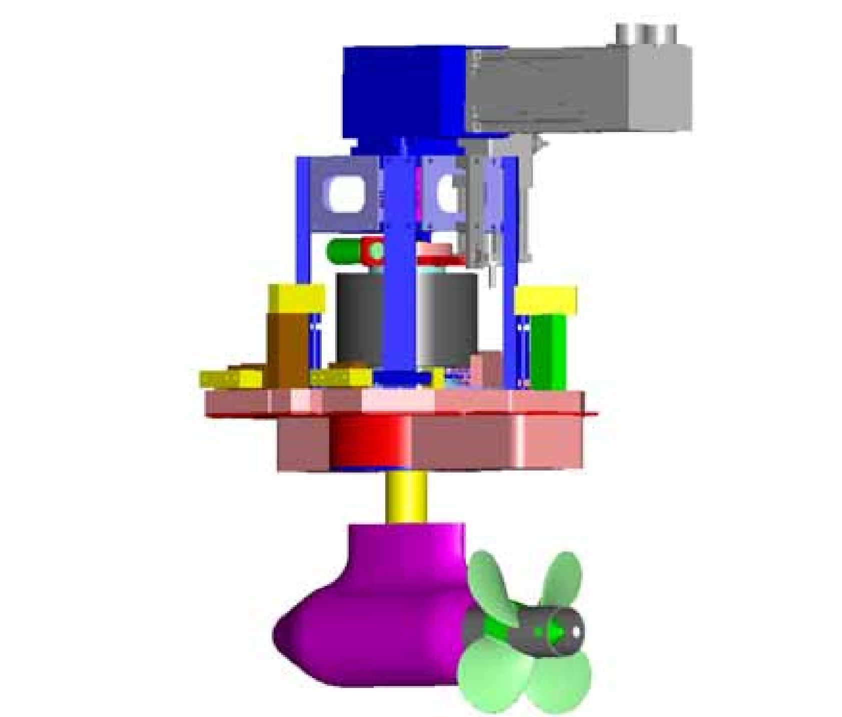

Figure 4: TDC Podded Props – General Arrangement

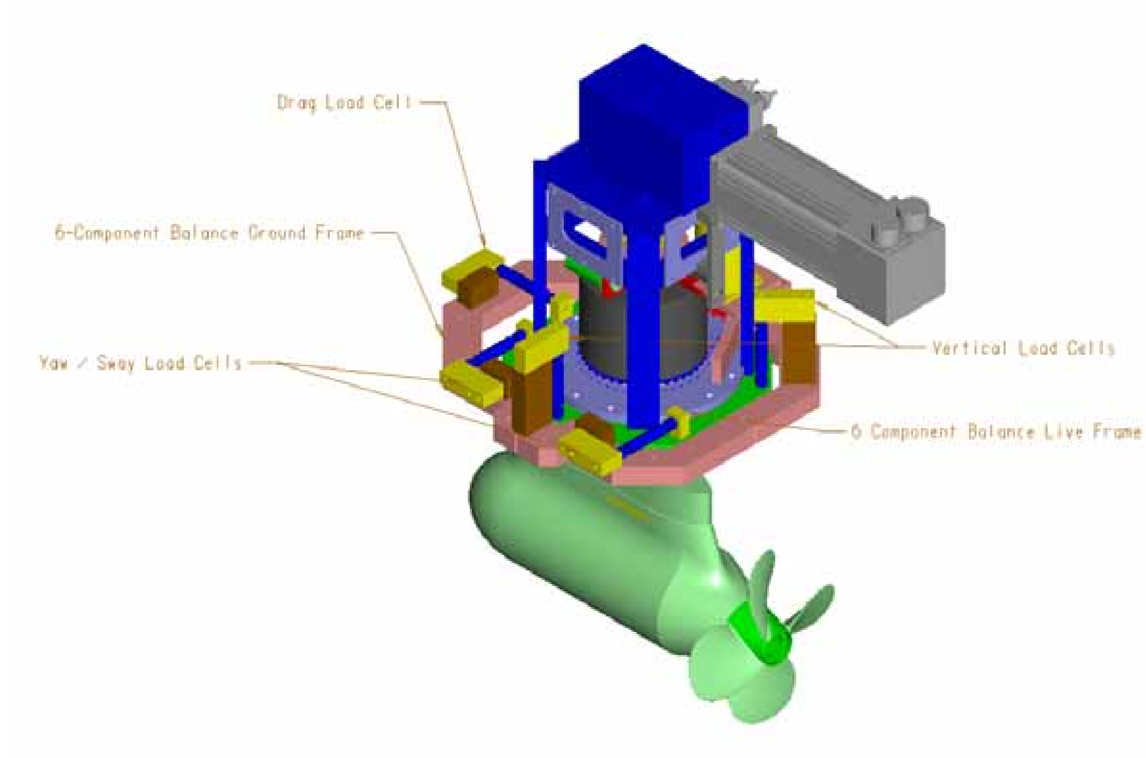

Figure 5: 6-Component Balance

4.1.2 NSERC-NRC pod dynamometer (or MUN dynamometer)

The NSERC-NRC pod dynamometer system, custom designed, was used during the experiments. The system has the ability to measure the propeller and pods forces and moments. It was used to measure unit thrust (T_{unit}), propeller thrust at hub end (T_{prop}), propeller thrust at pod end (T_{pod}), propeller torque (Q), as well as forces in the three coordinate directions.[3] The unit thrust is of particular interest, as it used for powering predictions for podded propellers. The unit thrust is the net available thrust available for propelling the ship. It not only includes the thrust of the propeller, but also the drag and other hydrodynamic forces acting on the pod-strut body. The water temperature, carriage speed (V), and the rotational speed of the propeller (n) were also measured.

As can be seen below in Figure 3, the unit consists of two major components. The first part is the pod dynamometer, which measures the thrust and torque of the propeller at the propeller shaft. The second part of the unit is the global dynamometer, which measures the unit forces in the three coordinate directions at a location above the propeller boat. Also, a boat shaped body called a wave shroud was attached to the frame of the test equipment and placed just above the water surface. Further details of the experimental apparatus can be found in MacNeill et al. (2004).[5]

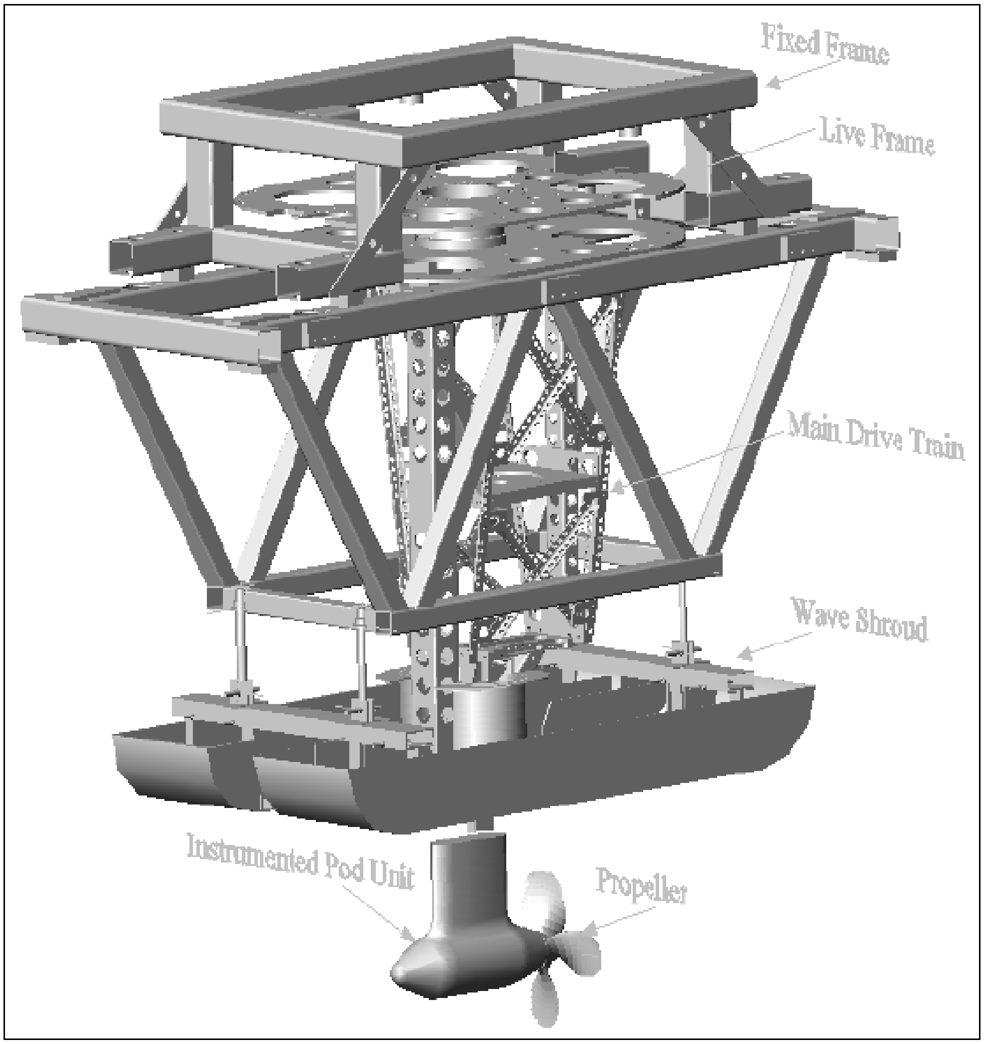

Figure 6: NSERC-NRC Pod Dynamometer System

Figure 7: Global dynamometer looking from below

Figure 8: Side view of system

4.2 Opens Boat

For the experiments conducted in the NRC-IOT Ice Tank an opens boat was constructed out of plywood, foam and glass. The opens boat floor was provided with slots that the pod drives fit into to allow the distance between the drives to be varied from as close as the drives could safely be run together to 3 times the width spacing of the pods.[4]

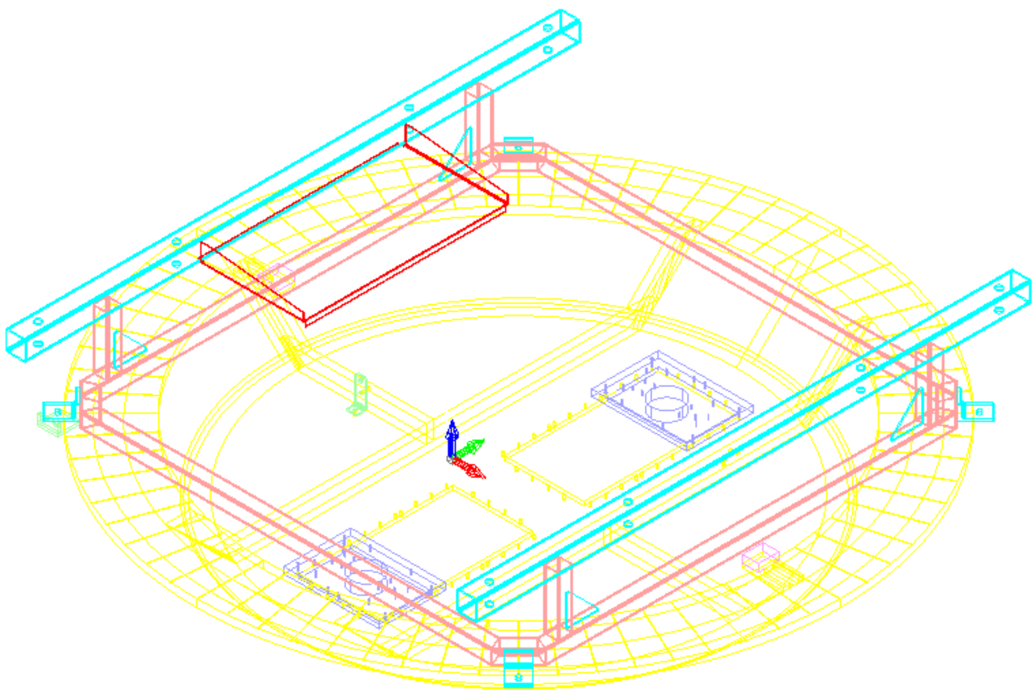

Figure 9: Round Opens Boat

4.3 Data Acquisition System (DAS)

4.3.1 NRC-IOT tests

The Data Acquisition System (DAS) for this project is custom built with IOTech gear and RS232 data from the U500 controller. The system components were chosen to allow for the system to be placed into a free running model. The data was collected through a total of 26 channels; a detailed outline of the channel set-up is in *Appendix C*. The system consisted of the following:

- 1 - Panasonic CF-51 Laptop, PC4026, S/N
- 1 – Panasonic Docking Station
- 1 – D-Link DI-624 Wireless Router
- 1 - IOTech Daqbook 2001, S/N 802671
- 2 - IOTech DBK 43A, 8 Channel Stain Gage Modules
- 1 – Custom 16 Channel DBK 43A to 10 Pin breakout box
- 2 - IOTech DBK 45, 4-Channel SSH and Low-Pass Filter Cards
- 1 – IOTech DBK 10, Expansion Chassis
- 1 – Custom 8-Channel Isolation Amp box

Figure 10: DAS set-up used for calibrations

4.3.2 MUN tests

The data for each of the test conditions was collected through 13 channels (three channels for propeller and pod thrusts and torque, two channels for shell drag, six channels for global loads, one channel for propeller rotational speed and one channel for carriage speed). The voltage data outputs for the tests were collected using an IOTech Daqbook data acquisition system (Daqbook 2000) connected to a computer running DaqView software. For these tests, the data were collected with a sampling rate of 59Hz. The raw data was collected in .txt format and post processed using Microsoft Excel. For each test run, data was collected for at least 10 second when the propeller run at very low rps (0.5 or less). Then the test data was collected following a standard procedure. The data collected at low rps was used to tare the test value. In this way the friction correction for thrust and torque was avoided.

5.0 DESCRIPTION OF CASES

As stated above, there were a total of seven sets of tests conducted. This section is intended to give a brief explanation of each case and the tests that were performed for each set of tests. A general test plan will be provided in each sub-section for each case.

5.1 Case 1

The tests were performed in the MUN Towing Tank in January 2005. The experiments conducted were on a single podded propeller with a diameter of 270mm. The following is a list of the types of experiments conducted: Reynolds Number Effects Tests, Air Friction and Bollard Runs, Opens Tests (0 deg azimuth), Oblique Flow Tests, and Third Quadrant Runs.

Reynolds Number Effects	
Mode	Pull Mode
RPS	8, 9, 10, 11, 12, 13, 14
Carriage Velocity (m/s)	1.728, 1.944, 2.16, 1.944, 2.187, 2.43, 2.16, 2.43, 2.7, 2.376, 2.673, 2.97, 2.592, 2.916, 3.24, 2.808, 3.159, 3.51, 3.024, 3.402, 3.78
Azimuth Angle (deg)	0

Table 2: General test plan for Reynolds Effects Tests

Air Friction Tests	
Mode	Pull Mode
RPS	1,2 (in both positive and negative directions)
Carriage Velocity (m/s)	0
Azimuth Angle (deg)	0

Table 3: General test plan for Air Friction Tests

Bollard Runs	
Mode	Pull Mode
RPS	-11 to 10
Carriage Velocity (m/s)	0
Azimuth Angle (deg)	0

Table 4: General test plan for Bollards Tests

Opens Tests	
Mode	Pull Mode
RPS	12
Carriage Velocity (m/s)	0.324, 0.648, 0.972, 1.296, 1.62, 1.944, 2.268, 2.592, 2.916, 3.24, 3.564
Azimuth Angle (deg)	0

Table 5: General test plan for Open Tests

Oblique Flow Tests	
Mode	Pull Mode
RPS	12
Run #1	
Carriage Velocity (m/s)	2.268, 1.62, 0.324, 3.24, 0.648, 0.972, 2.592, 1.944, 3.564, 1.296, 2.916, 4.0
Azimuth Angle (deg)	-9
Run #2	
Carriage Velocity (m/s)	-1.62, -1.296, -0.324, -0.648, -0.972, -1.944
Azimuth Angle (deg)	-9
Run #3	
Carriage Velocity (m/s)	2.268, 1.62, 0.324, 3.24, 0.648, 0.972, 2.592, 1.944, 3.564, 1.296, 2.916, 4.0
Azimuth Angle (deg)	9
Run #4	
Carriage Velocity (m/s)	-1.62, -1.296, -0.972, -1.944, -1.05
Azimuth Angle (deg)	9

Table 6: General test plan for Oblique Flow Tests

Third Quadrant Tests	
Mode	Pull Mode
RPS	12
Carriage Velocity (m/s)	0.324, 0.648, 0.972, 1.296, 1.62, 1.944
Azimuth Angle (deg)	0

Table 7: General test pan for Third Quadrant Tests

5.2 Case 2

This is the numerical results of the same set-up as case 1; and was completed on Oct 24/04. They were computed for a single podded propeller with a 270mm diameter. Mohammed Islam and Dr. Pengfei Liu completed the test using the program PROPELLA.

5.3 Case 3

Tests were conducted in the NRC-IOT Ice Tank in March of 2006 on a single podded propeller of 200mm diameter. The following is a list of the types of experiments performed: Reynolds Number Effect Tests, Air Friction and Bollard Runs, and Open Tests.

Air Friction Tests	
Mode	Pull Mode
Carriage Velocity (m/s)	0
Run #1	
RPS	0.01. 0.1, 1, 14, 15
Azimuth Angle (deg)	0
Run #2	
RPS	0.01. 0.1, 1, 14, 15
Azimuth Angle	0
Run #3	
RPS	0.01, 0.1, 1, 7, 10, 13, 14, 15
Azimuth Angle	0

Table 8: General test plan for Air Friction Tests

Bollard Runs	
Mode	Pull Mode
Carriage Velocity (m/s)	0
Run #1	
RPS	0.01, 0.1, 1, 14, 15
Azimuth Angle (deg)	0
Run #2	
RPS	0.01, 0.1, 1, 14, 15
Azimuth Angle	0
Run #3	
RPS	0.01, 0.1, 1, 7, 10, 13, 14, 15
Azimuth Angle	0

Table 9: General test plan for Bollard Runs

Opens Tests	
Mode	Pull Mode
Run #1	
Carriage Velocity (m/s)	0.66, 2.64, 3.30, 3.63, 3.96
RPS	16.5
Azimuth Angle (deg)	0
Run #2	
Carriage Velocity (m/s)	0.60, 2.40, 3.00, 3.30, 3.60
RPS	15
Azimuth Angle (deg)	0
Run #3	
Carriage Velocity (m/s)	0.52, 2.08, 2.60, 2.86, 3.12
RPS	13
Azimuth Angle (deg)	0
Run #4	
Carriage Velocity (m/s)	0.40, 1.60, 2.00, 2.20, 2.40
RPS	10
Azimuth Angle (deg)	0
Run #5	
Carriage Velocity (m/s)	0.28, 1.40, 1.68
RPS	7
Azimuth Angle (deg)	0

Table 10: General test plan for Opens Tests

5.4 Case 4 (a and b)

These tests were completed in the NRC-IOT Ice Tank in May of 2006 on a single podded propeller with a diameter of 200mm. For case 4a Pod B was static while for case 4b Pod A was static. The only test completed for this case was Opens Tests at low Froude numbers. This was mainly due to time constraints on the ice tank, and means that comparing the results with the other cases is difficult.

Opens Tests	
Mode	Pull Mode
Run #1	
Carriage Velocity (m/s)	0, 0.13, 0.26, 0.39, 0.52, 0.65, 0.78, 0.91, 1.04
Pod 1	
RPS	0
Azimuth Angle (deg)	0
Pod 2	

RPS	13
Azimuth Angle (deg)	0
Run #2	
Carriage Velocity (m/s)	0, 0.13, 0.26, 0.39, 0.52, 0.65, 0.78, 0.91, 1.04
Pod 1	
RPS	13
Azimuth Angle (deg)	0
Pod 2	
RPS	0
Azimuth Angle (deg)	0

Table 11: General test plan for Opens Tests

5.5 Case 5 (a and b)

Case 5a and 5b were also completed in the NRC-IOT Ice Tank in May of 2006. The tests were completed on two podded propellers operating simultaneously with a diameter of 200mm. Case 5a is the data collected for Pod A only while case 5b is the data collected for Pod B only. The following is a list of the types of experiments conducted: Air Friction and Bollard Runs, Opens Tests (0 deg azimuth), Oblique Flow Tests, and Dynamic Tests.

Air Friction Tests	
Mode	Pull Mode
Carriage Velocity (m/s)	0
Run #1	
Pod 1	
RPS	0, 0.01, 0.1, 0.2, 0.5, 1, 2, 3, 4, 5, 6, 7, 8, 9, 10, 11, 12, 13, 14, 15
Azimuth Angle (deg)	0
Pod 2	
RPS	0
Azimuth Angle (deg)	0
Run #2	
Pod 1	
RPS	0
Azimuth Angle (deg)	0
Pod 2	
RPS	0, 0.01, 0.1, 0.2, 0.5, 1, 2, 3, 4, 5, 6, 7, 8, 9, 10, 11, 12, 13, 14, 15
Azimuth Angle (deg)	0
Run #4	
Pod 1	
RPS	0

Azimuth Angle (deg)	0
Pod 2	
RPS	0, 0.01, 0.1, 0.2, 0.5, 1, 2, 3, 4, 5, 6, 7, 8, 9, 10, 11, 12, 13, 14, 15
Azimuth Angle (deg)	0

Table 12: General test plan for Air Friction Tests

Bollard Runs	
Mode	Pull Mode
Carriage Velocity (m/s)	0
Run #1	
Pod 1	
RPS	0, 0.01, 0.1, 0.2, 0.5, 1, 2, 3, 4, 5, 11, 12, 13
Azimuth Angle (deg)	0
Pod 2	
RPS	0
Azimuth Angle (deg)	0
Run #2	
Pod 1	
RPS	0
Azimuth Angle (deg)	0
Pod 2	
RPS	0, 0.01, 0.1, 0.2, 0.5, 1, 2, 3, 4, 5, 11, 12, 13
Azimuth Angle (deg)	0
Run #3	
Pod 1	
RPS	0, 0.01, 0.1, 0.2, 0.5, 1, 2, 3, 4, 5, 11, 12, 13
Azimuth Angle (deg)	0
Pod 2	
RPS	0, 0.01, 0.1, 0.2, 0.5, 1, 2, 3, 4, 5, 11, 12, 13
Azimuth Angle (deg)	0

Table 13: General test plan for Bollards Tests

Opens Tests	
Mode	Pull Mode
Run #1	
Carriage Velocity (m/s)	0, 0.13, 0.26, 0.39, 0.52, 0.65, 0.78, 0.91, 1.04, 1.17, 1.3, 1.56, 1.82, 2.08, 2.34, 2.47, 2.6, 2.86, 3.12
Pod 1	

RPS	0, 0.1, 13
Azimuth Angle (deg)	0
Pod 2	
RPS	0, 0.1, 13
Azimuth Angle (deg)	0

Table 14: General test plan for Open Tests

Oblique Flow Tests	
Mode	Pull Mode
Run #1	
Carriage Velocity (m/s)	0, 0.13, 0.26, 0.39, 0.52, 0.65, 0.78, 0.91, 1.04, 1.3, 1.56, 1.82, 2.08, 2.34, 2.47, 2.6, 2.86, 3.12
Pod 1	
RPS	0, 0.1, 13
Azimuth Angle (deg)	5
Pod 2	
RPS	0, 0.1, 13
Azimuth Angle (deg)	0
Run #2	
Carriage Velocity (m/s)	0, 0.13, 0.26, 0.39, 0.52, 0.65, 0.78, 0.91, 1.04
Pod 1	
RPS	0, 0.1, 13
Azimuth Angle (deg)	10
Pod 2	
RPS	0, 0.1, 13
Azimuth Angle (deg)	0
Run #3	
Carriage Velocity (m/s)	0, 0.13, 0.26, 0.39, 0.52, 0.65, 0.78, 0.91, 1.04
Pod 1	
RPS	0, 0.1, 13
Azimuth Angle (deg)	30
Pod 2	
RPS	0, 0.1, 13
Azimuth Angle (deg)	0
Run #4	
Carriage Velocity (m/s)	0, 0.13, 0.26, 0.39, 0.52, 0.65, 0.78, 0.91, 1.04
Pod 1	
RPS	0, 0.1, 13
Azimuth Angle (deg)	60

Pod 2	
RPS	0, 0.1, 13
Azimuth Angle (deg)	0
Run #5	
Carriage Velocity (m/s)	0, 0.13, 0.26, 0.39, 0.52, 0.65, 0.78, 0.91, 1.04
Pod 1	
RPS	0, 0.1, 13
Azimuth Angle (deg)	60
Pod 2	
RPS	0, 0.1, 13
Azimuth Angle (deg)	60

Table 15: General test plan for Oblique Flow Tests

Dynamic Tests	
Mode	Pull Mode
Run#1	
RPS	13
Carriage Velocity (m/s)	0, 0.13, 0.26, 0.39, 0.52, 0.65, 0.78, 0.91, 1.04, 1.17
Azimuth Rate	2, 5, 10, 20
Pod 1	
Azimuth Angle (deg)	5
Pod 2	
Azimuth Angle (deg)	0
Run #2	
RPS	13
Carriage Velocity (m/s)	0, 0.13, 0.26, 0.39, 0.52, 0.65, 0.78, 0.91, 1.04, 1.17
Azimuth Rate	2, 5, 10, 20
Pod 1	
Azimuth Angle (deg)	10
Pod 2	
Azimuth Angle (deg)	0
Run #3	
RPS	13
Carriage Velocity (m/s)	0, 0.13, 0.26, 0.39, 0.52, 0.65, 0.78, 0.91, 1.04, 1.17
Azimuth Rate	2, 5, 10, 20
Pod 1	
Azimuth Angle (deg)	5

Pod 2	
Azimuth Angle (deg)	5
Run #4	
RPS	13
Carriage Velocity (m/s)	0, 0.13, 0.26, 0.39, 0.52, 0.65, 0.78, 0.91, 1.04, 1.17
Azimuth Rate	2, 5, 10, 20
Pod 1	
Azimuth Angle (deg)	10
Pod 2	
Azimuth Angle (deg)	10

Table 16: General test plan for Dynamic Tests

5.6 Case 6

This was another numerical simulation of the average pod geometry. They were computed for a single podded propeller with a 200mm diameter. Mohammed Islam and Dr. Pengfei Liu also completed the test using the program PROPELLA.

5.7 Case 7

Tests were conducted in May of 2006 in the NRC-IOT Ice Tank. The tests were conducted on a single podded propeller with a diameter of 200mm. The types of experiments conducted were Air Friction and Bollard Runs, Opens Tests, and Oblique Flow Tests.

Air Friction Tests	
Mode	Pull Mode
Carriage Velocity (m/s)	0
Run #1	
RPS	0, 0.01, 0.1, 0.2, 0.5, 1, 2, 3, 4, 5, 11, 12, 13
Azimuth Angle (deg)	0
Run #2	
RPS	0, 0.01, 0.1, 0.2, 0.5, 1, 2, 3, 4, 5, 11, 12, 13
Azimuth Angle (deg)	0
Run #3	
RPS	0, 0.01, 0.1, 0.2, 0.5, 1, 2, 3, 4, 5, 11, 12, 13
Azimuth Angle (deg)	0

Table 17: General test plan for Air Friction Tests

Bollard Runs	
Mode	Pull Mode
Carriage Velocity (m/s)	0
Run #1	
RPS	0, 0.01, 0.1, 0.2, 0.5, 1, 2, 3, 4, 5, 11, 12, 13
Azimuth Angle (deg)	0
Run #2	
RPS	0, 0.05, 0.1, 0.2, 0.3, 0.4, 0.5
Azimuth Angle (deg)	0
Run #3	
RPS	0, 0.01, 0.1, 0.2, 0.5, 1, 2, 3, 4, 5, 11, 12, 13
Azimuth Angle (deg)	0
Run #4	
RPS	0, 0.05, 0.1, 0.2, 0.3, 0.4, 0.5
Azimuth Angle (deg)	0
Run #5	
RPS	0, 0.01, 0.1, 0.2, 0.5, 1, 2, 3, 4, 5, 11, 12, 13
Azimuth Angle (deg)	0
Run #6	
RPS	0, 0.05, 0.1, 0.2, 0.3, 0.4, 0.5
Azimuth Angle (deg)	0
Run #7	
RPS	13
Azimuth Angle (deg)	90
Run #8	
RPS	13
Azimuth Angle (deg)	45

Table 18: General test plan for Bollard Runs

Opens Tests	
Mode	Pull Mode
Run #1	
Carriage Velocity (m/s)	1.30, 1.56, 1.82, 2.08, 2.34, 2.47, 2.60, 2.86, 3.12
RPS	13
Azimuth Angle (deg)	0

Table 19: General test plan for Opens Tests

Oblique Flow Tests	
Mode	Pull Mode
Run #1	
Carriage Velocity (m/s)	1.30, 1.56, 1.82, 2.08, 2.34, 2.47, 2.60, 2.86, 3.12
RPS	13
Azimuth Angle (deg)	5
Run #2	
Carriage Velocity (m/s)	1.30, 1.56, 1.82, 2.08, 2.34, 2.47, 2.60, 2.86, 3.12
RPS	13
Azimuth Angle (deg)	5

Table 20: General test plan for Oblique Flow Tests

6.0 DESCRIPTION OF EXPERIMENTS

6.1 Reynolds Number Effect Tests

Flow over full-scale propellers is fully turbulent at operating condition. Flow visualizations on propeller models have found that on model propellers with diameters between 168 and 355mm the boundary layer flow is mainly laminar on both the suction and pressure sides of the propeller blade at propeller $R_n = nD^2/\nu$ below $1*10^6$. Between $R_n = 1*10^6$ and $1*10^7$ the boundary layer develops into fully developed turbulent flow, first on the suction side and then later on the pressure side. The exact or critical R_n at which the flow becomes fully turbulent is dependent on factors such as the geometry, load conditions and flow conditions.[6]

Testing on model propellers must be at rotational speeds that allow the propeller to operate in a flow regime that minimizes laminar flow on the suction side or flow separation on the trailing edge. With respect to podded propulsion open water tests; this flow becomes particularly important in pulling pod configurations because the flow into the propeller is not affected by the turbulent wakes of the strut and pod.[6]

Through open water testing, researchers have found that the propeller performance becomes independent of the R_n at a level where the laminar flow is developing into turbulent flow and this value can be found by completing Reynolds Number Effect Tests.

The performance measurements are Thrust and Torque; the non-dimensional coefficients of Torque and Thrust are K_Q and K_T. If these values are plotted against Reynolds Numbers there will be a point at which the Reynolds numbers does not affect the performance measurements. The performance parameters for both the large (D = 406mm) and small (D = 238mm) propellers stabilize at approximately $1\text{-}1.2 *10^6$.

Reynolds effects tests are performed at a number of different Reynolds numbers.

To perform a set of Reynolds effect tests a range of J values are chosen and then tested at a selection of rotation rates. The speed of advance is varied to give a selection of Reynolds Numbers. These Reynolds numbers are then plotted against performance parameters to see if the increase is having a significant effect on performance. The performance parameters are thrust and torque; the non-dimensional coefficients are K_Q and K_T. The equations for both coefficients are shown above.

The following equation is used to determine Reynolds Number:

$$R_n = \frac{c_{0.75}\sqrt{{V_A}^2 + (0.75\pi nD)^2}}{\upsilon}$$

Where: $c_{0.75}$ = Chord length at 0.75 radius fraction of propeller = 0.095m
V_A = Speed of advance
n = Shaft speed
D = Propeller diameter = 0.27m
ν = Kinematic viscosity = $1.139 \cdot 10^{-6}$ m^2/s

6.2 Air Friction Tests

Conducted by taking the pod(s) out of the water and running them in air. By completing these tests one can estimate the frictional losses in the system. This then allows the researcher to tare the torque values by subtracting this value from all the torque readings measured during the Opens Tests.

6.3 Bollard Runs

These are conducted when the carriage is at a stop. The propeller is run at operating speed (rps); which allows for the computation of Bollard Pull. The Bollard Pull for a propeller is the amount of thrust produced by the propeller when the vessel is stopped. This is particularly important for vessels such as tugboats and icebreakers as they frequently operate at very low, next to zero, velocities.

6.4 Opens Tests (0 degree azimuth)

To illustrate the open water performance characteristics of the propeller a plot of K_T, $10K_Q$, η vs. J would be created, this is called the propeller performance chart. The equations to obtain these characteristics are described below in *Table 5*. For clarification, the definitions of all non-dimensional coefficients and terms shown in *Table 5* are explained in further detail in *Table 6*. For completeness efficiency curves would be created and displayed for the data. These curves tend to be more sensitive to errors than thrust and torque coefficients, so therefore more emphasis is placed on observations in the thrust and torque coefficient data.

Performance Characteristic	Data Reduction Equation
K_{Tprop} (Propeller Thrust Coefficient)	$T_{prop} /(\rho n^2 D^4)$
K_{Tunit} (Unit Thrust Coefficient)	$T_{unit} /(\rho n^2 D^4)$
K_Q (Torque Coefficient)	$Q /(\rho n^2 D^5)$
J (Advance Coefficient)	$V /(nD)$
η_{prop} (Propeller Efficiency (on Pod))	$(K_{Tprop} J) /(2\pi K_Q)$
η_{unit} (Unit Efficiency (on Pod))	$(K_{Tunit} J) /(2\pi K_Q)$
Where: T_{prop} = Propeller Thrust T_{unit} = Unit Thrust Q = Torque ρ = Density	n = Shaft Speed D = Propeller Diameter V = Speed of Advance

Table 21: Data Reduction Equations used in analysis

	Podded Propeller Test Definition
$\mathbf{K_{Tprop}}$	Non-dimensional form of the thrust of the propeller installed on the pod
$\mathbf{K_{Tunit}}$	Non-dimensional form of the unit thrust of the podded propeller
$\mathbf{K_Q}$	Non-dimensional form of the torque on the propeller shaft
J	Non-dimensional ratio of the advance speed to the shaft speed
η_{prop}	Open water efficiency of the propeller operating on the pod unit
η_{unit}	Overall efficiency of the entire pod unit, which factors in the drag of the pod and strut
$\mathbf{T_{prop}}$	Axial component of force generated by the propeller when installed on the pod unit
$\mathbf{T_{unit}}$	Net axial thrust generated by the pod unit; includes the drag of the pod and its influence on the prop
Q	The axial moment required to rotate the propeller at the desired shaft speed

Table 22: Definitions of Data Reduction Terms

7.0 DESCRIPTION OF DATA ANALYSIS

For both the tests carried out in the NRC-IOT Ice Tank as well as the test case performed in the MUN Towing Tank ASCII data files were compiled for transfer to researchers personal computers when the trials were completed.

7.1 Interpreting the Raw Data (MUN Towing Tank Tests)

When the data is transferred it is ready to be post-processed. The interpretation was completed using Microsoft Excel 2000. A time series is plotted and averages are taken for each defined section of the run; these final averages are then used in the final analysis. *Figure 19* shows a typical run down the tank while performing an opens test. In the plot below there are four sections; 1st. Nothing is on – both the carriage and propeller are still, 2nd. The carriage is turned on, but still doesn't move forward, 3rd. The prop starts to move at a very low rps while the carriage remains stopped, 4th. The carriage is up to running speed (approximately 2 m/s below) and the prop is running at desired rps. It should be noted that the plot below does not actually show rps, but shows the reading in volts. This would be changed to rps by multiplying by the appropriate constant.

After the averages are taken for each run the interpreted data can be transferred to a new Excel sheet where it is sorted according to run type (i.e. Third Quadrant Tests, Opens Tests, etc.) and advance coefficient, *J*. The physical quantities can then be non-dimensionalzed using the appropriate expression, as discussed in *Section 7.4*.

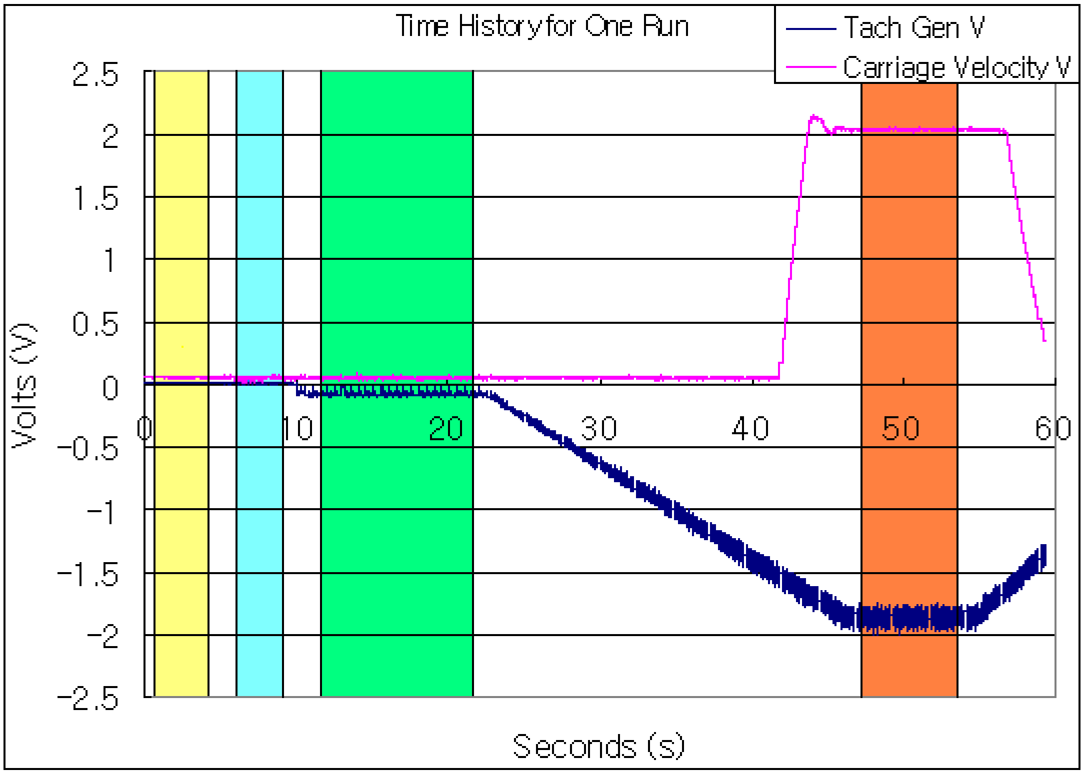

Figure 11: Typical plot of rps and Carriage Velocity for one run down the tank

7.2 Interpreting the Raw Data (NRC-IOT Ice Tank Tests)

Analysis of the tests was on going at the same time as the tests were running. A time series is plotted and averages are taken for each defined section of the run; these final averages are then used in the final analysis. *Figure 24* shows a typical run down the tank while performing an opens test. In the plot below there are three defined sections; 1st. Nothing is on – both the carriage and propeller are still, 2nd. The propeller is up to desired rps (in this case approximately 15), 3rd. The carriage is up to running speed (below at about 3.1 m/s) and the prop is running at desired rps.

After the averages are taken for each run the interpreted data can be transferred to a Microsoft Excel sheet where it is sorted according to run type (i.e. Third Quadrant Tests, Opens Tests, etc.) and advance coefficient, *J* (It's customary to sort from *J* = 0 to *J* = 1.2). The physical quantities measured can then be non-dimensionalzed using the appropriate expressions, as discussed in *Section 7.4.*

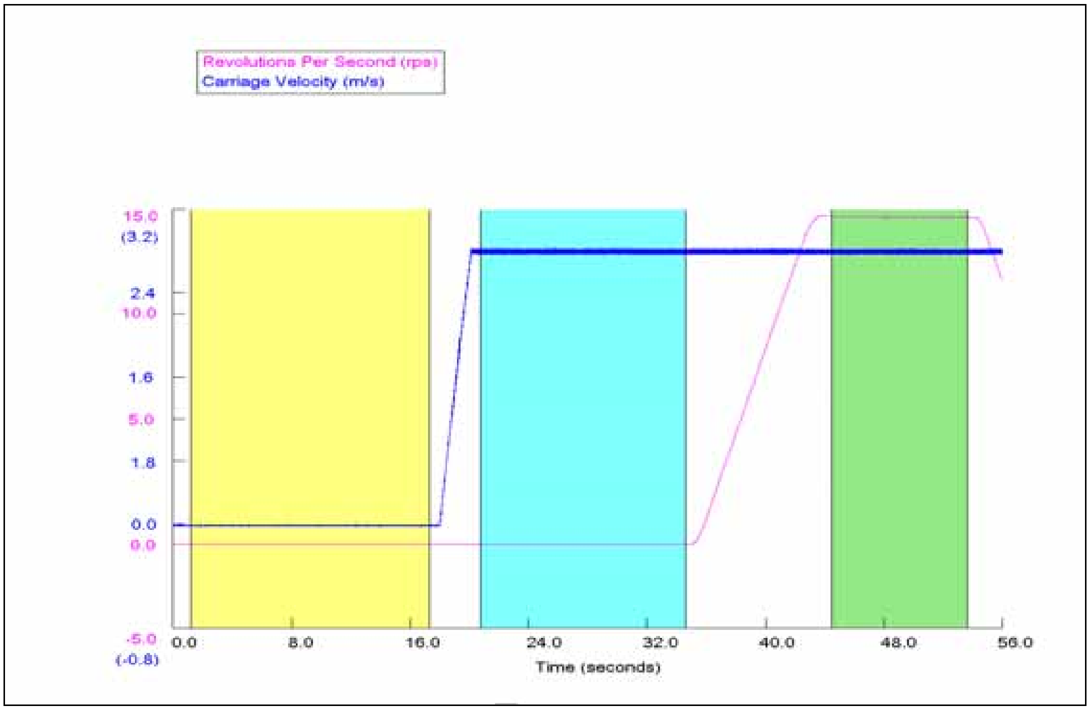

Figure 12: Typical plot of rps and Carriage Velocity for one run down the tank

8.0 CALIBRATIONS

The method used to calibrate the global dynamometer as well as thrust and torque load cells was the linear least squares method. This method theorizes that if enough varied loads are applied in varied directions an accurate estimate of the calibration matrix can be obtained using an optimized linear least square fit. In other words, if the test apparatus can be loaded with enough independent loading cases to cover the expected use of the model during actual testing, then an accurate calibration matrix can be derived.

The algorithm used to obtain the linear least squares calibration matrix is:

$$\underset{(n,m)}{[C]} = \underset{(m,z)}{[L]}\underset{(z,n)}{[a]^T}\left(\underset{(n,z)}{[a]}\underset{(z,n)}{[a]^T}\right)^{-1}$$

Where: n is the number of balance components
m is the number of calibration coefficients per component, [m = n(n+3)/2]
z is the number of loading cases
[C] contains the calibration coefficients

[L] defines the calculated distribution of the applied load P between the balance components for each loading case

[a] defines the actual distribution of the applied load P between the balance components for each loading case

8.1 Global Dynamometer

As stated above, the global dynamometer was calibrated using the linear least squares method. A total of forty-three cases were performed on the test set-up. This provided enough loading cases to provide an accurate calibration matrix.

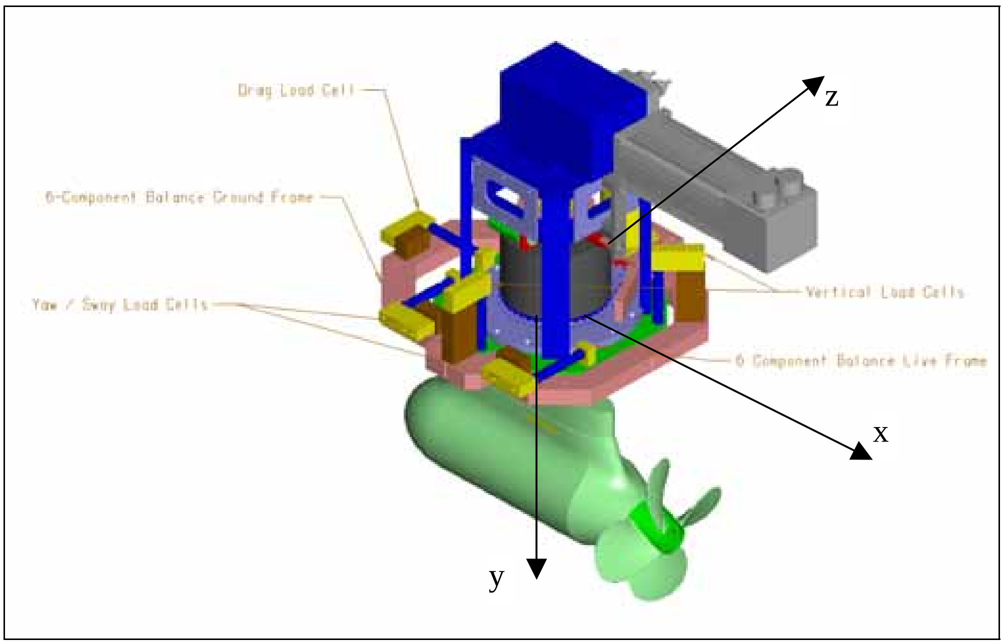

Figure 13: Positive coordinate directions in 3-D space

From the above equation the following matrix of calibration coefficients can be obtained. The calibration coefficients can then be applied directly to the measured data to estimate the actual force reading. [L] and [a] matrices can be found in *Appendix A.*

[C] =	35.065	-0.62753	0.62753	-0.15249	0.08896	0.04254
	4.702	61.447	-61.447	4.7079	-47.924	71.247
	5.2784	24.211	-24.211	5.0931	-49.897	73.751
	0.20125	0.97173	-0.97173	32.769	0.71655	1.5015
	-0.00214	0.72505	-0.72505	-2.8303	36.846	1.6438
	-0.17728	0.20692	-0.20692	-2.5681	0.75165	39.253

8.2 Thrust and Torque Load Cells

Calibrated in much the same way as the global dynamometer. Torque was produced by way of an adapter on the front of the pod where an arm could be attached (figure shown below). The results of the calibration are shown below in tables. [L] and [a] matrices for thrust and torque calibrations can be found in *Appendix B.*

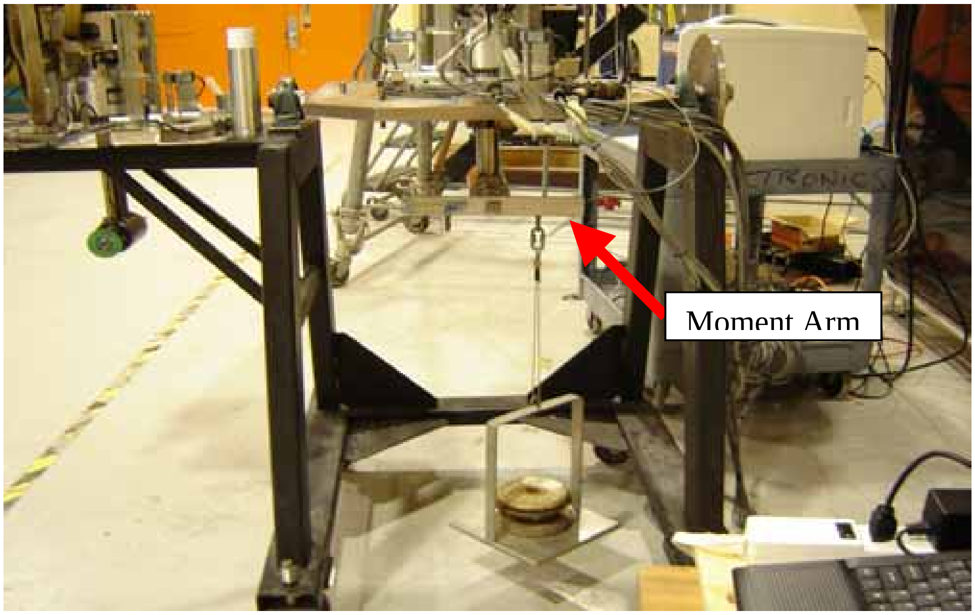

Figure 14: Photo showing how torque can be induced on the system

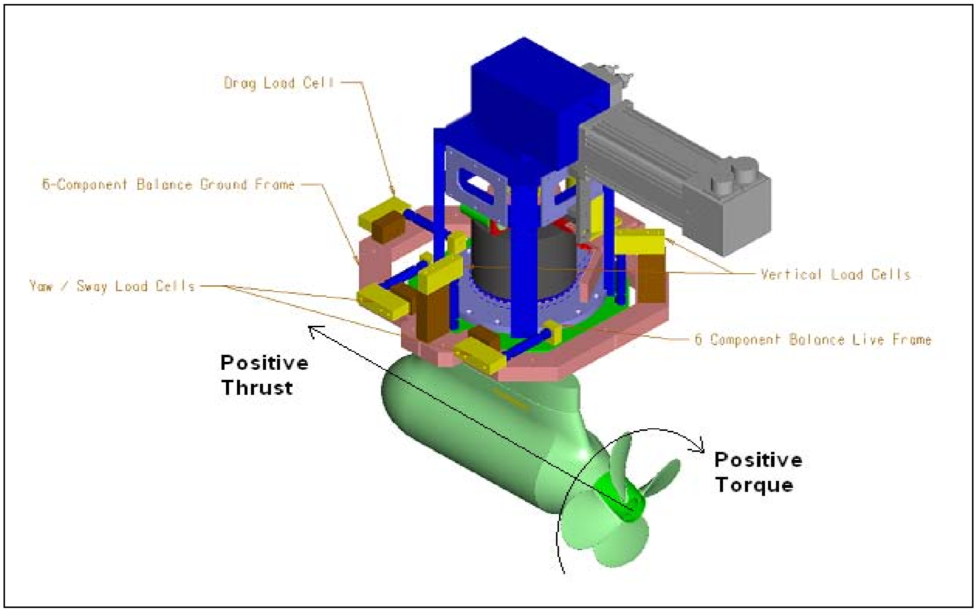

Figure 15: Positive thrust and torque directions during calibrations

From the equation in *Section 8.0* the following matrix of calibration coefficients can be obtained. The calibration coefficients can then be applied directly to the measured data to estimate the actual thrust and torque.

$$[C] = \begin{matrix} 65.9407 & 0.0064 \\ 0.0407 & 0.0115 \end{matrix}$$

9.0 RESULTS AND DISCUSSION

In the current study configurations of podded propellers were tested in either the NRC-IOT ice tank or the MUN Towing tank. The propellers were four bladed and in puller configuration. There were also two cases where numerical methods were used to determine the performance characteristics of the podded propeller. The flowing is the results obtained from the Opens Tests along with comments on the experiments performed.

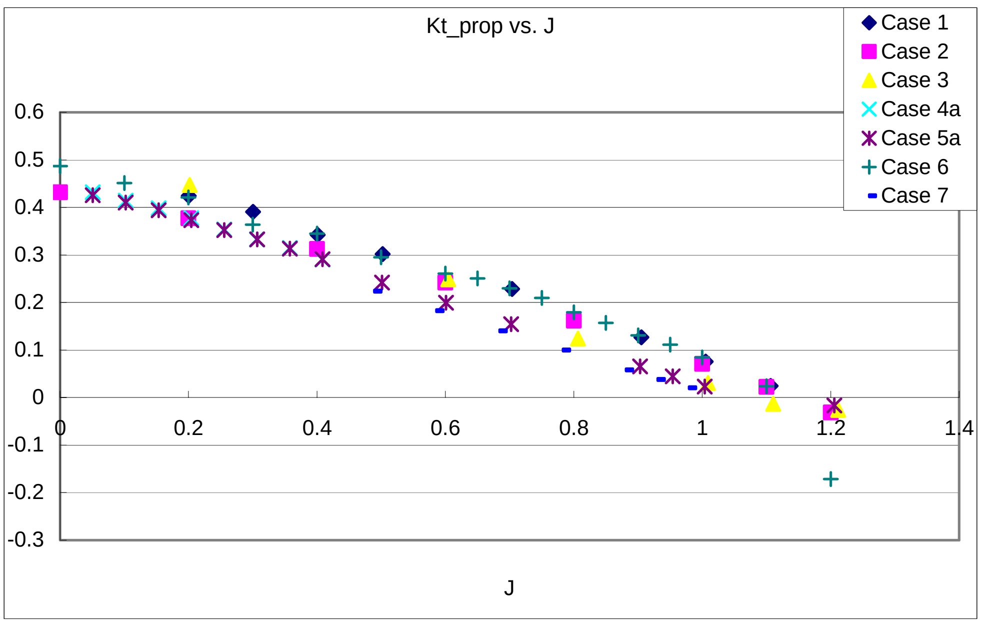

Figure 16: Comparison of K_{T_prop} versus J

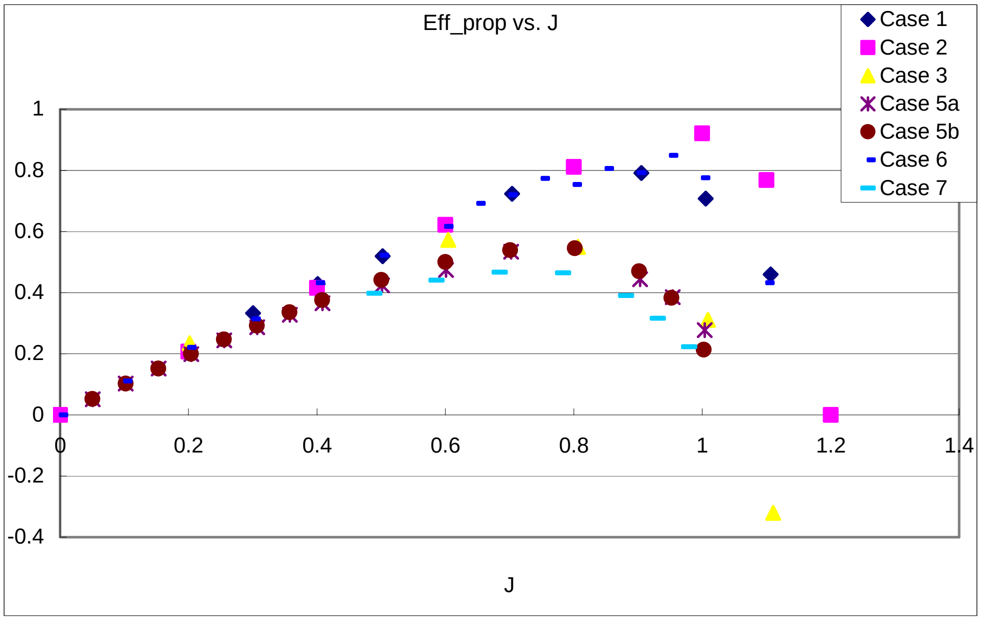

Figure 17: Comparison of η_{prop} versus J

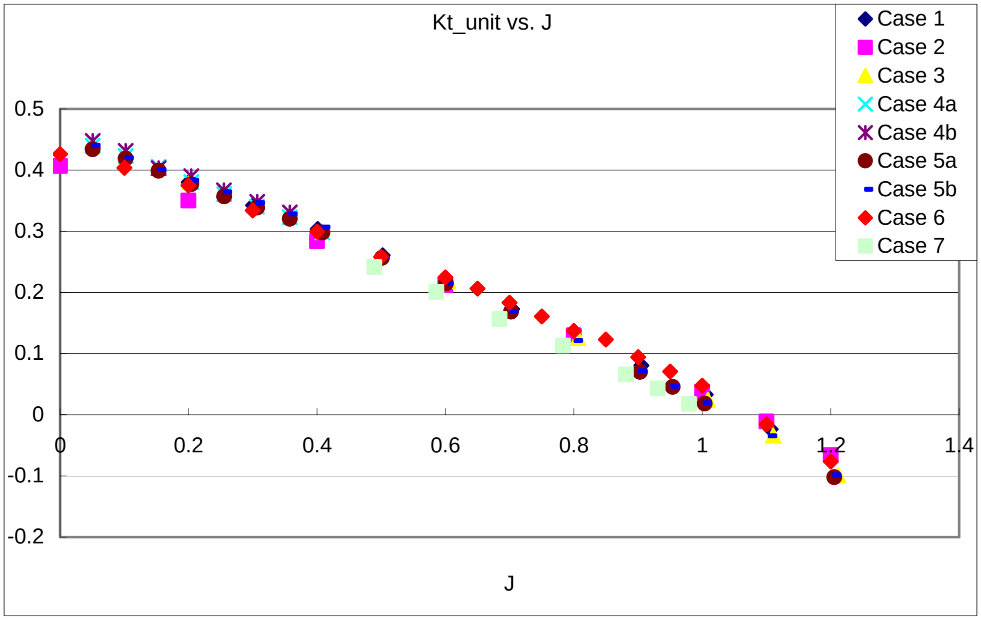

Figure 18: Comparison of K_{T_unit} versus J

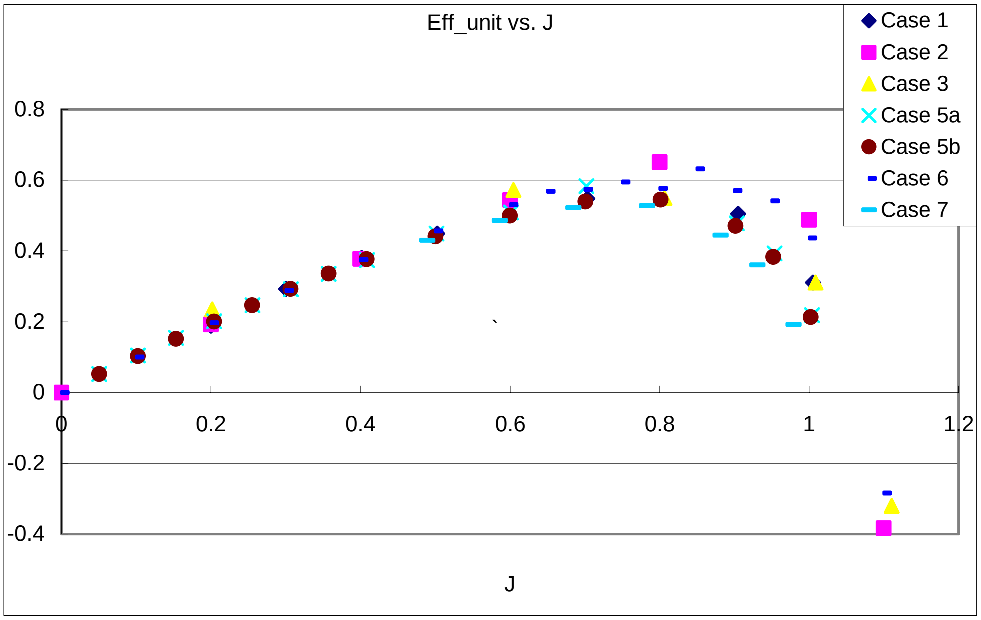

Figure 19: Comparison of η_{unit} versus J

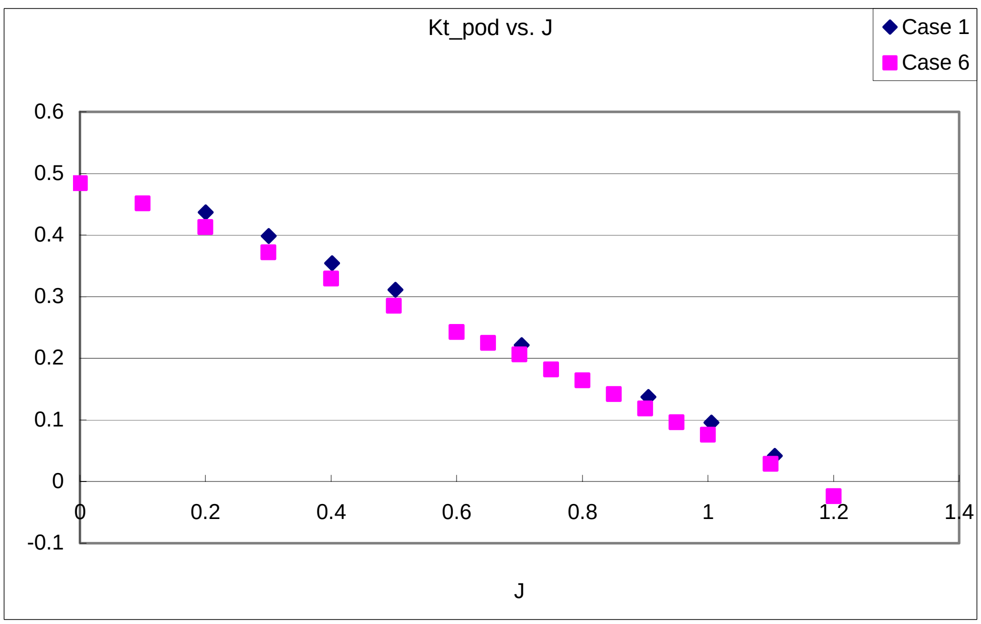

Figure 20: Comparison of K_{T_pod} versus J

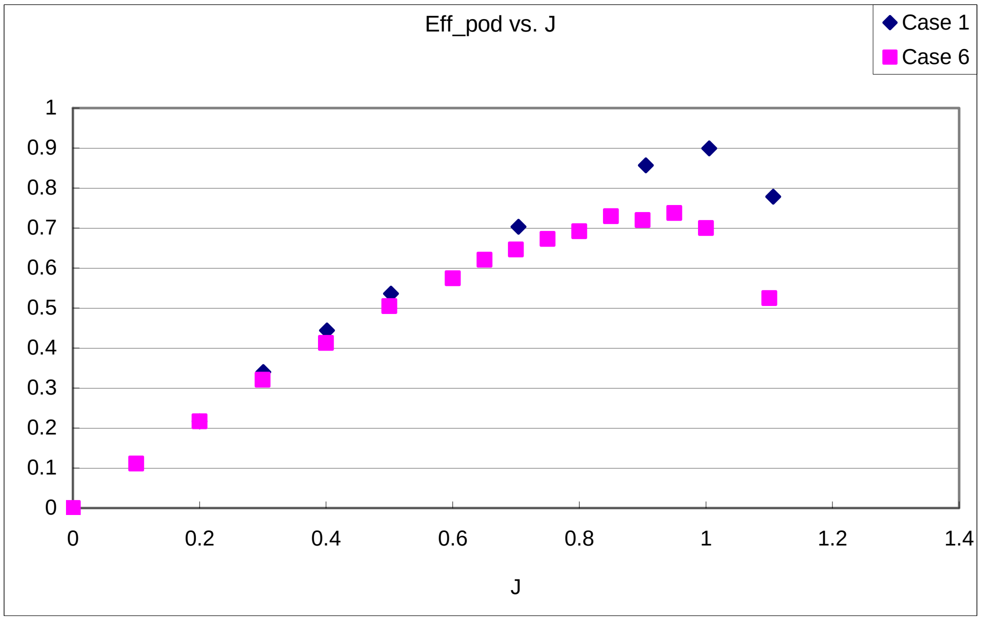

Figure 21: Comparison of η_{pod} versus J

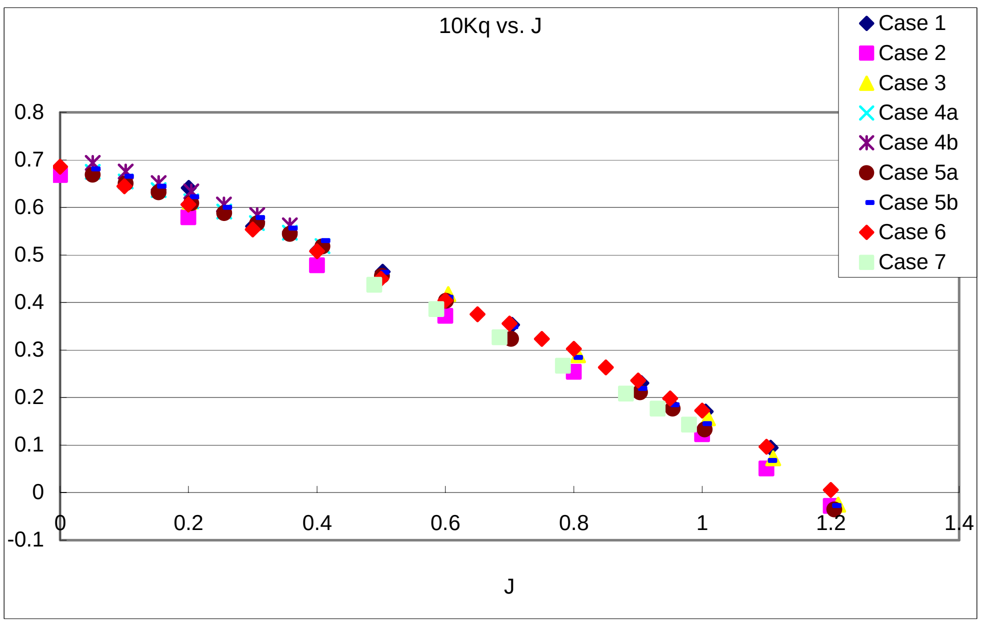

Figure 22: Comparison of $10K_Q$ versus J

From the above set of plots good comparison can be viewed for K_{T_unit}, K_{T_pod}, and $10K_Q$; with fairly good results for K_{T_prop}. K_{T_prop}: all of the cases go negative between J = 1.05 and 1.15 approximately; K_{T_unit}: all cases go negative between approximately J = 1.05 and 1.1; K_{T_pod}: both cases go negative between J = 1.15 and 1.2; and $10K_Q$: the cases go negative around approximately J = 1.2.

The efficiency curves show poorer quality results than the K_T and $10K_Q$ curves. This could be possibly due to mechanical errors encountered during testing or a whole range of other possible sources. Whatever the cause may be it is not of great concern at this time, as the remainder of the opens tests show promising results; and as was stated earlier emphasis is placed on thrust and torque coefficients.

Unfortunately cases 4a and 4b were not completely finished and therefore it is difficult to compare the results to the rest of the cases. However, from the comparisons that can be made, it looks as though if the runs had been completed it is likely that the trend would have continued and the results would have been similar to the remainder of the results.

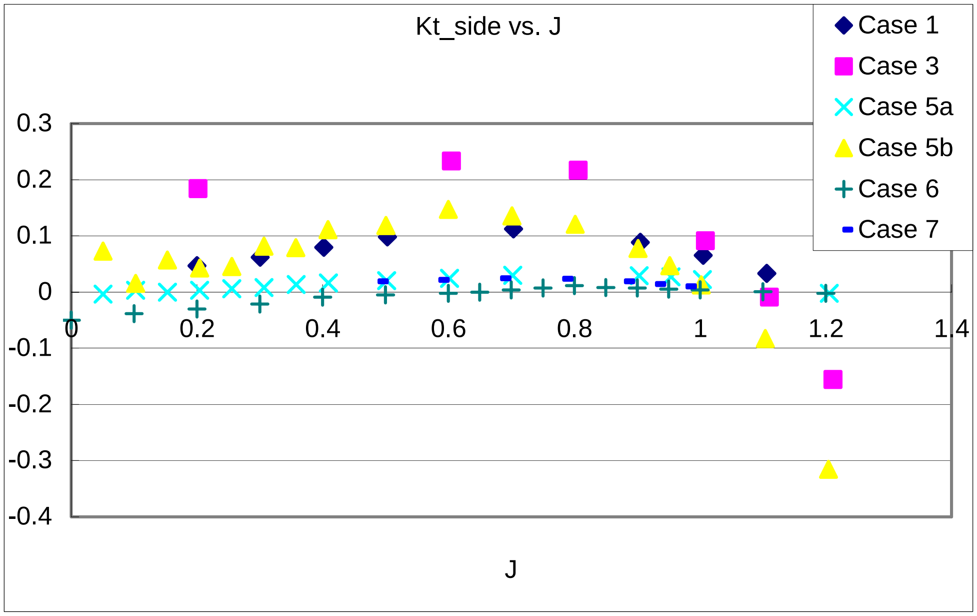

Figure 23: Comparison of K_{T_side} versus J

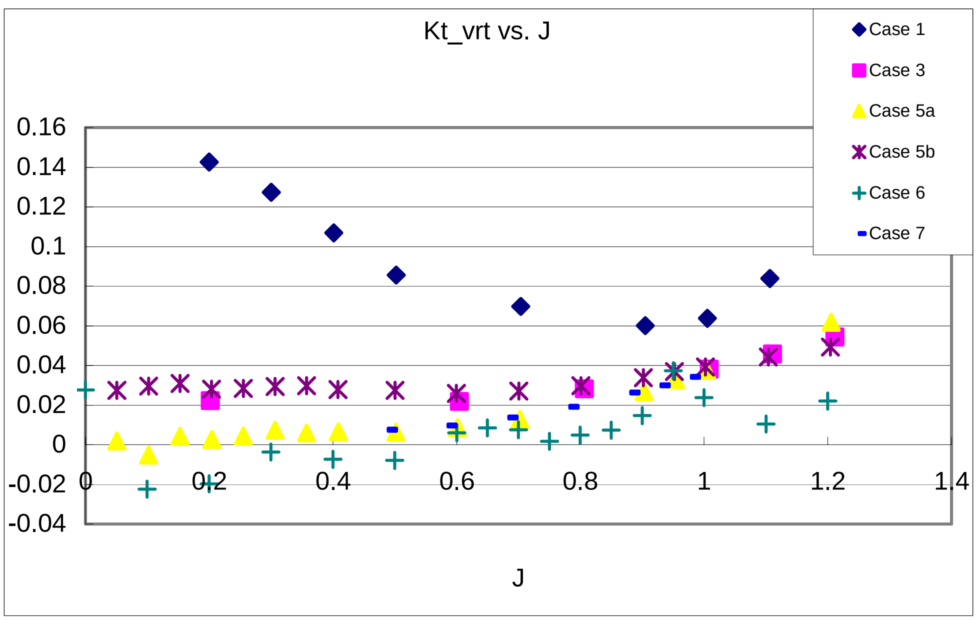

Figure 24: Comparison of K_{T_vrt} versus J

The above two plots are the non-dimensional force coefficients obtained from the global dynamometer. The agreement between the cases isn't very good; however there does seem to be a general trend in each of the plots.

10.0 RECOMMENDATIONS AND CONCLUSIONS

The following is a series of comments on the experiments performed and what steps should be taken in the future to confirm the results obtained.

Overall, the Opens Tests show good results. The tests correspond well with *Principles of Naval Architecture* section on open water tests (page 145).[5] However, since testing on podded propellers is still not as well know as conventional screw propellers, additional testing should be conducted to compare with this data analyzed. Further testing would provide researchers with valuable knowledge about podded propellers as well as providing a solid base to compare future tests.

Further Reynolds effect tests should be conducted on podded propellers to verify if testing on podded propellers can be completed at lower Reynolds Numbers than recommended by ITTC (i.e. less than $1*10^6$).

Testing thus far by NRC has provided the institute with priceless information and knowledge about the performance characteristics of podded propulsors. Further testing would compliment the testing executed so far and would help to further expand the researcher's knowledge. Plans now being made include the building of a model icebreaker hull to which two podded propellers will be fitted and self-propulsion tests will be conducted.

11.0 ACKNOWLEDGMENTS

I would like to express their gratitude to the National Research Council (NRC) and Memorial University of Newfoundland (MUN) for their financial and other support. Thanks are also extended to the staff in both the Ice tank at Institute for Ocean Technology (IOT) and the staff in the MUN Towing tank, without whose assistance the tests would not have been completed. I would also like to thank Dr. Ayhan Akinturk, whose support and guidance throughout my work term has allowed me to expand my engineering knowledge.

12.0 REFERENCES

1) Islam, M., Veitch, B., Bose, N., Liu, P., (2006). "Hydrodynamic Characteristics of Puller Podded Propulsors with Tapered Hub Propellers."
2) National Research Council – Institute for Ocean Technology website. *URL: http://iot-ito.nrc-cnrc.gc.ca/facilities/it_e.html*
3) Oceanic Consulting Corporation Website>Facilities>58m Towing Tank. *URL: http://www.oceaniccorp.com/FacilityDetails.asp?id=2*
4) Bell, J., (2005). "TDC Podded Propeller Drive." Institute for Ocean Technology, NRC: Report No. LM – 2005 – 01
5) MacNeill, A., Taylor, R., Malloy, S., Bose, N., Veitch, B., Randell, T., Liu, P., (2004). "Design of Model Pod Test Unit." Proceedings of the 1st International

Conference on Technological Advances in Podded Propulsion. Newcastle University, UK, April.

6) Jessup, S., Bose, N., Dugué, C., Esposito, P.G., Holtrop, J., Lee, J.T., Mewis, F., Pustoshny, A., Salvatore, F., Shirose, Y., (2003). Proceedings of the 23rd ITTC - Volume 1: The Propulsion Committee, ITTC 23 USA
7) Taylor, R., (2005). “Experimental Investigation of the Influence of Hub Taper Angle on the Performance of Push and Pull Configuration Podded Propellers.” Masters of Engineering Thesis, Memorial University of Newfoundland, Canada.
8) Lewis, E., “Principles of Naval Architecture. Volume 2: Resistance, Propulsion and Vibration.” Jersey City, NJ: SNAME, 1988, pp 145.

APPENDIX A: Calibration Data for Global Dynamometer

A-1: Matrix of coefficients obtained from measured data ([a] matrix)

$a_{1\,1}$	0.000195	$a_{1\,2}$	-0.000002	$a_{1\,3}$	-0.000324	$a_{1\,4}$	-0.014440	$a_{1\,5}$	0.009645	$a_{1\,6}$	0.031223
$a_{2\,1}$	0.000203	$a_{2\,2}$	-0.000092	$a_{2\,3}$	-0.000196	$a_{2\,4}$	-0.018068	$a_{2\,5}$	0.022992	$a_{2\,6}$	0.021882
$a_{3\,1}$	0.000217	$a_{3\,2}$	-0.000170	$a_{3\,3}$	-0.000059	$a_{3\,4}$	-0.014240	$a_{3\,5}$	0.032529	$a_{3\,6}$	0.009249
$a_{4\,1}$	0.000216	$a_{4\,2}$	-0.000239	$a_{4\,3}$	0.000063	$a_{4\,4}$	-0.004432	$a_{4\,5}$	0.036409	$a_{4\,6}$	-0.003590
$a_{5\,1}$	0.020020	$a_{5\,2}$	0.000525	$a_{5\,3}$	-0.000728	$a_{5\,4}$	0.018484	$a_{5\,5}$	0.005772	$a_{5\,6}$	-0.003839
$a_{6\,1}$	0.019963	$a_{6\,2}$	-0.006626	$a_{6\,3}$	0.006172	$a_{6\,4}$	0.015276	$a_{6\,5}$	0.013996	$a_{6\,6}$	-0.008683
$a_{7\,1}$	0.019914	$a_{7\,2}$	-0.012950	$a_{7\,3}$	0.012284	$a_{7\,4}$	0.015068	$a_{7\,5}$	0.021208	$a_{7\,6}$	-0.015380
$a_{8\,1}$	0.019877	$a_{8\,2}$	-0.016941	$a_{8\,3}$	0.016174	$a_{8\,4}$	0.020498	$a_{8\,5}$	0.025721	$a_{8\,6}$	-0.024769
$a_{9\,1}$	0.028344	$a_{9\,2}$	-0.000764	$a_{9\,3}$	0.000544	$a_{9\,4}$	0.034327	$a_{9\,5}$	-0.000415	$a_{9\,6}$	-0.032013
$a_{10\,1}$	0.028194	$a_{10\,2}$	-0.014058	$a_{10\,3}$	0.013405	$a_{10\,4}$	0.034140	$a_{10\,5}$	-0.000459	$a_{10\,6}$	-0.031759
$a_{11\,1}$	0.028117	$a_{11\,2}$	-0.024495	$a_{11\,3}$	0.023504	$a_{11\,4}$	0.032846	$a_{11\,5}$	-0.000490	$a_{11\,6}$	-0.030490
$a_{12\,1}$	0.028090	$a_{12\,2}$	-0.027440	$a_{12\,3}$	0.026370	$a_{12\,4}$	0.033828	$a_{12\,5}$	-0.000502	$a_{12\,6}$	-0.031385
$a_{13\,1}$	-0.019738	$a_{13\,2}$	-0.000275	$a_{13\,3}$	-0.000008	$a_{13\,4}$	-0.038168	$a_{13\,5}$	0.005998	$a_{13\,6}$	0.049189
$a_{14\,1}$	-0.019698	$a_{14\,2}$	0.010259	$a_{14\,3}$	-0.010146	$a_{14\,4}$	-0.040563	$a_{14\,5}$	0.018221	$a_{14\,6}$	0.039655
$a_{15\,1}$	-0.019731	$a_{15\,2}$	0.015956	$a_{15\,3}$	-0.015600	$a_{15\,4}$	-0.035808	$a_{15\,5}$	0.024800	$a_{15\,6}$	0.028816
$a_{16\,1}$	-0.019746	$a_{16\,2}$	0.016634	$a_{16\,3}$	-0.016238	$a_{16\,4}$	-0.026980	$a_{16\,5}$	0.025666	$a_{16\,6}$	0.019722
$a_{17\,1}$	-0.028211	$a_{17\,2}$	-0.000968	$a_{17\,3}$	0.000681	$a_{17\,4}$	-0.034967	$a_{17\,5}$	-0.000371	$a_{17\,6}$	0.032725
$a_{18\,1}$	-0.028311	$a_{18\,2}$	-0.014139	$a_{18\,3}$	0.013359	$a_{18\,4}$	-0.034467	$a_{18\,5}$	-0.000213	$a_{18\,6}$	0.032102
$a_{19\,1}$	-0.028385	$a_{19\,2}$	-0.024052	$a_{19\,3}$	0.022892	$a_{19\,4}$	-0.034383	$a_{19\,5}$	-0.000095	$a_{19\,6}$	0.031908
$a_{20\,1}$	-0.028418	$a_{20\,2}$	-0.027663	$a_{20\,3}$	0.026368	$a_{20\,4}$	-0.034127	$a_{20\,5}$	-0.000048	$a_{20\,6}$	0.031622
$a_{21\,1}$	0.000057	$a_{21\,2}$	-0.000042	$a_{21\,3}$	-0.000181	$a_{21\,4}$	0.023576	$a_{21\,5}$	-0.018298	$a_{21\,6}$	0.022486
$a_{22\,1}$	0.000329	$a_{22\,2}$	0.000155	$a_{22\,3}$	-0.000452	$a_{22\,4}$	-0.023445	$a_{22\,5}$	0.008822	$a_{22\,6}$	0.040493
$a_{23\,1}$	0.000261	$a_{23\,2}$	-0.000034	$a_{23\,3}$	-0.000258	$a_{23\,4}$	-0.029015	$a_{23\,5}$	0.028406	$a_{23\,6}$	0.026982
$a_{24\,1}$	0.000213	$a_{24\,2}$	-0.000215	$a_{24\,3}$	-0.000053	$a_{24\,4}$	-0.023606	$a_{24\,5}$	0.041982	$a_{24\,6}$	0.008951
$a_{25\,1}$	0.000139	$a_{25\,2}$	-0.000339	$a_{25\,3}$	0.000111	$a_{25\,4}$	-0.009037	$a_{25\,5}$	0.047180	$a_{25\,6}$	-0.009609
$a_{26\,1}$	0.000015	$a_{26\,2}$	-0.000066	$a_{26\,3}$	-0.000159	$a_{26\,4}$	0.029226	$a_{26\,5}$	-0.029007	$a_{26\,6}$	0.027356
$a_{27\,1}$	0.020077	$a_{27\,2}$	-0.000223	$a_{27\,3}$	-0.000021	$a_{27\,4}$	0.011221	$a_{27\,5}$	0.006718	$a_{27\,6}$	0.001966
$a_{28\,1}$	0.019971	$a_{28\,2}$	-0.010421	$a_{28\,3}$	0.009842	$a_{28\,4}$	0.007381	$a_{28\,5}$	0.018352	$a_{28\,6}$	-0.005547
$a_{29\,1}$	0.019851	$a_{29\,2}$	-0.018892	$a_{29\,3}$	0.018062	$a_{29\,4}$	0.009533	$a_{29\,5}$	0.027997	$a_{29\,6}$	-0.016769
$a_{30\,1}$	0.019215	$a_{30\,2}$	-0.023189	$a_{30\,3}$	0.022280	$a_{30\,4}$	0.018896	$a_{30\,5}$	0.033847	$a_{30\,6}$	-0.030591
$a_{31\,1}$	0.028280	$a_{31\,2}$	0.000682	$a_{31\,3}$	-0.000855	$a_{31\,4}$	0.033118	$a_{31\,5}$	-0.000177	$a_{31\,6}$	-0.030320
$a_{32\,1}$	0.028144	$a_{32\,2}$	-0.017098	$a_{32\,3}$	0.016404	$a_{32\,4}$	0.032827	$a_{32\,5}$	0.000180	$a_{32\,6}$	-0.030297

$\mathbf{a}_{33\ 1}$	0.028026	$\mathbf{a}_{33\ 2}$	-0.030886	$\mathbf{a}_{33\ 3}$	0.029790	$\mathbf{a}_{33\ 4}$	0.032006	$\mathbf{a}_{33\ 5}$	0.000456	$\mathbf{a}_{33\ 6}$	-0.029720
$\mathbf{a}_{34\ 1}$	0.028040	$\mathbf{a}_{34\ 2}$	-0.029491	$\mathbf{a}_{34\ 3}$	0.028441	$\mathbf{a}_{34\ 4}$	0.032729	$\mathbf{a}_{34\ 5}$	0.000435	$\mathbf{a}_{34\ 6}$	-0.030377
$\mathbf{a}_{35\ 1}$	0.028527	$\mathbf{a}_{35\ 2}$	0.029442	$\mathbf{a}_{35\ 3}$	-0.028780	$\mathbf{a}_{35\ 4}$	0.034110	$\mathbf{a}_{35\ 5}$	-0.000845	$\mathbf{a}_{35\ 6}$	-0.030813
$\mathbf{a}_{36\ 1}$	-0.020171	$\mathbf{a}_{36\ 2}$	0.000493	$\mathbf{a}_{36\ 3}$	-0.000663	$\mathbf{a}_{36\ 4}$	0.007872	$\mathbf{a}_{36\ 5}$	0.007335	$\mathbf{a}_{36\ 6}$	0.004525
$\mathbf{a}_{37\ 1}$	-0.020194	$\mathbf{a}_{37\ 2}$	-0.012607	$\mathbf{a}_{37\ 3}$	0.011942	$\mathbf{a}_{37\ 4}$	0.012466	$\mathbf{a}_{37\ 5}$	-0.007498	$\mathbf{a}_{37\ 6}$	0.014456
$\mathbf{a}_{38\ 1}$	-0.019379	$\mathbf{a}_{38\ 2}$	0.018198	$\mathbf{a}_{38\ 3}$	-0.017706	$\mathbf{a}_{38\ 4}$	-0.037984	$\mathbf{a}_{38\ 5}$	0.027990	$\mathbf{a}_{38\ 6}$	0.028190
$\mathbf{a}_{39\ 1}$	-0.019522	$\mathbf{a}_{39\ 2}$	0.020608	$\mathbf{a}_{39\ 3}$	-0.020022	$\mathbf{a}_{39\ 4}$	-0.028954	$\mathbf{a}_{39\ 5}$	0.030784	$\mathbf{a}_{39\ 6}$	0.016922
$\mathbf{a}_{40\ 1}$	-0.028262	$\mathbf{a}_{40\ 2}$	-0.001292	$\mathbf{a}_{40\ 3}$	0.001015	$\mathbf{a}_{40\ 4}$	-0.033571	$\mathbf{a}_{40\ 5}$	-0.000138	$\mathbf{a}_{40\ 6}$	0.031957
$\mathbf{a}_{41\ 1}$	-0.028133	$\mathbf{a}_{41\ 2}$	0.015615	$\mathbf{a}_{41\ 3}$	-0.015197	$\mathbf{a}_{41\ 4}$	-0.034279	$\mathbf{a}_{41\ 5}$	0.000035	$\mathbf{a}_{41\ 6}$	0.032476
$\mathbf{a}_{42\ 1}$	-0.028425	$\mathbf{a}_{42\ 2}$	-0.026347	$\mathbf{a}_{42\ 3}$	0.025061	$\mathbf{a}_{42\ 4}$	-0.033592	$\mathbf{a}_{42\ 5}$	-0.000433	$\mathbf{a}_{42\ 6}$	0.032207
$\mathbf{a}_{43\ 1}$	-0.028444	$\mathbf{a}_{43\ 2}$	-0.029187	$\mathbf{a}_{43\ 3}$	0.027782	$\mathbf{a}_{43\ 4}$	-0.034047	$\mathbf{a}_{43\ 5}$	-0.000482	$\mathbf{a}_{43\ 6}$	0.032664

Matrix of coefficients obtained from measured data

A-2: Matrix of coefficients obtained from calculated data ([L] matrix)

$f_{1\,1}$	0.000000	$f_{1\,2}$	0.000000	$f_{1\,3}$	0.000000	$f_{1\,4}$	-0.532872	$f_{1\,5}$	0.352286	$f_{1\,6}$	1.180636
$f_{2\,1}$	0.000000	$f_{2\,2}$	0.000000	$f_{2\,3}$	0.000000	$f_{2\,4}$	-0.657899	$f_{2\,5}$	0.831907	$f_{2\,6}$	0.826042
$f_{3\,1}$	0.000000	$f_{3\,2}$	0.000000	$f_{3\,3}$	0.000000	$f_{3\,4}$	-0.519859	$f_{3\,5}$	1.183014	$f_{3\,6}$	0.336895
$f_{4\,1}$	0.000000	$f_{4\,2}$	0.000000	$f_{4\,3}$	0.000000	$f_{4\,4}$	-0.155739	$f_{4\,5}$	1.311528	$f_{4\,6}$	-0.155739
$f_{5\,1}$	0.707135	$f_{5\,2}$	0.000000	$f_{5\,3}$	0.000000	$f_{5\,4}$	0.467414	$f_{5\,5}$	0.249101	$f_{5\,6}$	-0.009380
$f_{6\,1}$	0.707135	$f_{6\,2}$	-0.301072	$f_{6\,3}$	0.301072	$f_{6\,4}$	0.379007	$f_{6\,5}$	0.588241	$f_{6\,6}$	-0.260113
$f_{7\,1}$	0.707135	$f_{7\,2}$	-0.521473	$f_{7\,3}$	0.521473	$f_{7\,4}$	0.476615	$f_{7\,5}$	0.836509	$f_{7\,6}$	-0.605989
$f_{8\,1}$	0.707135	$f_{8\,2}$	-0.602145	$f_{8\,3}$	0.602145	$f_{8\,4}$	0.734085	$f_{8\,5}$	0.927381	$f_{8\,6}$	-0.954331
$f_{9\,1}$	1.000050	$f_{9\,2}$	0.000000	$f_{9\,3}$	0.000000	$f_{9\,4}$	1.193901	$f_{9\,5}$	0.000000	$f_{9\,6}$	-1.193901
$f_{10\,1}$	1.000050	$f_{10\,2}$	-0.425785	$f_{10\,3}$	0.425785	$f_{10\,4}$	1.193901	$f_{10\,5}$	0.000000	$f_{10\,6}$	-1.193901
$f_{11\,1}$	1.000050	$f_{11\,2}$	-0.737481	$f_{11\,3}$	0.737481	$f_{11\,4}$	1.193901	$f_{11\,5}$	0.000000	$f_{11\,6}$	-1.193901
$f_{12\,1}$	1.000050	$f_{12\,2}$	-0.851093	$f_{12\,3}$	0.851093	$f_{12\,4}$	1.193901	$f_{12\,5}$	0.000000	$f_{12\,6}$	-1.193901
$f_{13\,1}$	-0.707135	$f_{13\,2}$	0.000000	$f_{13\,3}$	0.000000	$f_{13\,4}$	-1.221001	$f_{13\,5}$	0.249101	$f_{13\,6}$	1.679035
$f_{14\,1}$	-0.707135	$f_{14\,2}$	0.301072	$f_{14\,3}$	-0.301072	$f_{14\,4}$	-1.309408	$f_{14\,5}$	0.588241	$f_{14\,6}$	1.428302
$f_{15\,1}$	-0.707135	$f_{15\,2}$	0.521473	$f_{15\,3}$	-0.521473	$f_{15\,4}$	-1.211800	$f_{15\,5}$	0.836509	$f_{15\,6}$	1.082426
$f_{16\,1}$	-0.707135	$f_{16\,2}$	0.602145	$f_{16\,3}$	-0.602145	$f_{16\,4}$	-0.954331	$f_{16\,5}$	0.927381	$f_{16\,6}$	0.734085
$f_{17\,1}$	-1.000050	$f_{17\,2}$	0.000000	$f_{17\,3}$	0.000000	$f_{17\,4}$	-1.193901	$f_{17\,5}$	0.000000	$f_{17\,6}$	1.193901
$f_{18\,1}$	-1.000050	$f_{18\,2}$	-0.425785	$f_{18\,3}$	0.425785	$f_{18\,4}$	-1.193901	$f_{18\,5}$	0.000000	$f_{18\,6}$	1.193901
$f_{19\,1}$	-1.000050	$f_{19\,2}$	-0.737481	$f_{19\,3}$	0.737481	$f_{19\,4}$	-1.193901	$f_{19\,5}$	0.000000	$f_{19\,6}$	1.193901
$f_{20\,1}$	-1.000050	$f_{20\,2}$	-0.851570	$f_{20\,3}$	0.851570	$f_{20\,4}$	-1.193901	$f_{20\,5}$	0.000000	$f_{20\,6}$	1.193901
$f_{21\,1}$	0.000000	$f_{21\,2}$	0.000000	$f_{21\,3}$	0.000000	$f_{21\,4}$	0.803503	$f_{21\,5}$	-0.606956	$f_{21\,6}$	0.803503
$f_{22\,1}$	0.000000	$f_{22\,2}$	0.000000	$f_{22\,3}$	0.000000	$f_{22\,4}$	-0.895679	$f_{22\,5}$	0.352286	$f_{22\,6}$	1.543442
$f_{23\,1}$	0.000000	$f_{23\,2}$	0.000000	$f_{23\,3}$	0.000000	$f_{23\,4}$	-1.073651	$f_{23\,5}$	1.035011	$f_{23\,6}$	1.038690
$f_{24\,1}$	0.000000	$f_{24\,2}$	0.000000	$f_{24\,3}$	0.000000	$f_{24\,4}$	-0.877155	$f_{24\,5}$	1.534800	$f_{24\,6}$	0.342405
$f_{25\,1}$	0.000000	$f_{25\,2}$	0.000000	$f_{25\,3}$	0.000000	$f_{25\,4}$	-0.358843	$f_{25\,5}$	1.717735	$f_{25\,6}$	-0.358843
$f_{26\,1}$	0.000000	$f_{26\,2}$	0.000000	$f_{26\,3}$	0.000000	$f_{26\,4}$	1.006606	$f_{26\,5}$	-1.013163	$f_{26\,6}$	1.006606
$f_{27\,1}$	0.707135	$f_{27\,2}$	0.000000	$f_{27\,3}$	0.000000	$f_{27\,4}$	0.268720	$f_{27\,5}$	0.249101	$f_{27\,6}$	0.189314
$f_{28\,1}$	0.707135	$f_{28\,2}$	-0.428567	$f_{28\,3}$	0.428567	$f_{28\,4}$	0.085029	$f_{28\,5}$	0.731856	$f_{28\,6}$	-0.109750
$f_{29\,1}$	0.707135	$f_{29\,2}$	-0.742299	$f_{29\,3}$	0.742299	$f_{29\,4}$	0.223971	$f_{29\,5}$	1.085257	$f_{29\,6}$	-0.602093
$f_{30\,1}$	0.707135	$f_{30\,2}$	-0.857133	$f_{30\,3}$	0.857133	$f_{30\,4}$	0.590470	$f_{30\,5}$	1.214610	$f_{30\,6}$	-1.097945
$f_{31\,1}$	1.000050	$f_{31\,2}$	0.000000	$f_{31\,3}$	0.000000	$f_{31\,4}$	1.193901	$f_{31\,5}$	0.000000	$f_{31\,6}$	-1.193901
$f_{32\,1}$	1.000050	$f_{32\,2}$	-0.606091	$f_{32\,3}$	0.606091	$f_{32\,4}$	1.193901	$f_{32\,5}$	0.000000	$f_{32\,6}$	-1.193901

$f_{33\ 1}$	1.000050	$f_{33\ 2}$	-1.128514	$f_{33\ 3}$	1.128514	$f_{33\ 4}$	1.193901	$f_{33\ 5}$	0.000000	$f_{33\ 6}$	-1.193901
$f_{34\ 1}$	1.000050	$f_{34\ 2}$	-1.115207	$f_{34\ 3}$	1.115207	$f_{34\ 4}$	1.193901	$f_{34\ 5}$	0.000000	$f_{34\ 6}$	-1.193901
$f_{35\ 1}$	1.000050	$f_{35\ 2}$	1.115207	$f_{35\ 3}$	-1.115207	$f_{35\ 4}$	1.193901	$f_{35\ 5}$	0.000000	$f_{35\ 6}$	-1.193901
$f_{36\ 1}$	-0.707135	$f_{36\ 2}$	0.000000	$f_{36\ 3}$	0.000000	$f_{36\ 4}$	0.210873	$f_{36\ 5}$	0.249101	$f_{36\ 6}$	0.247160
$f_{37\ 1}$	-0.707135	$f_{37\ 2}$	-0.428567	$f_{37\ 3}$	0.428567	$f_{37\ 4}$	0.373005	$f_{37\ 5}$	-0.233653	$f_{37\ 6}$	0.567784
$f_{38\ 1}$	-0.707135	$f_{38\ 2}$	0.682915	$f_{38\ 3}$	-0.682915	$f_{38\ 4}$	-1.396504	$f_{38\ 5}$	1.018365	$f_{38\ 6}$	1.085275
$f_{39\ 1}$	-0.707135	$f_{39\ 2}$	0.857133	$f_{39\ 3}$	-0.857133	$f_{39\ 4}$	-1.097945	$f_{39\ 5}$	1.214610	$f_{39\ 6}$	0.590470
$f_{40\ 1}$	-1.000050	$f_{40\ 2}$	0.000000	$f_{40\ 3}$	0.000000	$f_{40\ 4}$	-1.193901	$f_{40\ 5}$	0.000000	$f_{40\ 6}$	1.193901
$f_{41\ 1}$	-1.000050	$f_{41\ 2}$	0.606091	$f_{41\ 3}$	-0.606091	$f_{41\ 4}$	-1.193901	$f_{41\ 5}$	0.000000	$f_{41\ 6}$	1.193901
$f_{42\ 1}$	-1.000050	$f_{42\ 2}$	-1.049780	$f_{42\ 3}$	1.049780	$f_{42\ 4}$	-1.193901	$f_{42\ 5}$	0.000000	$f_{42\ 6}$	1.193901
$f_{43\ 1}$	-1.000050	$f_{43\ 2}$	-1.212181	$f_{43\ 3}$	1.212181	$f_{43\ 4}$	-1.193901	$f_{43\ 5}$	0.000000	$f_{43\ 6}$	1.193901

Matrix of coefficients obtained from calculated data

APPENDIX B: Calibration Data for Thrust and Torque Load Cells

B-1: Matrix of coefficients obtained from measured data

$\mathbf{a}_{1\,1}$	0.008517	$\mathbf{a}_{1\,2}$	4.799733
$\mathbf{a}_{2\,1}$	-0.010700	$\mathbf{a}_{2\,2}$	-4.780244
$\mathbf{a}_{3\,1}$	-0.000339	$\mathbf{a}_{3\,2}$	6.713952
$\mathbf{a}_{4\,1}$	-0.000337	$\mathbf{a}_{4\,2}$	-6.676090
$\mathbf{a}_{5\,1}$	0.014632	$\mathbf{a}_{5\,2}$	0.001815
$\mathbf{a}_{6\,1}$	-0.015982	$\mathbf{a}_{6\,2}$	-0.000193
$\mathbf{a}_{7\,1}$	-0.016897	$\mathbf{a}_{7\,2}$	-0.002923
$\mathbf{a}_{8\,1}$	0.014210	$\mathbf{a}_{8\,2}$	-0.003161

Matrix of coefficients obtained from measured data

B-2: Matrix of coefficients obtained from calculated data

$\mathbf{f}_{1\,1}$	0.707100	$\mathbf{f}_{1\,2}$	0.053881
$\mathbf{f}_{2\,1}$	-0.707100	$\mathbf{f}_{2\,2}$	-0.053881
$\mathbf{f}_{3\,1}$	0.000000	$\mathbf{f}_{3\,2}$	0.076200
$\mathbf{f}_{4\,1}$	0.000000	$\mathbf{f}_{4\,2}$	-0.076200
$\mathbf{f}_{5\,1}$	1.000000	$\mathbf{f}_{5\,2}$	0.000000
$\mathbf{f}_{6\,1}$	-1.000000	$\mathbf{f}_{6\,2}$	0.000000
$\mathbf{f}_{7\,1}$	-1.000000	$\mathbf{f}_{7\,2}$	0.000000
$\mathbf{f}_{8\,1}$	1.000000	$\mathbf{f}_{8\,2}$	0.000000

Matrix of coefficients obtained from calculated data

APPENDIX C: Data Acquisition System Channel Set-up for NRC-IOT Tests

C-1: Channel Set-up

DAS PLAN

Project Name: T.C. Azipod | **Project Number: 42_2085_16**

Signal Conditioner: Custom IOTech | **Date: 9-Dec-05**

Sampling Rate: 5Khz | **Generated by: James E. Williams**

GDAC	CHAN #	IOTech#	DESCRIPTION/DEVICE	SERIAL #	BAR-CODE	RANGE	FILTER	EXC. Volts	Gain	Offset	Cal. Factor
1	**0**	**Ch00-0-0**	Pod 1, Fxa, Port	E50407	200203	250 lbf	1Khz	10	150		
2	**1**	**Ch00-0-1**	Pod 1, Fy1a	E50185	200201	250 lbf	1Khz	10	150		
3	**2**	**Ch00-0-2**	Pod 1, Fy2a	E50406	200207	250 lbf	1Khz	10	150		
4	**3**	**Ch00-0-3**	Pod 1, Fz1a	E50400	200204	250 lbf	1Khz	10	150		
5	**4**	**Ch00-0-4**	Pod 1, Fz2a	E50204	200205	250 lbf	1Khz	10	150		
6	**5**	**Ch00-0-5**	Pod 1, FZ3a	E50184	200208	250 lbf	1Khz	10	150		
7	**6**	**Ch00-0-6**	spare				1Khz	5			
8	**7**	**Ch00-0-7**	spare				1Khz	5			
9	**8**	**Ch00-1-0**	Pod 2, Fxb, Starboard	E50413	200206	250 lbf	1Khz	10	150		
10	**9**	**Ch00-1-1**	Pod 2, Fy1b	E50384	200198	250 lbf	1Khz	10	150		
11	**10**	**Ch00-1-2**	Pod 2, Fy2b	E50170	200199	250 lbf	1Khz	10	150		
12	**11**	**Ch00-1-3**	Pod 2, Fz1b	E50417	200200	250 lbf	1Khz	10	150		
13	**12**	**Ch00-1-4**	Pod 2, Fz2b	E50403	200197	250 lbf	1Khz	10	150		
14	**13**	**Ch00-1-5**	Pod 2, FZ3b	E50194	200202	250 lbf	1Khz	10	150		
15	**14**	**Ch00-1-6**	spare				1Khz	5			
16	**15**	**Ch00-1-7**	spare				1Khz	5			
17	**16**	**Ch01-0-0**	Pod 1, Thrust, Ta	21316		50 lbf	1Khz	N/A	4.4		
18	**17**	**Ch01-0-1**	Pod 1, Torque, Qa	A			1Khz	N/A	5.39		
19	**18**	**Ch01-0-2**	Pod 1 RPS				1Khz	N/A	?		

20	**19**	**Ch01-0-3**					1Khz	N/A	
21	**20**	**Ch01-1-0**	Pod 2 Thrust ,Tb	21320		50 lbf	1Khz	N/A	3.45
22	**21**	**Ch01-1-1**	Pod 2, Torque,Qb	B			1Khz	N/A	5.39
23	**22**	**Ch01-1-2**	Pod 2 RPS				1Khz	N/A	?
24	**23**	**Ch01-1-3**	DAS Sync signal				1Khz	N/A	
25		**RS232 Ch1**	Pod 1 Azimithing angle			360 degs	na		
26		**RS232 Ch2**	Pod 2 Azumithing angle			360 degs	na		
27		**RS232 Ch3**	Pod 1 Blade Angle						
28		**RS232 Ch4**	Pod 2 Blade Angle						
29		**RS232 Ch5**	Pod 1 RPS						
30		**RS232 Ch6**	Pod 2 RPS						
30		**RS232 Ch7**	DAS Sync signal						
			Industrial pc:	Telem # : PC004026		IP #		Barcode:	
			Daq book:	S/N:		Barcode:			

APPENDIX D: Results for Case One

D-1: Reynolds Number Effect Tests

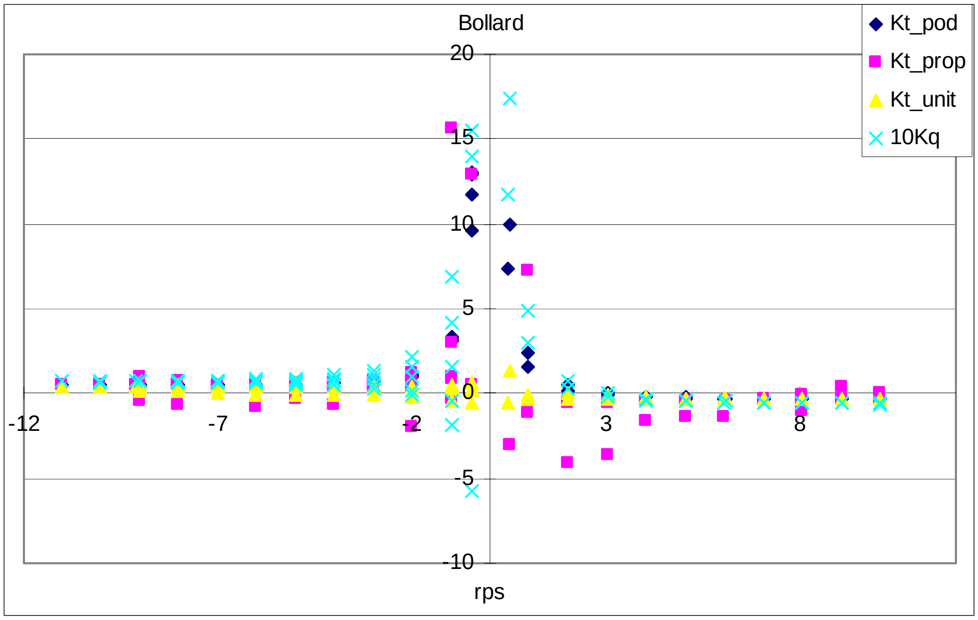

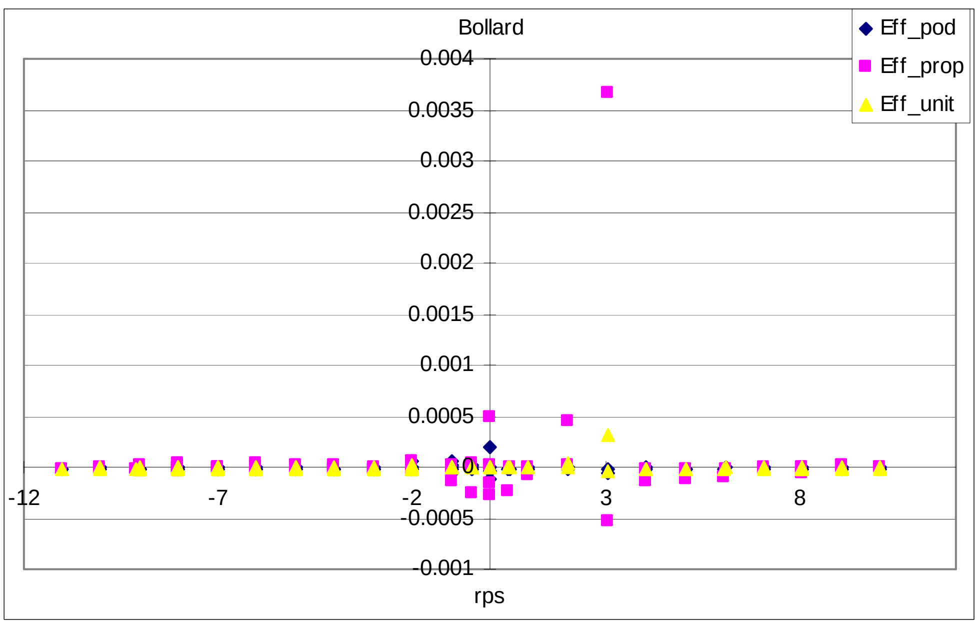

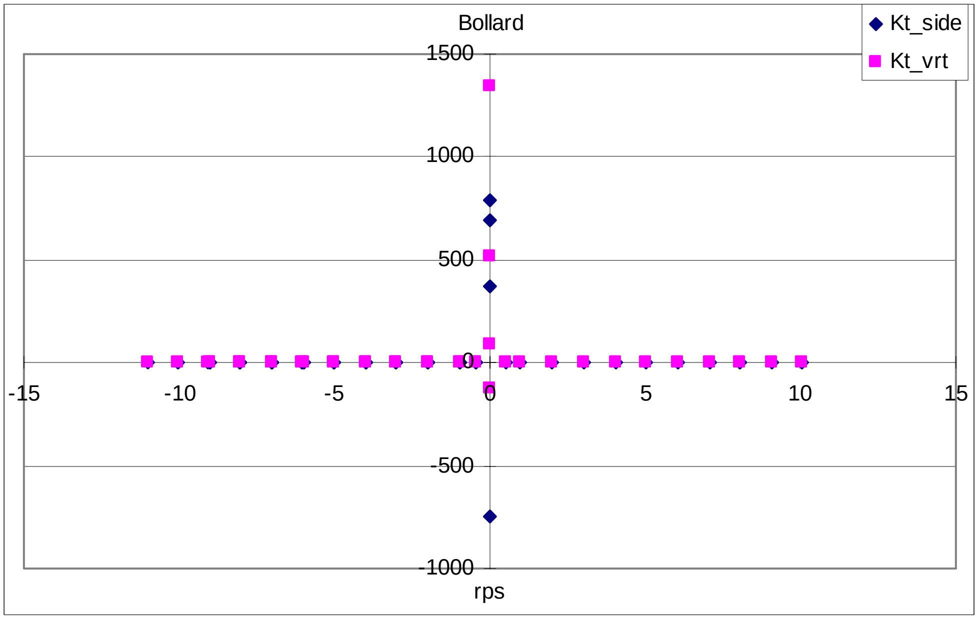
Bollard
Kt_side
Kt_vrt
1500
1000
500
0
-500
-1000
-15
-10
-5
0
5
10
15
rps

D-2: Opens Tests Results

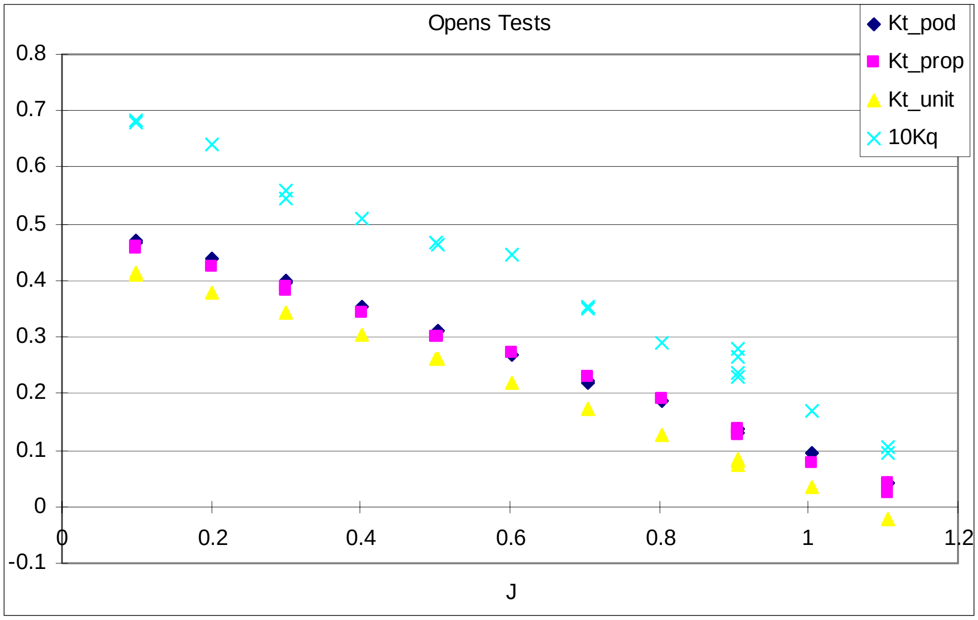

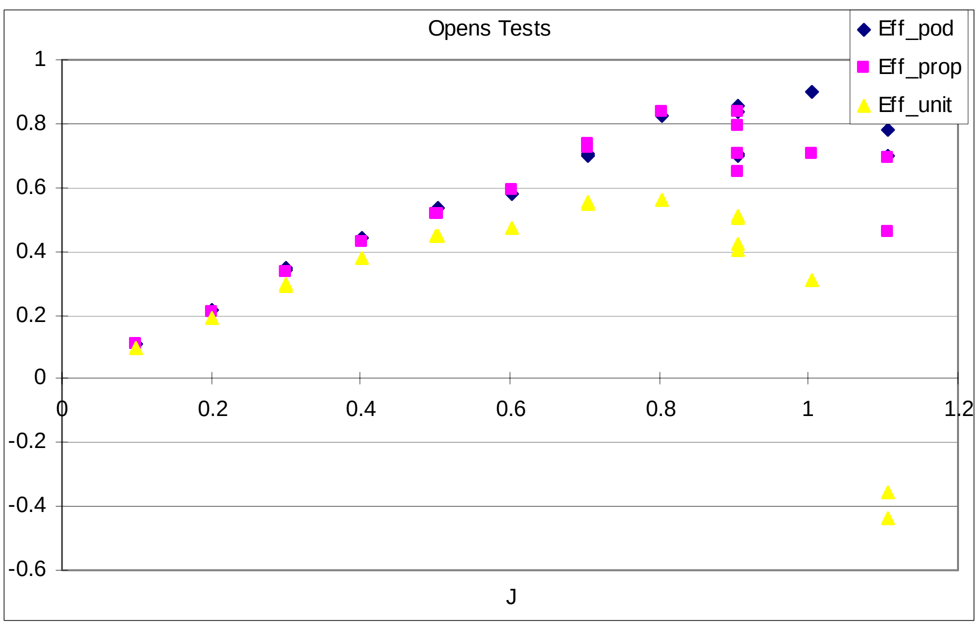

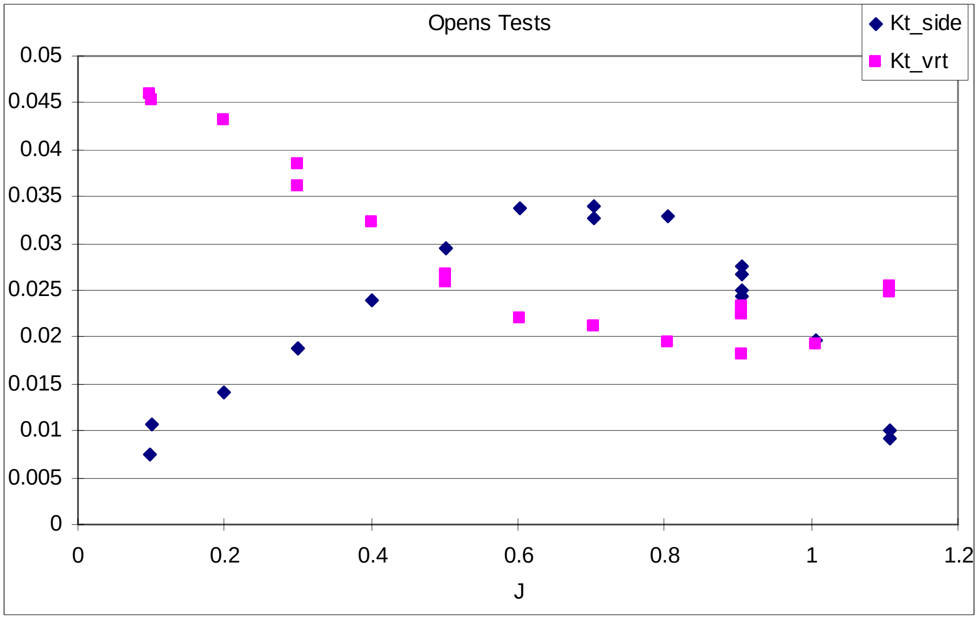
Opens Tests
Kt_side
Kt_vrt
0.05
0.045
0.04
0.035
0.03
0.025
0.02
0.015
0.01
0.005
0
0
0.2
0.4
0.6
0.8
1
1.2
J

D-3: Third Quadrant Runs

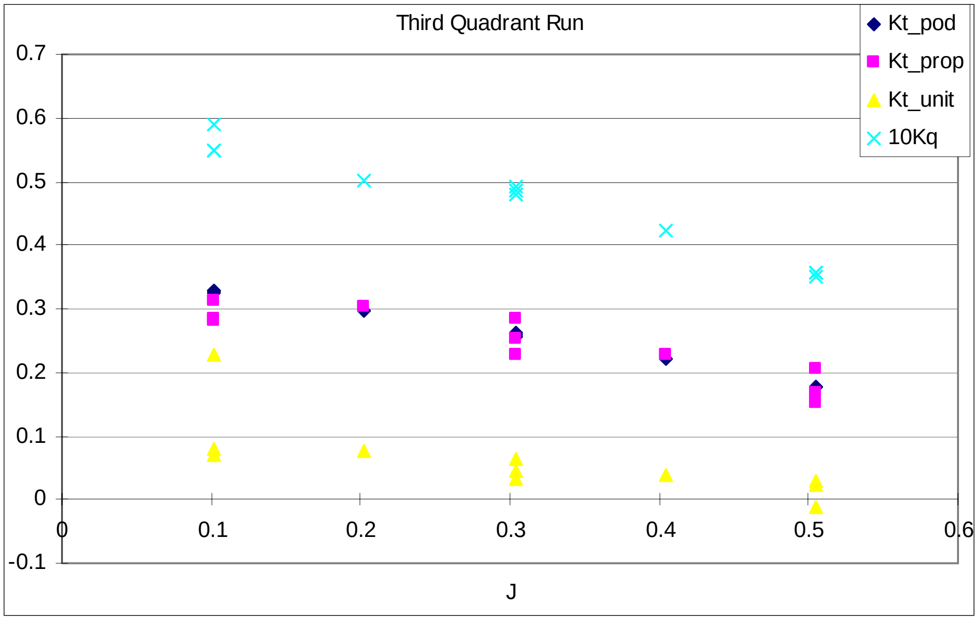

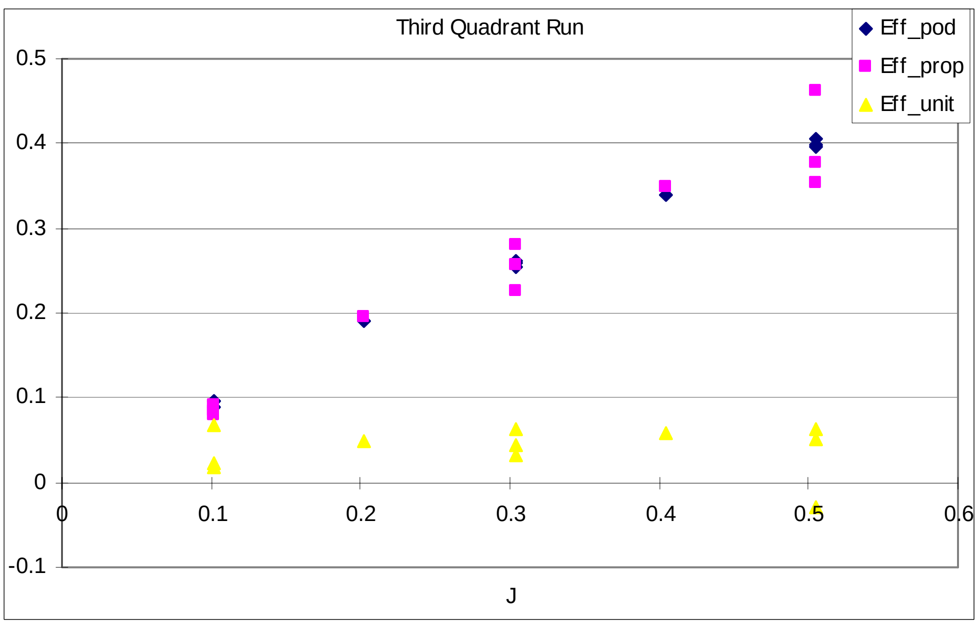

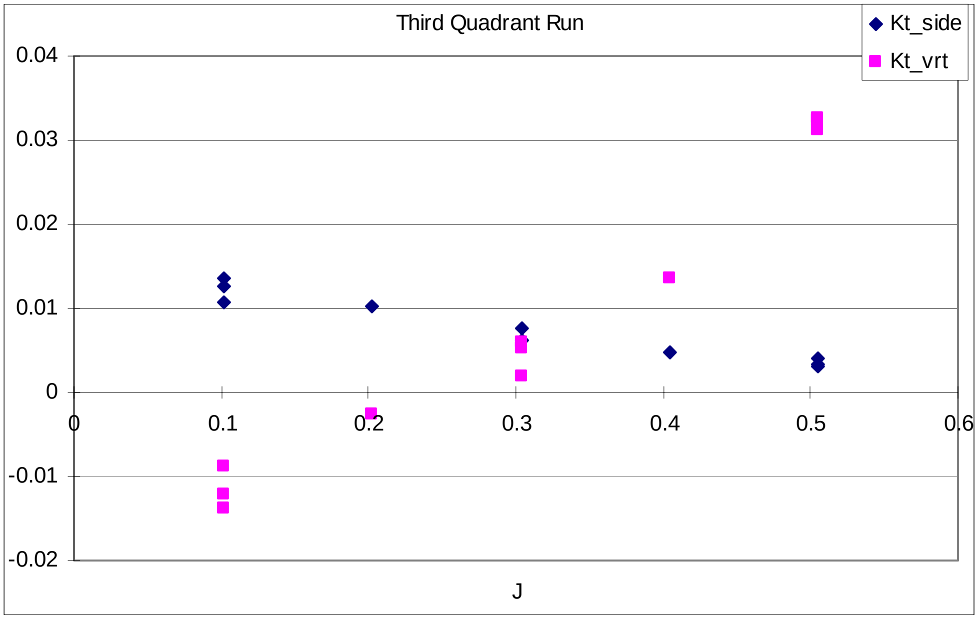
Third Quadrant Run
Kt_side
Kt_vrt
0.04
0.03
0.02
0.01
0
-0.01
-0.02
0
0.1
0.2
0.3
0.4
0.5
0.6
J

D-4: Oblique Flow Tests

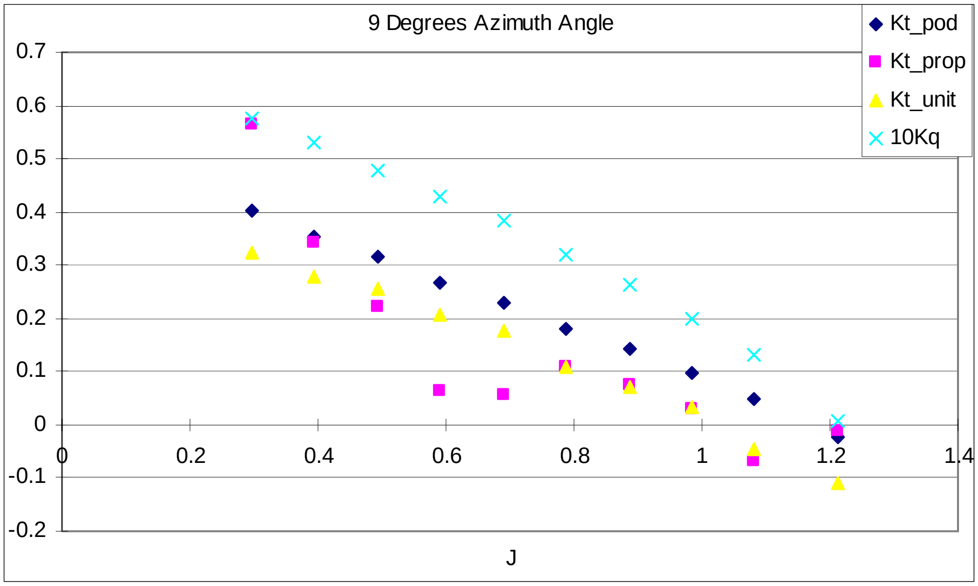

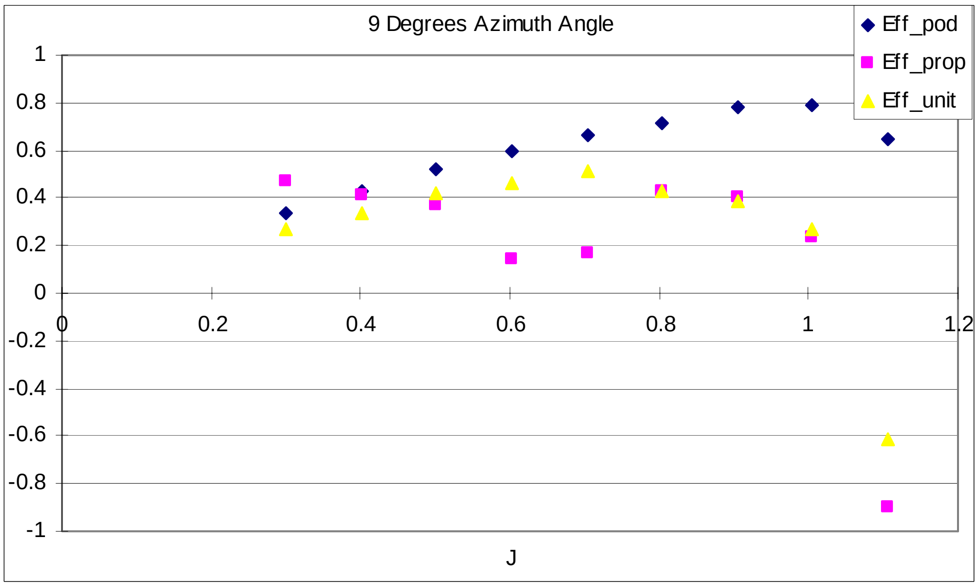

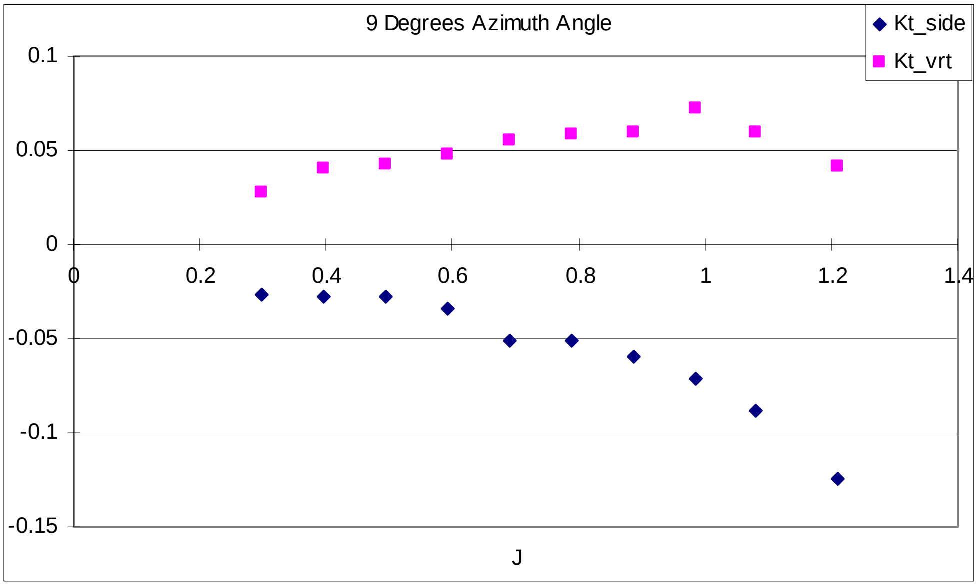
9 Degrees Azimuth Angle
Kt_side
Kt_vrt
0.1
0.05
0
-0.05
-0.1
-0.15
0
0.2
0.4
0.6
0.8
1
1.2
1.4
J

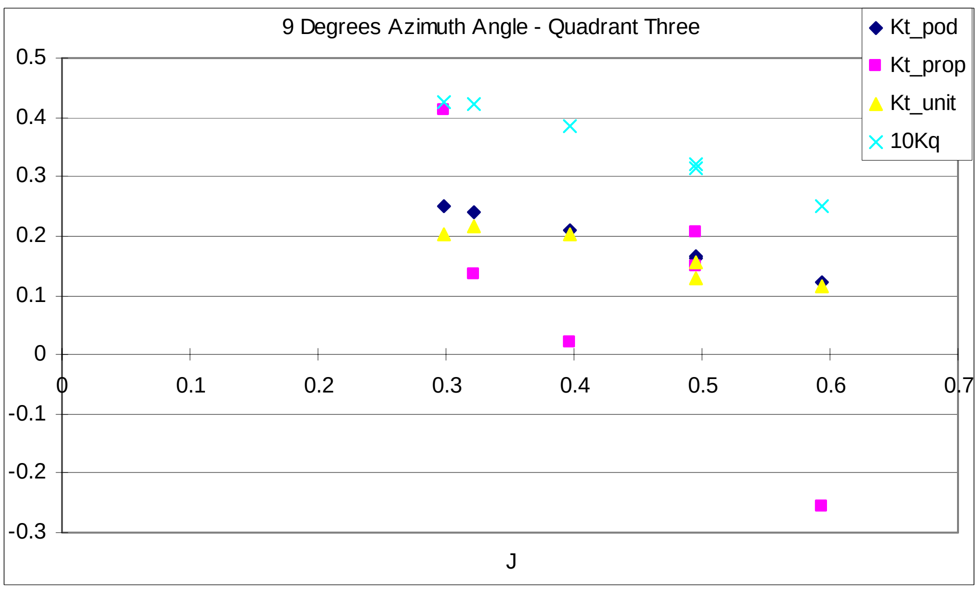
9 Degrees Azimuth Angle - Quadrant Three
Kt_pod
Kt_prop
Kt_unit
10Kq
0.5
0.4
0.3
0.2
0.1
0
-0.1
-0.2
-0.3
0
0.1
0.2
0.3
0.4
0.5
0.6
0.7
J

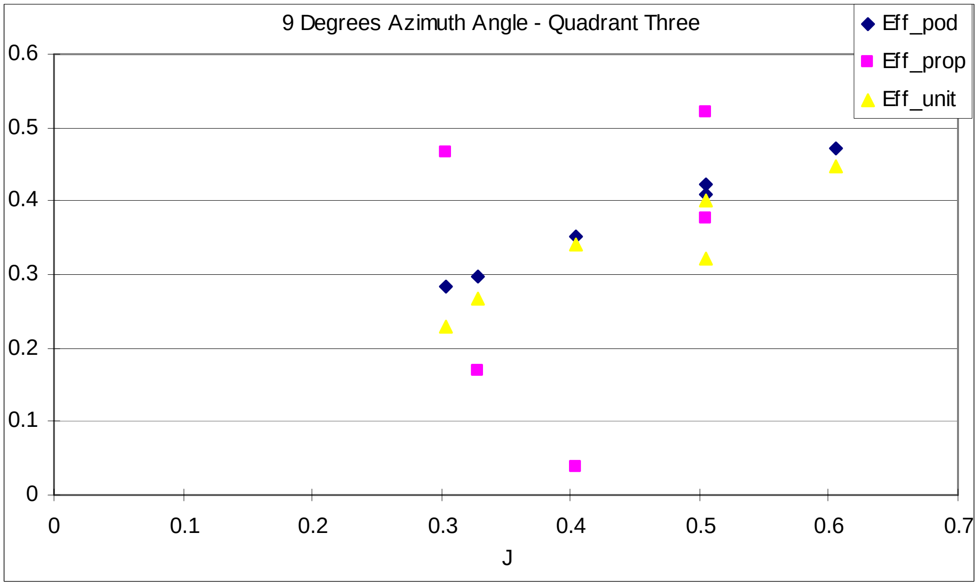
9 Degrees Azimuth Angle - Quadrant Three
Eff_pod
Eff_prop
Eff_unit
0.6
0.5
0.4
0.3
0.2
0.1
0
0
0.1
0.2
0.3
0.4
0.5
0.6
0.7
J

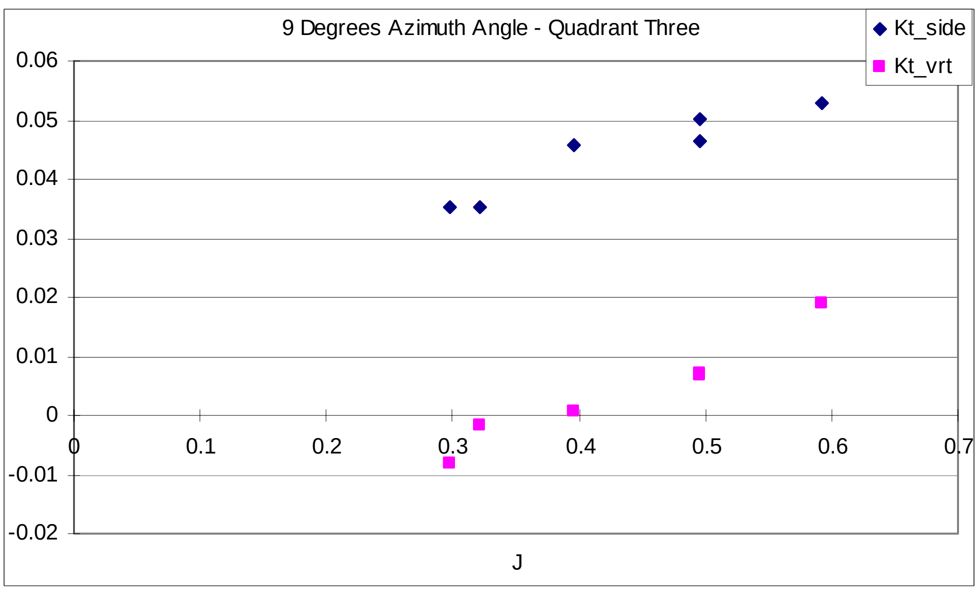
9 Degrees Azimuth Angle - Quadrant Three
Kt_side
Kt_vrt
0.06
0.05
0.04
0.03
0.02
0.01
0
-0.01
-0.02
0
0.1
0.2
0.3
0.4
0.5
0.6
0.7
J

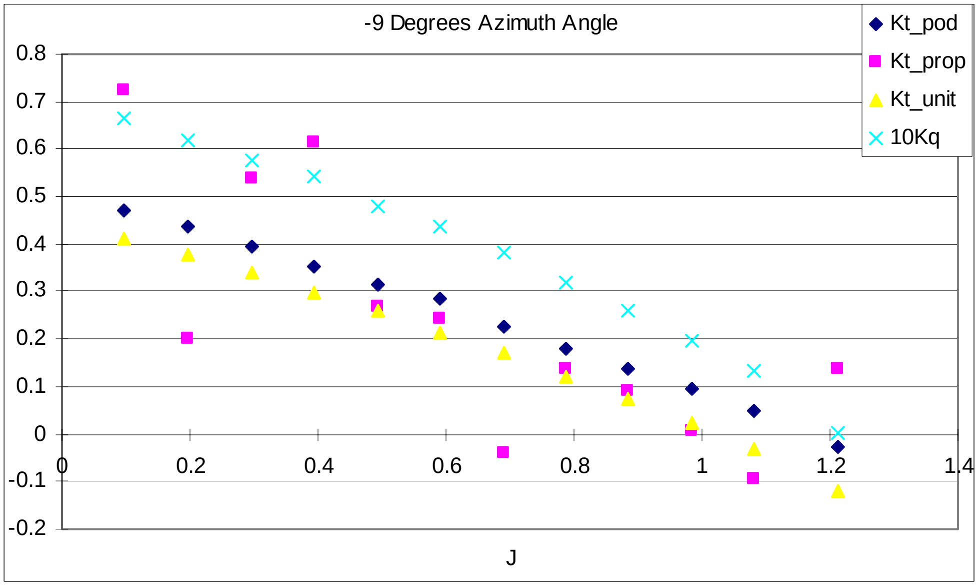
-9 Degrees Azimuth Angle
Kt_pod
Kt_prop
Kt_unit
10Kq
0.8
0.7
0.6
0.5
0.4
0.3
0.2
0.1
0
-0.1
-0.2
0
0.2
0.4
0.6
0.8
1
1.2
1.4
J

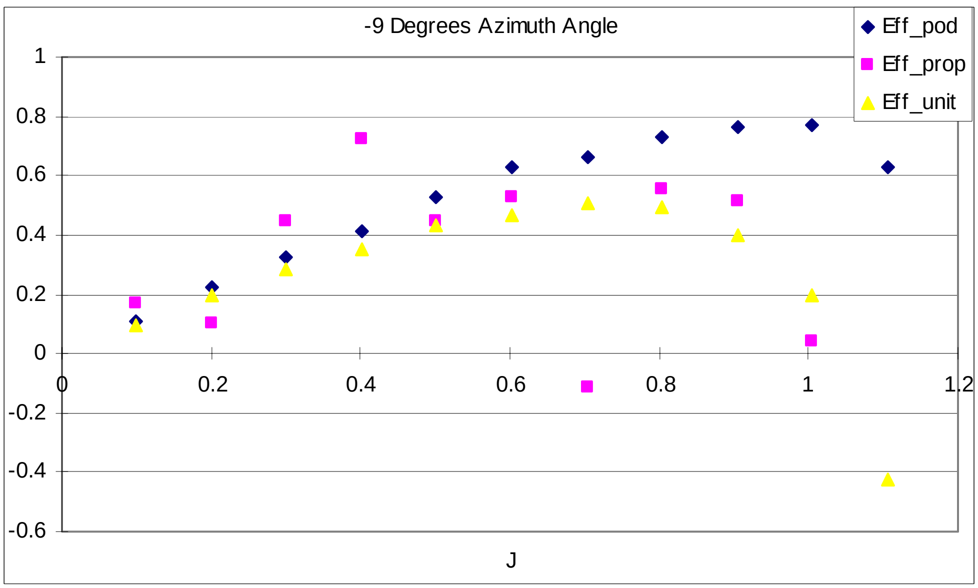
-9 Degrees Azimuth Angle
Eff_pod
Eff_prop
Eff_unit
1
0.8
0.6
0.4
0.2
0
-0.2
-0.4
-0.6
0
0.2
0.4
0.6
0.8
1
1.2
J

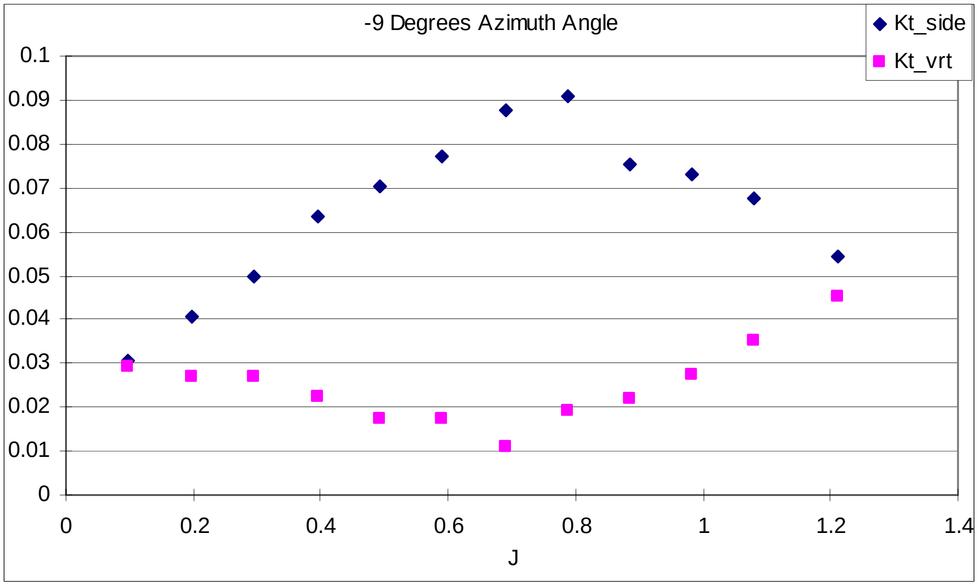
-9 Degrees Azimuth Angle
Kt_side
Kt_vrt
0.1
0.09
0.08
0.07
0.06
0.05
0.04
0.03
0.02
0.01
0
0
0.2
0.4
0.6
0.8
1
1.2
1.4
J

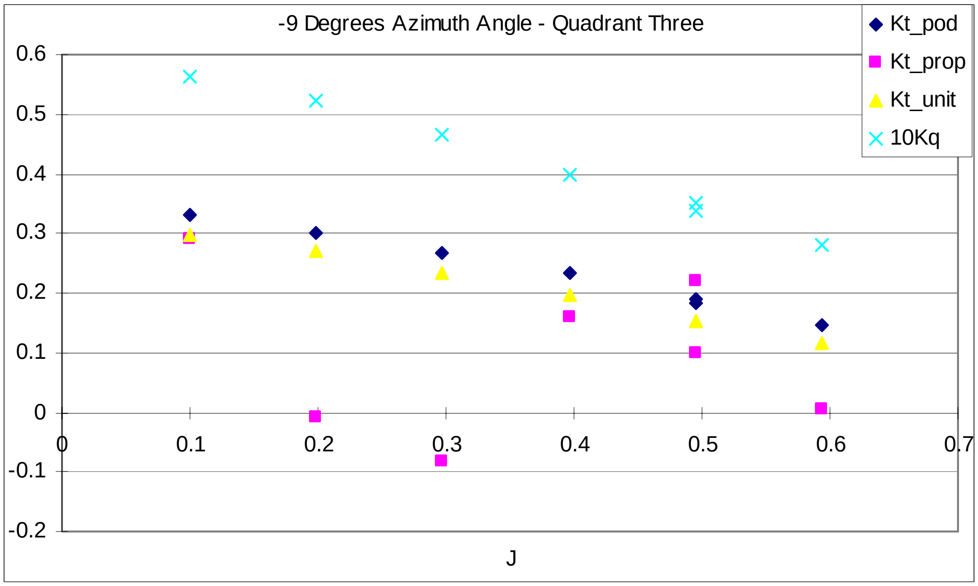
-9 Degrees Azimuth Angle - Quadrant Three
Kt_pod
Kt_prop
Kt_unit
10Kq
0.6
0.5
0.4
0.3
0.2
0.1
0
-0.1
-0.2
0
0.1
0.2
0.3
0.4
0.5
0.6
0.7
J

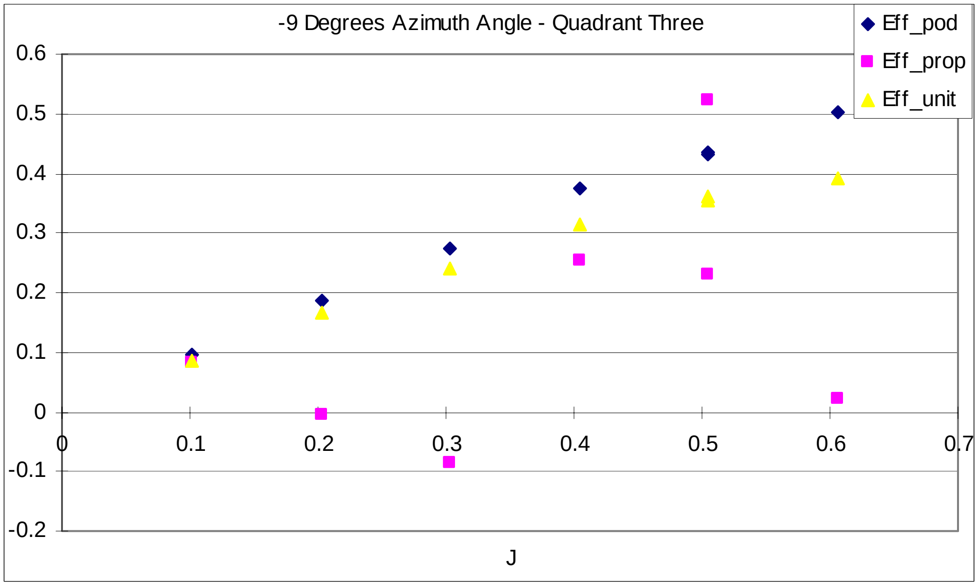

-9 Degrees Azimuth Angle - Quadrant Three
Eff_pod
Eff_prop
Eff_unit
0.6
0.5
0.4
0.3
0.2
0.1
0
-0.1
-0.2
0
0.1
0.2
0.3
0.4
0.5
0.6
0.7
J

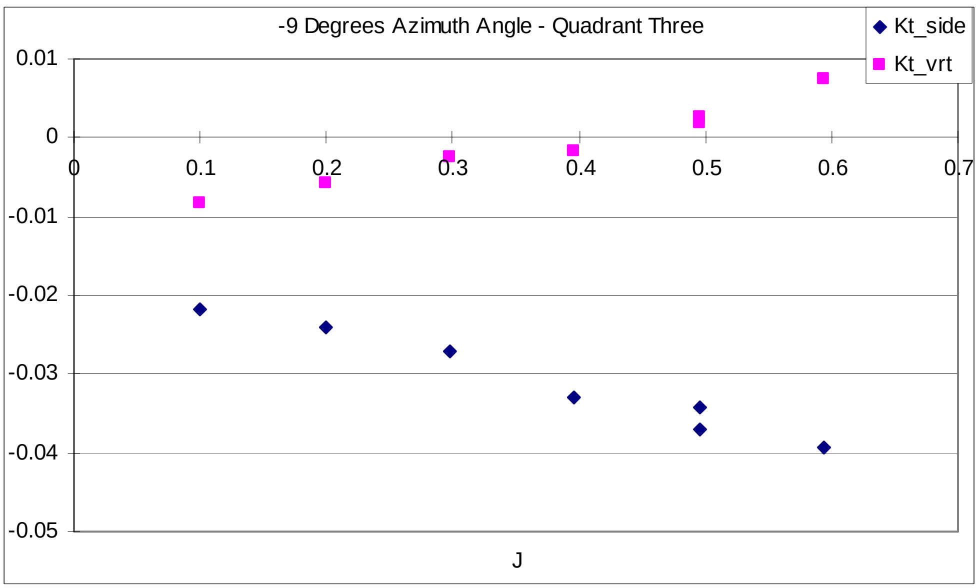

-9 Degrees Azimuth Angle - Quadrant Three
Kt_side
Kt_vrt
0.01
0
-0.01
-0.02
-0.03
-0.04
-0.05
0
0.1
0.2
0.3
0.4
0.5
0.6
0.7
J

APPENDIX E: Results for Case Three

E-1: Reynolds Number Effect Tests

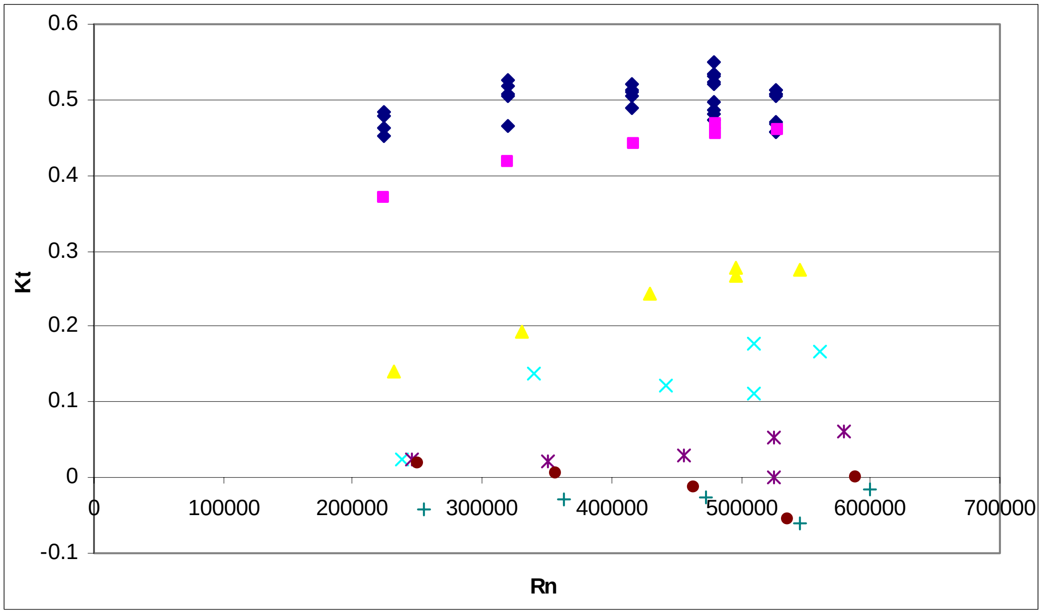

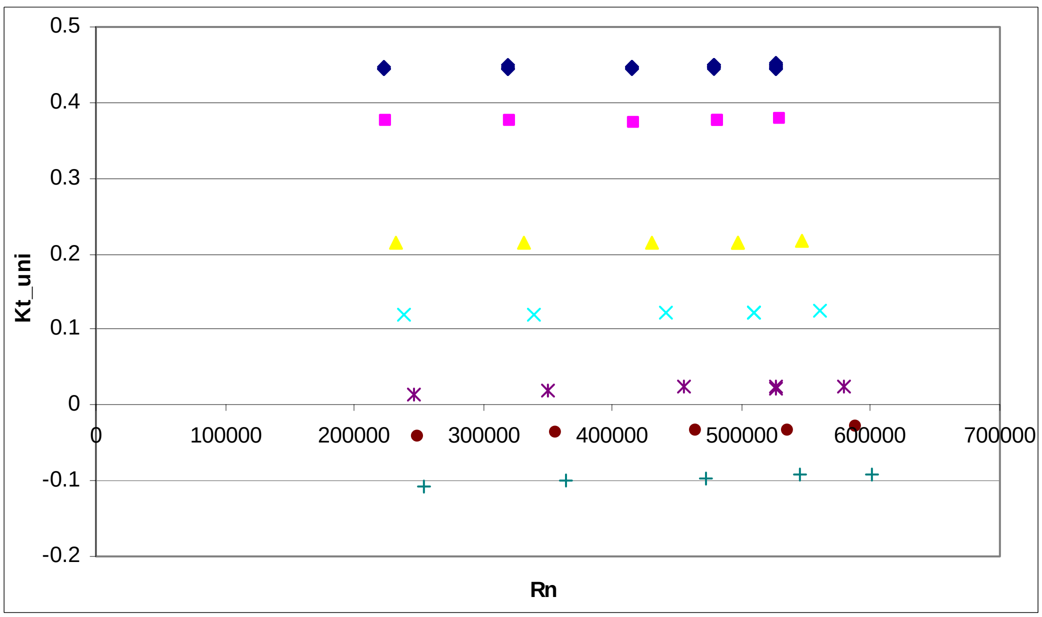

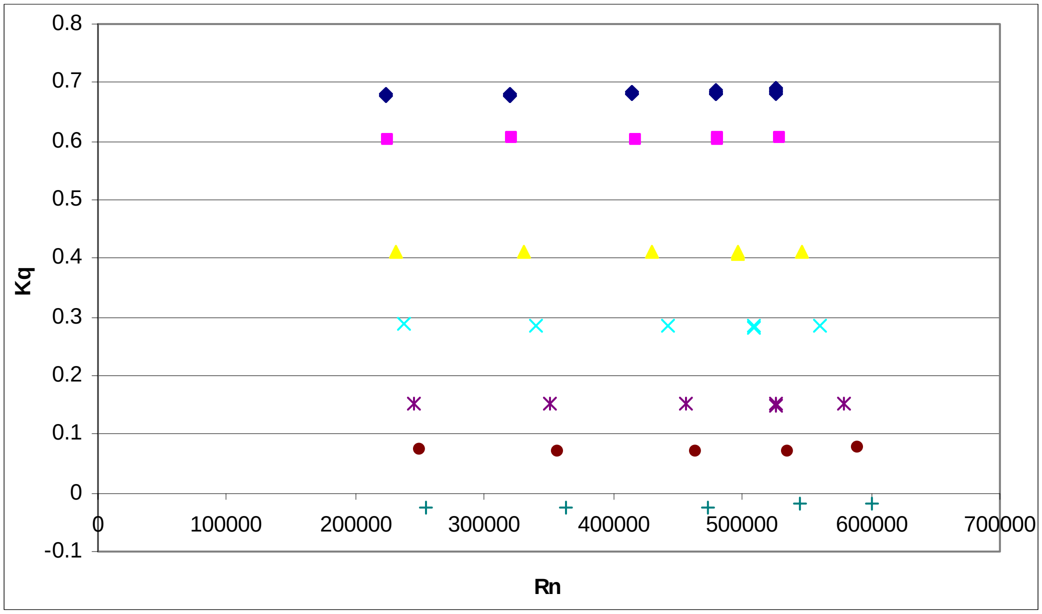
Kq
Rn
0.8
0.7
0.6
0.5
0.4
0.3
0.2
0.1
0
-0.1
0
100000
200000
300000
400000
500000
600000
700000

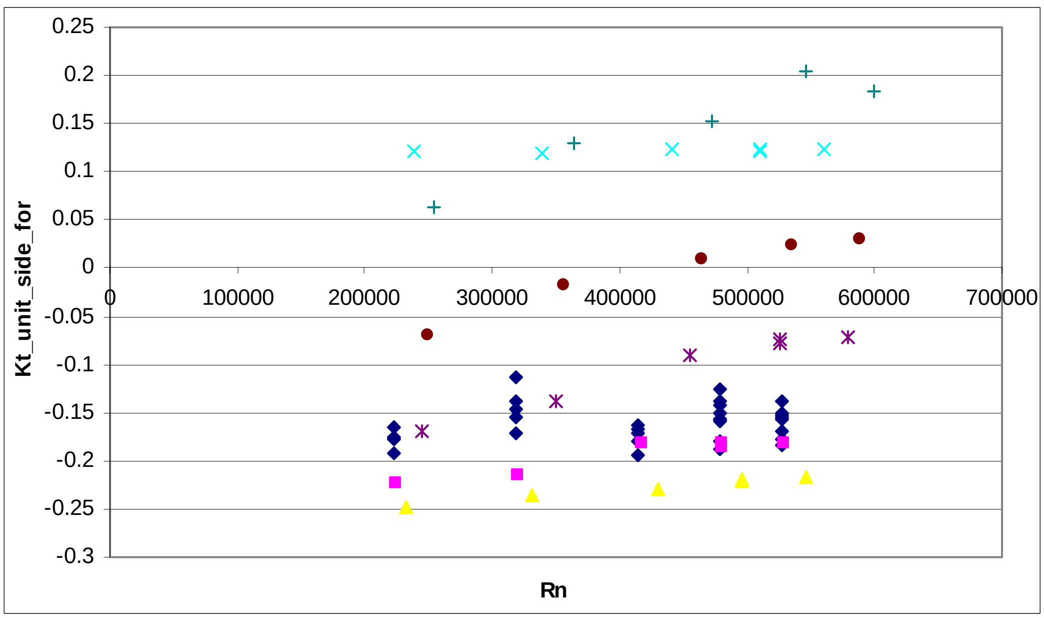
Kt_unit_side_for
Rn
0.25
0.2
0.15
0.1
0.05
0
-0.05
-0.1
-0.15
-0.2
-0.25
-0.3
0
100000
200000
300000
400000
500000
600000
700000

E-2: Air Friction Tests

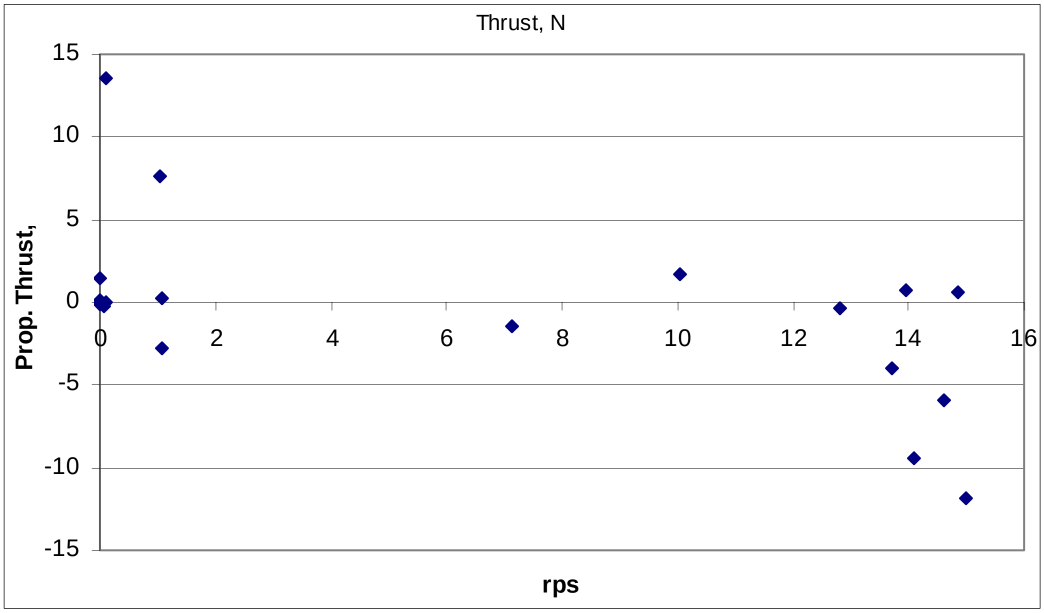

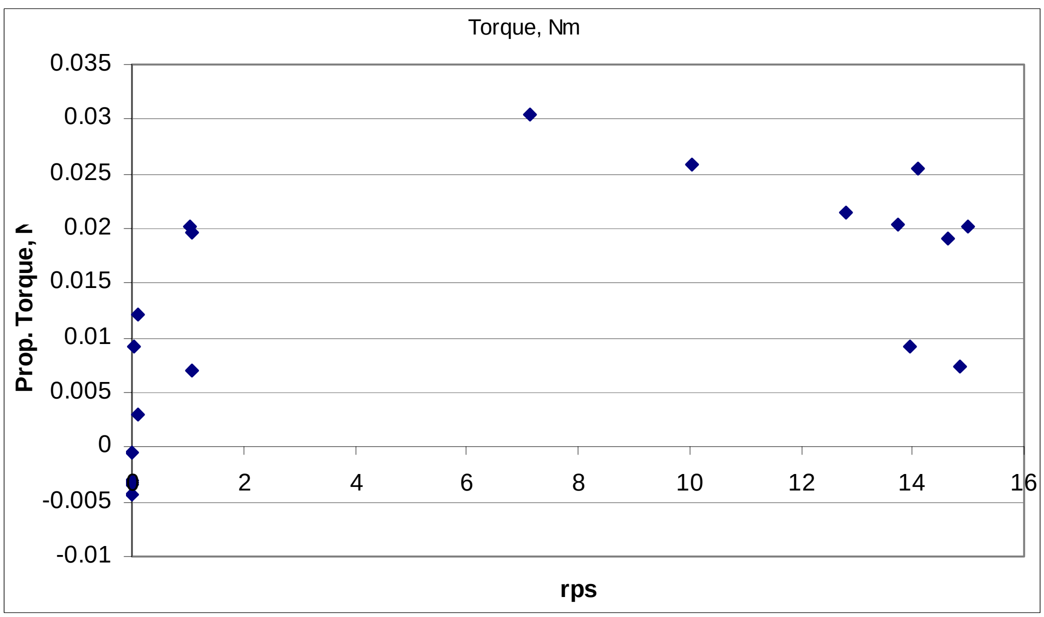

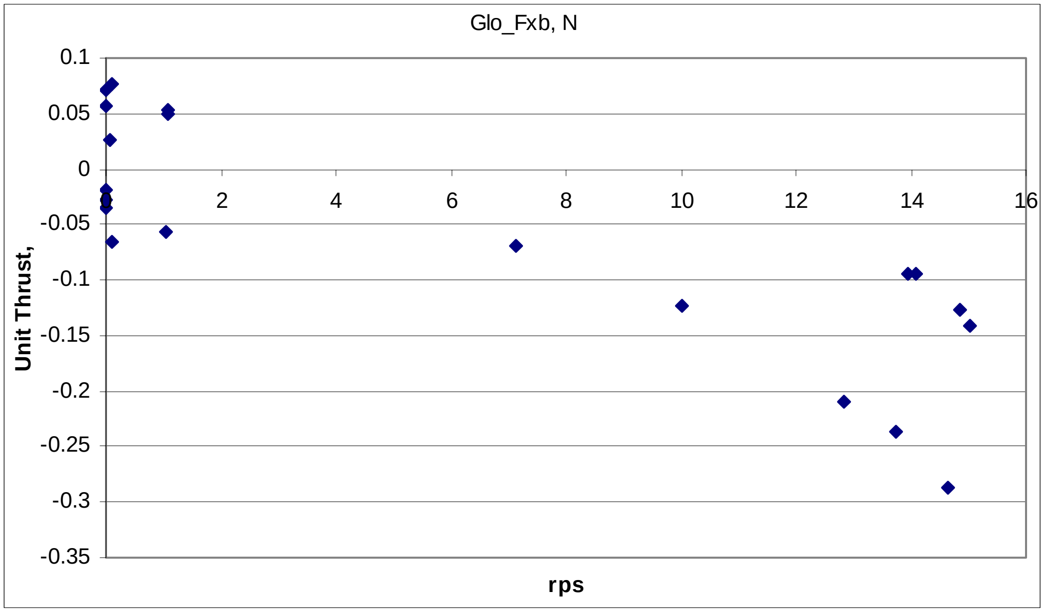
Glo_Fxb, N
0.1
0.05
0
-0.05
-0.1
-0.15
-0.2
-0.25
-0.3
-0.35
0
2
4
6
8
10
12
14
16
Unit Thrust,
rps

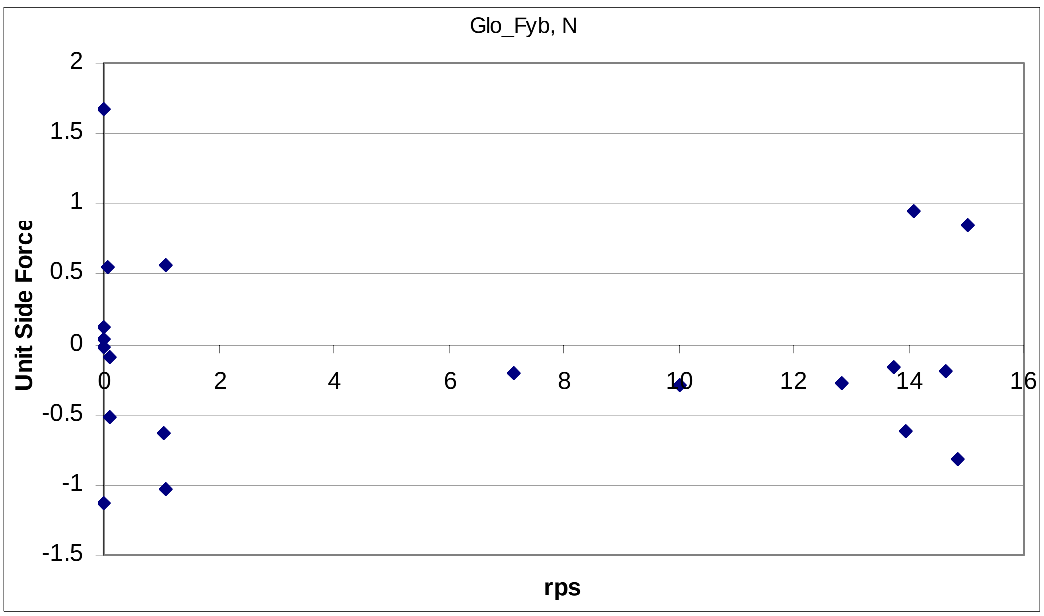
Glo_Fyb, N
2
1.5
1
0.5
0
-0.5
-1
-1.5
0
2
4
6
8
10
12
14
16
Unit Side Force
rps

E-3: Bollard Runs

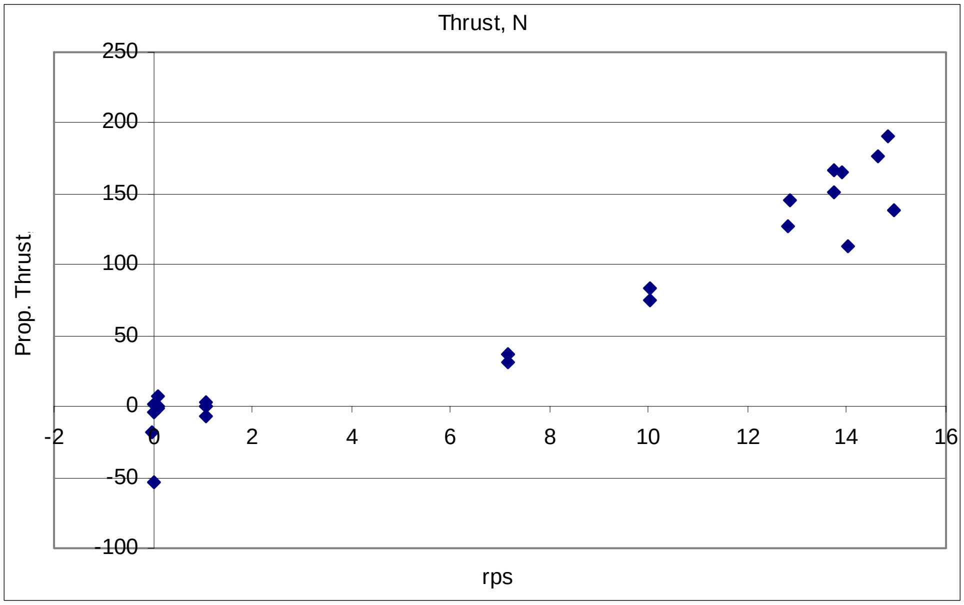

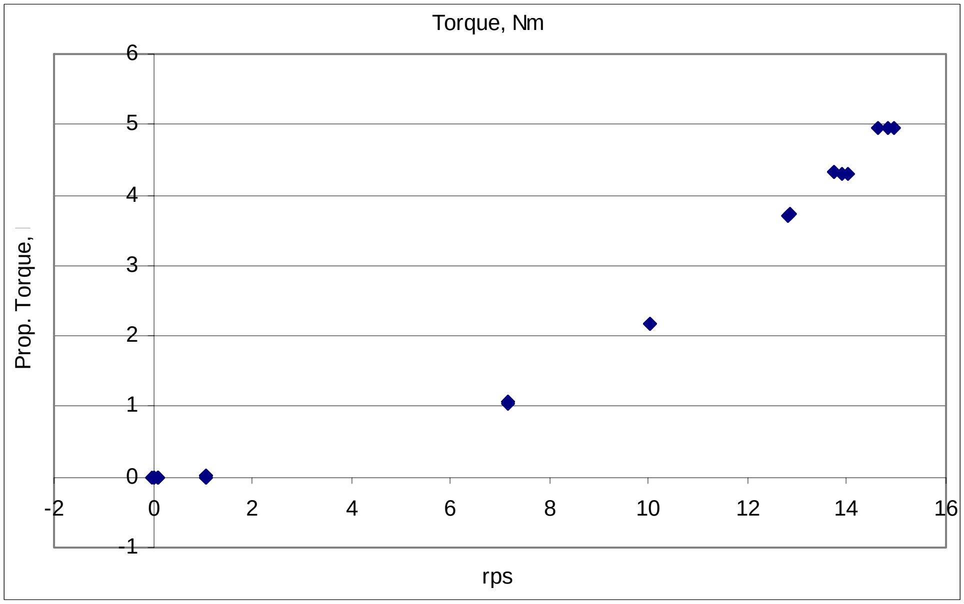

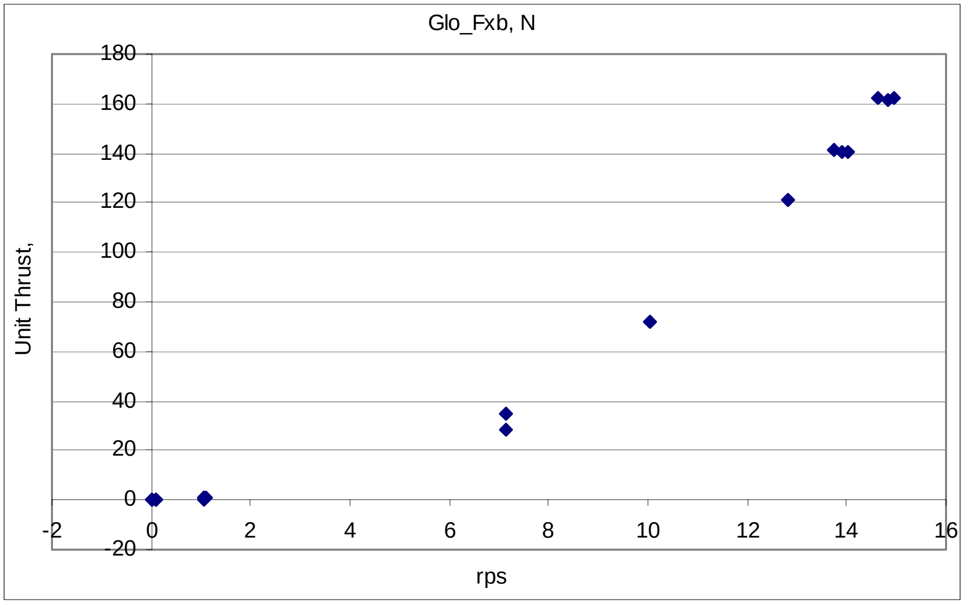
Glo_Fxb, N
Unit Thrust,
rps
180
160
140
120
100
80
60
40
20
0
-20
-2
0
2
4
6
8
10
12
14
16

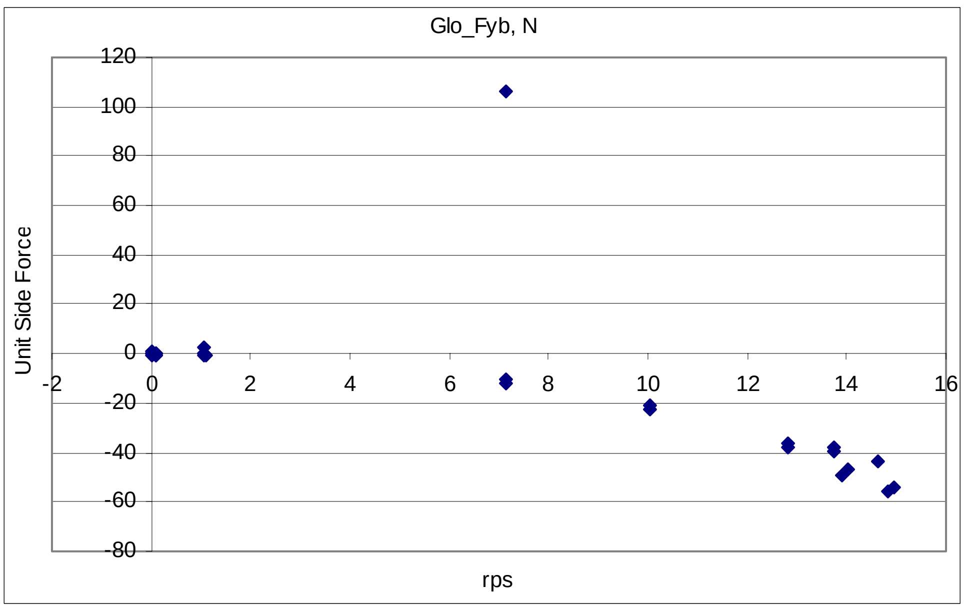
Glo_Fyb, N
Unit Side Force
rps
120
100
80
60
40
20
0
-20
-40
-60
-80
-2
0
2
4
6
8
10
12
14
16

E-4: Opens Tests

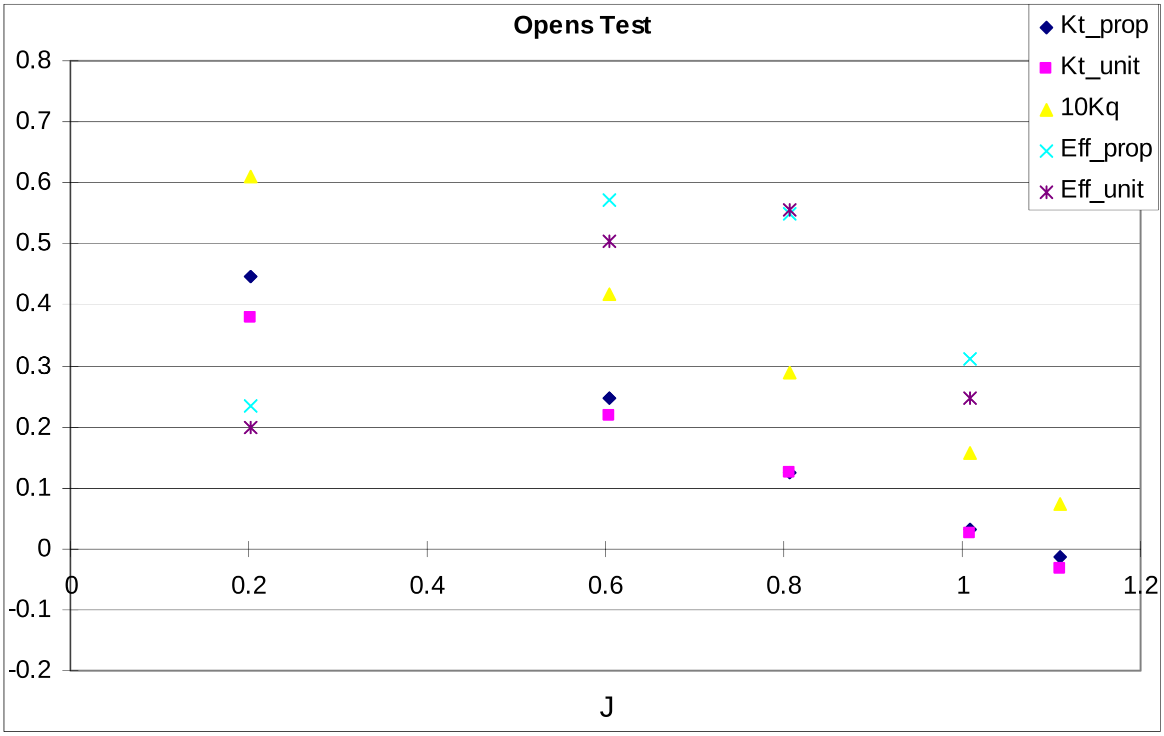

APPENDIX F: Results for Case 4

F-1: Opens Tests (Case 4a)

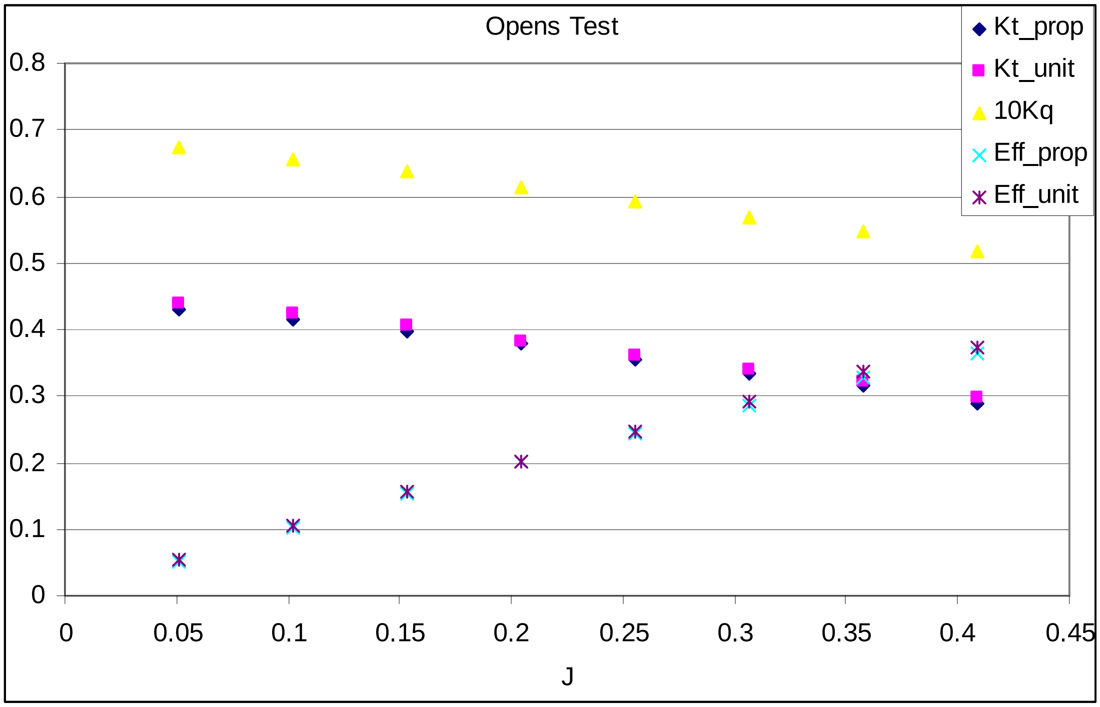

F-2: Opens Tests (Case 4b)

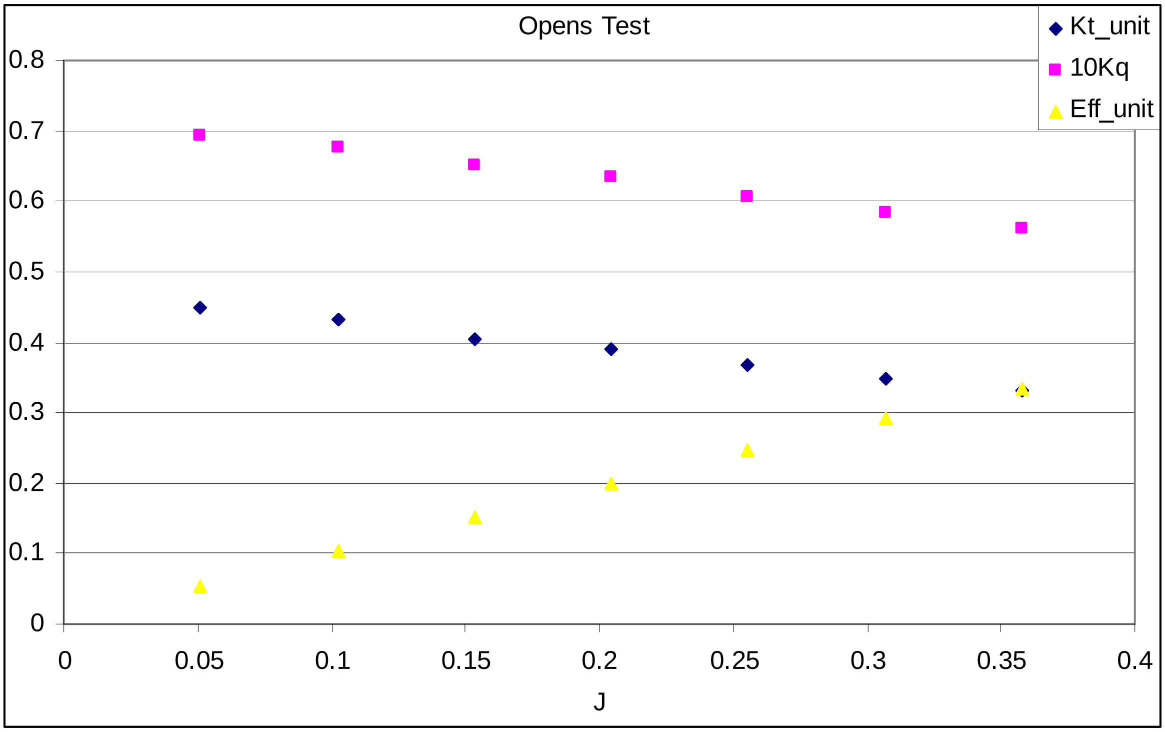

APPENDIX G: Results for Case 5

G-1: Air Friction Tests

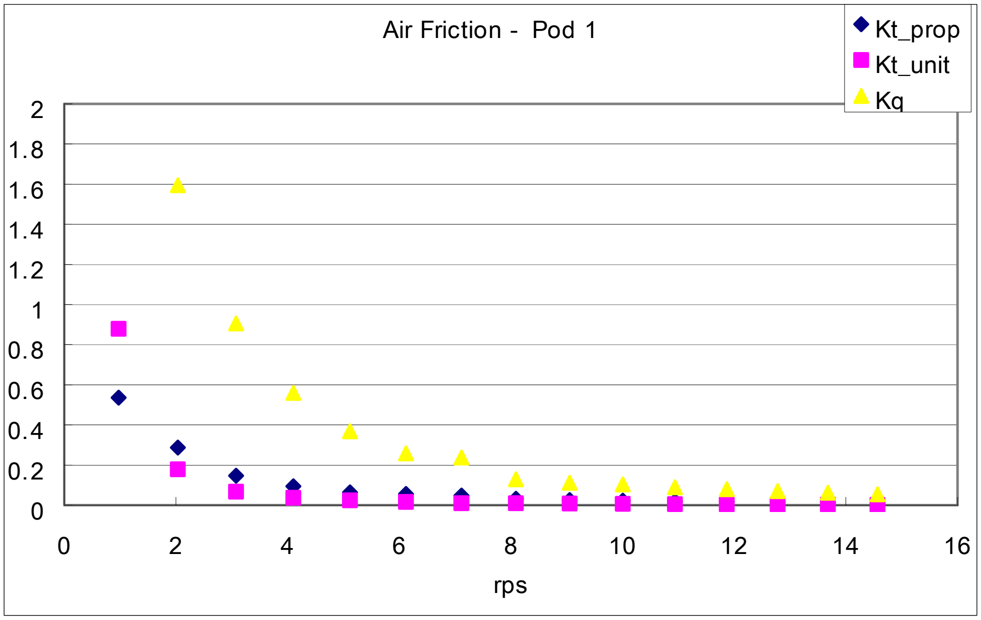

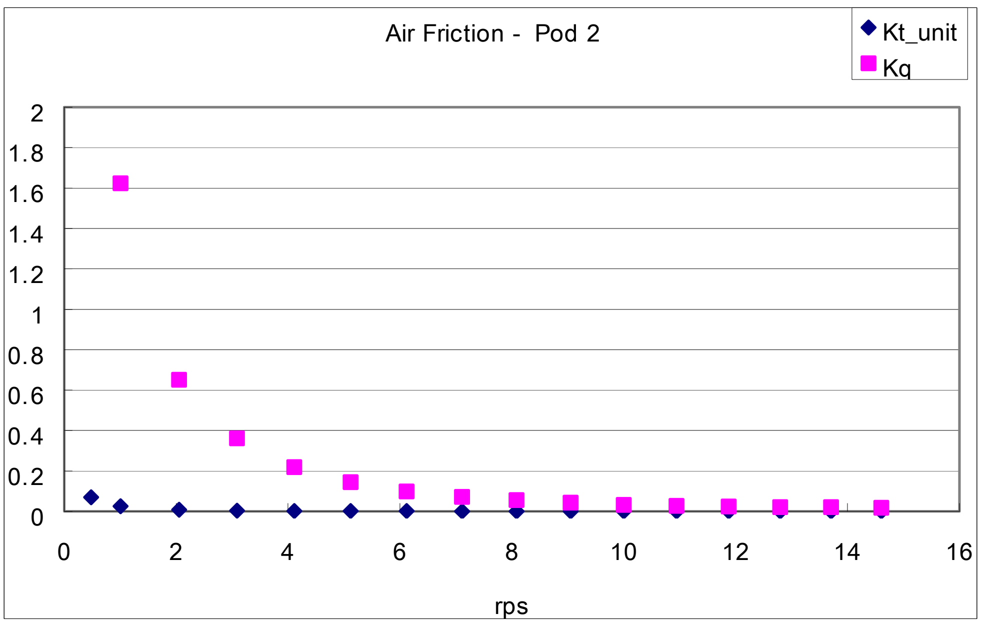

G-2: Bollard Runs

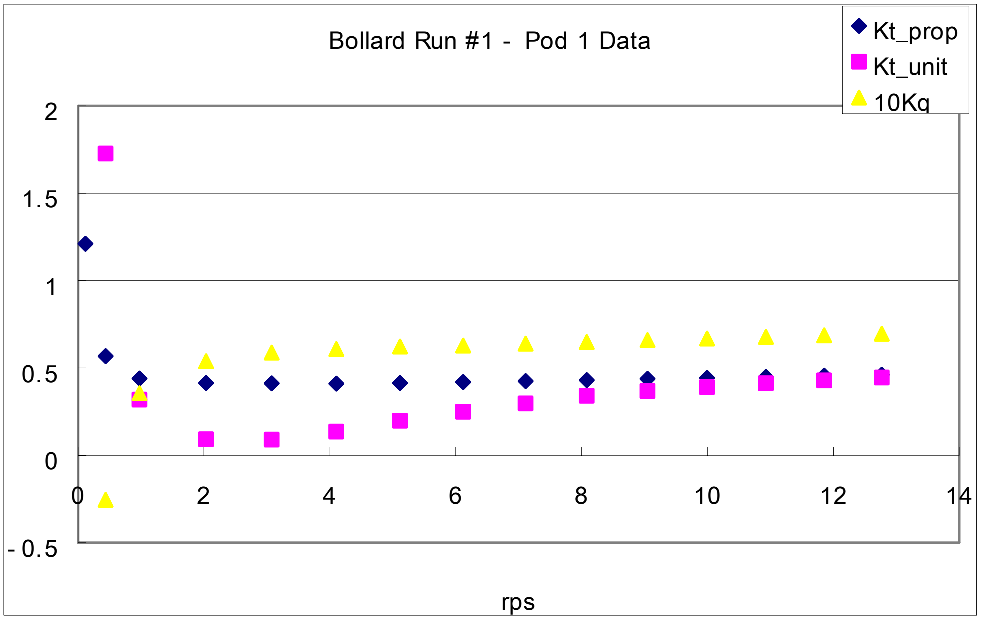

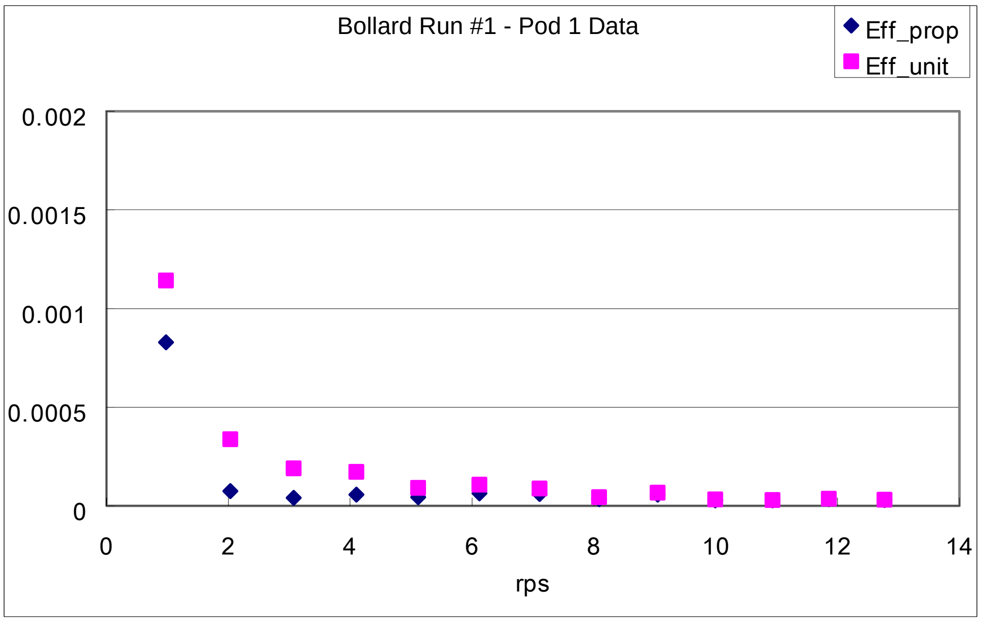

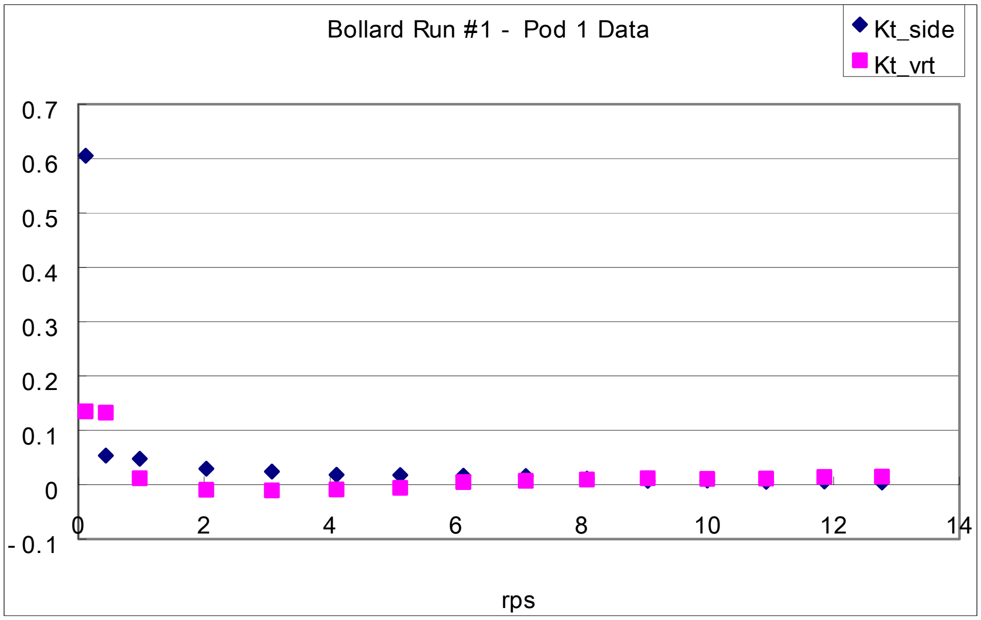
Bollard Run #1 - Pod 1 Data
Kt_side
Kt_vrt
0.7
0.6
0.5
0.4
0.3
0.2
0.1
0
- 0.1
0
2
4
6
8
10
12
14
rps

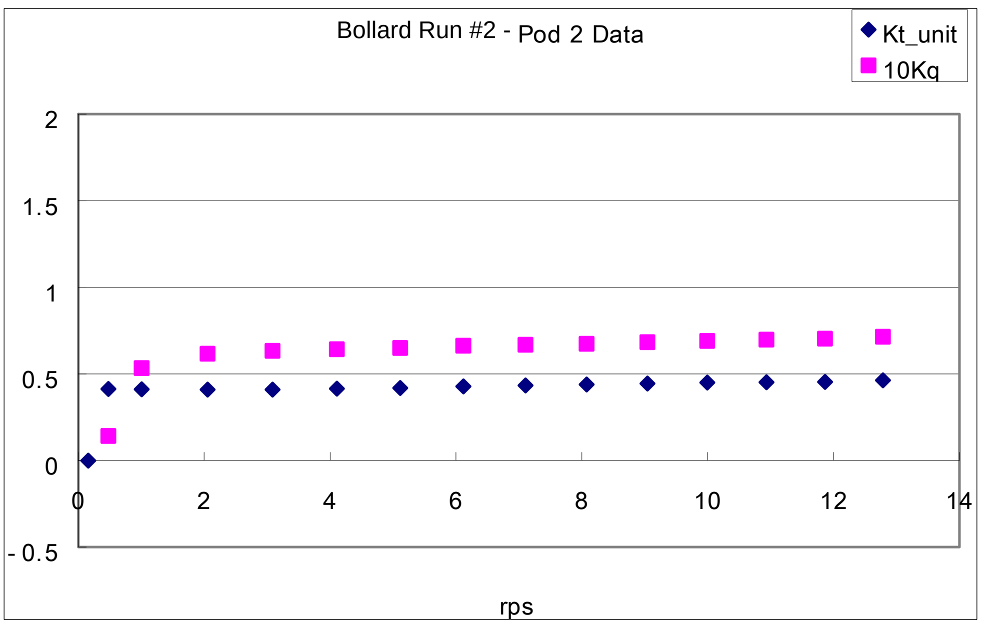
Bollard Run #2 - Pod 2 Data
Kt_unit
10Kq
2
1.5
1
0.5
0
- 0.5
0
2
4
6
8
10
12
14
rps

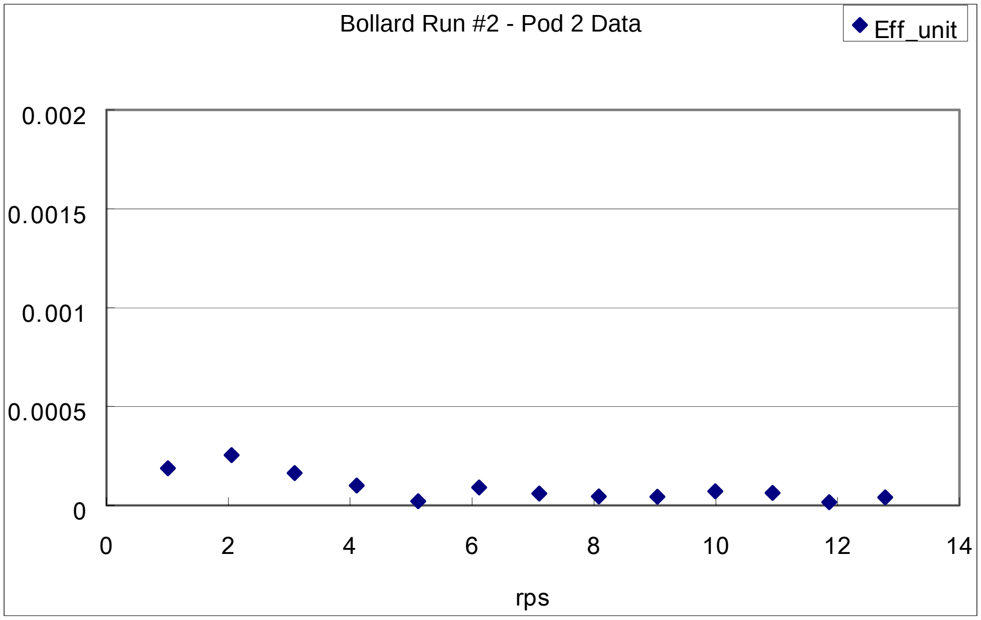
Bollard Run #2 - Pod 2 Data
Eff_unit
0.002
0.0015
0.001
0.0005
0
0
2
4
6
8
10
12
14
rps

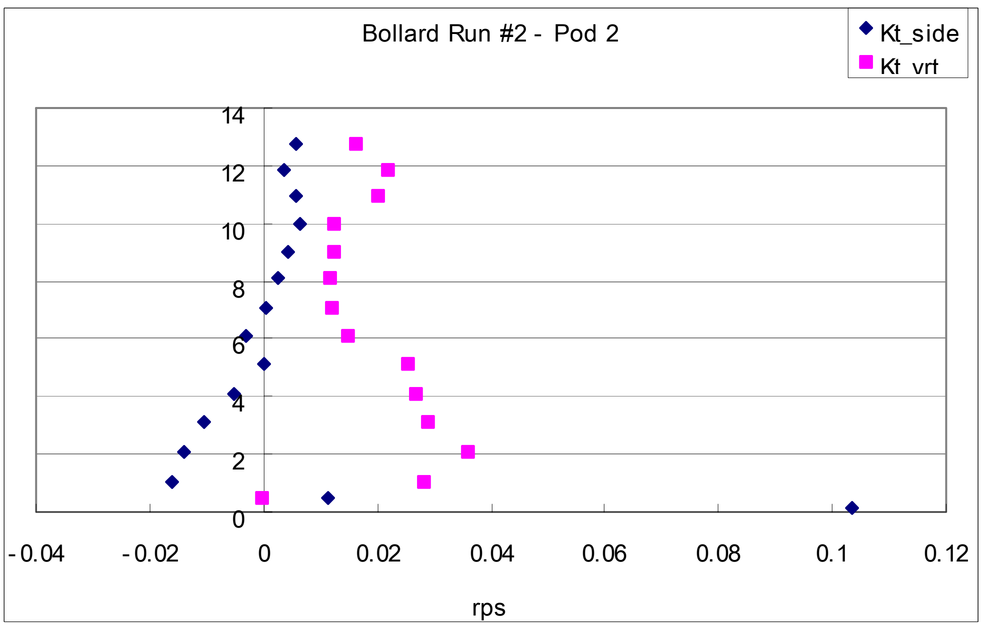
Bollard Run #2 - Pod 2
Kt_side
Kt_vrt
14
12
10
8
6
4
2
0
-0.04
-0.02
0
0.02
0.04
0.06
0.08
0.1
0.12
rps

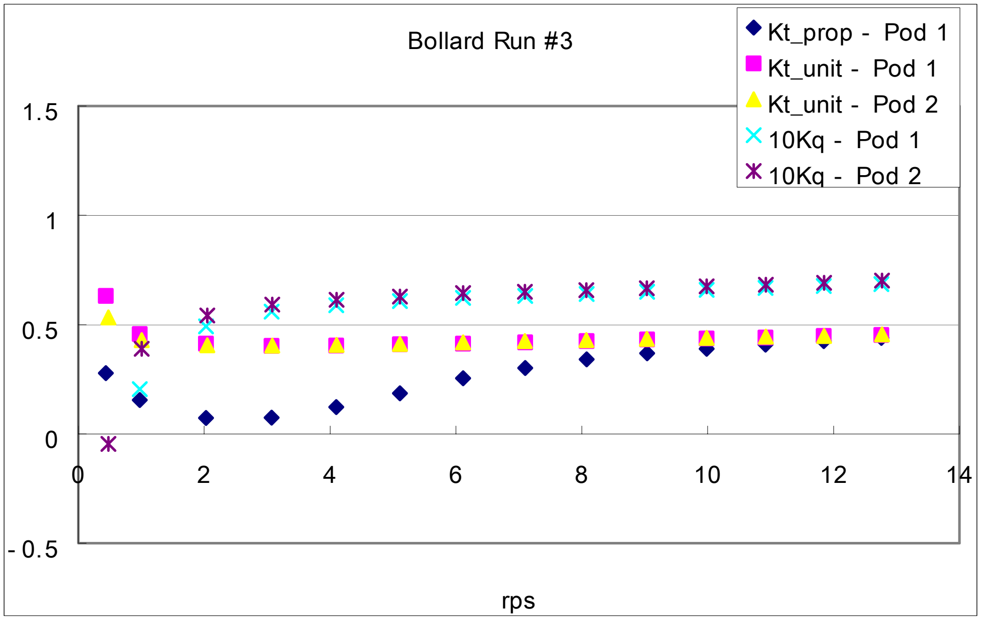
Bollard Run #3
Kt_prop - Pod 1
Kt_unit - Pod 1
Kt_unit - Pod 2
10Kq - Pod 1
10Kq - Pod 2
1.5
1
0.5
0
- 0.5
0
2
4
6
8
10
12
14
rps

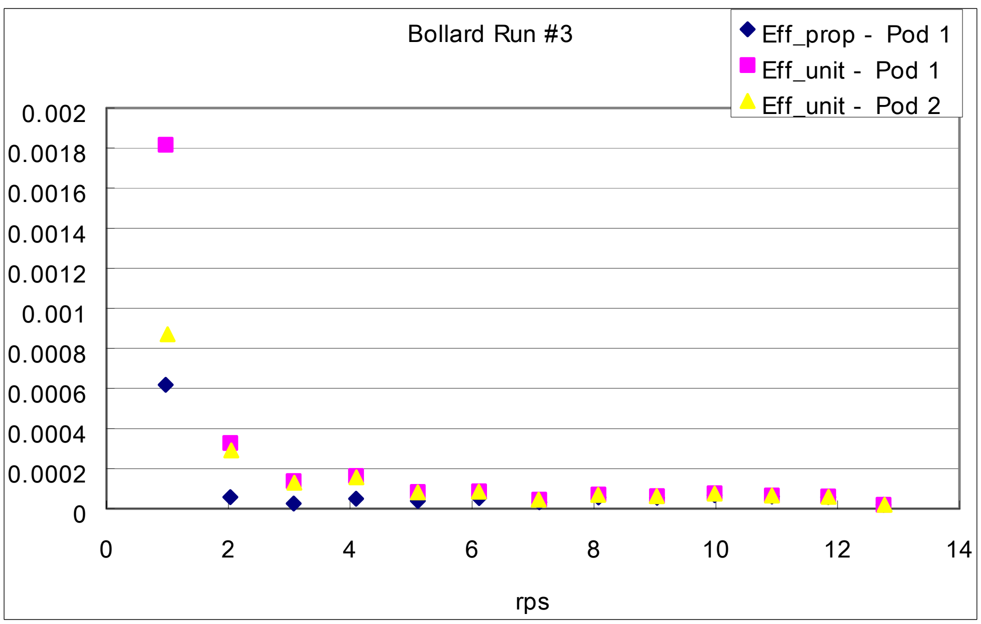
Bollard Run #3
Eff_prop - Pod 1
Eff_unit - Pod 1
Eff_unit - Pod 2
0.002
0.0018
0.0016
0.0014
0.0012
0.001
0.0008
0.0006
0.0004
0.0002
0
0
2
4
6
8
10
12
14
rps

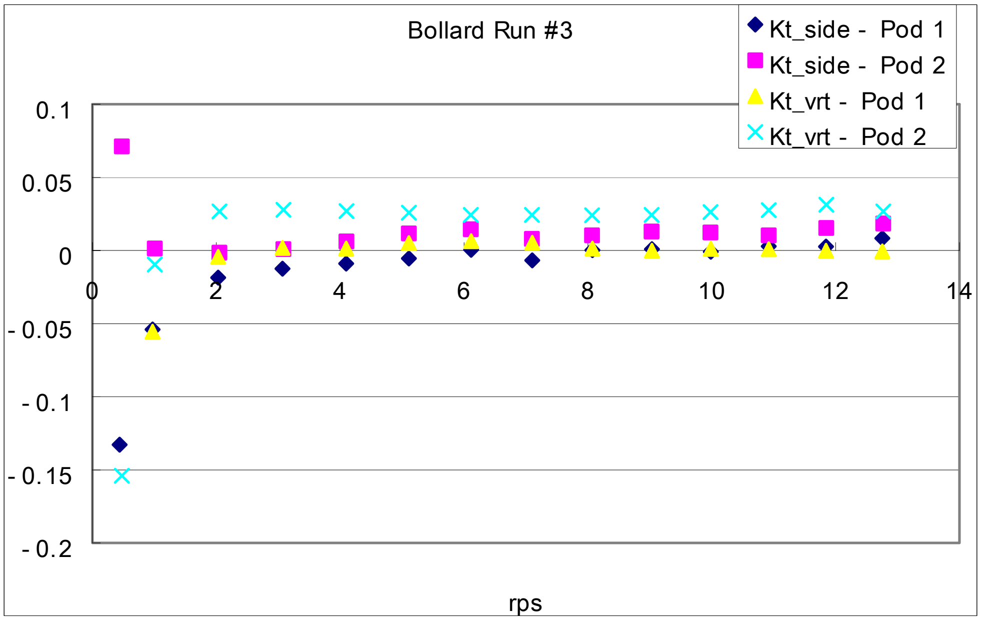
Bollard Run #3
Kt_side - Pod 1
Kt_side - Pod 2
Kt_vrt - Pod 1
Kt_vrt - Pod 2
0.1
0.05
0
- 0.05
- 0.1
- 0.15
- 0.2
0
2
4
6
8
10
12
14
rps

G-3: Opens Tests

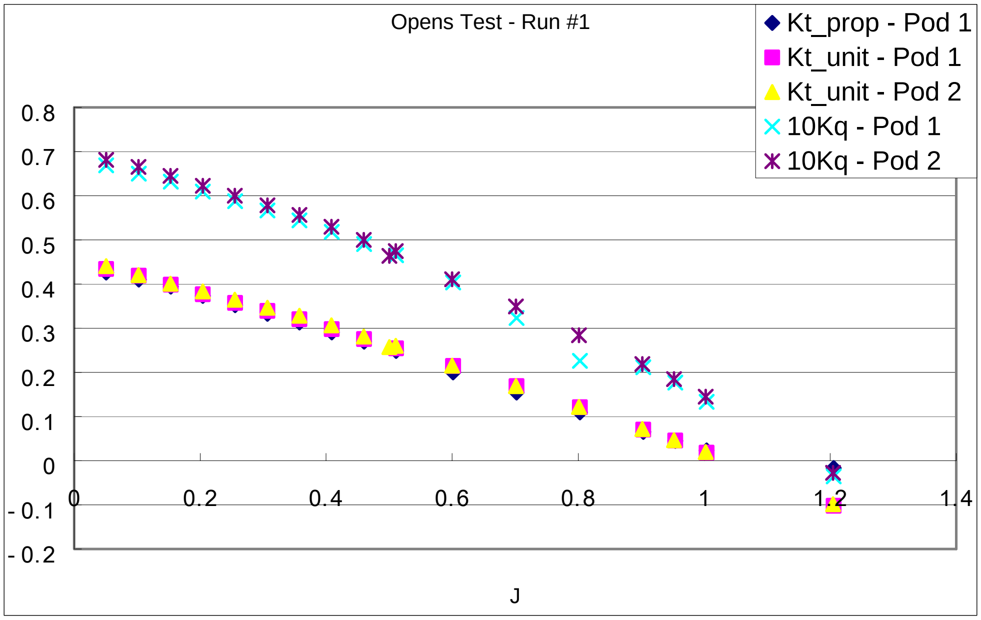

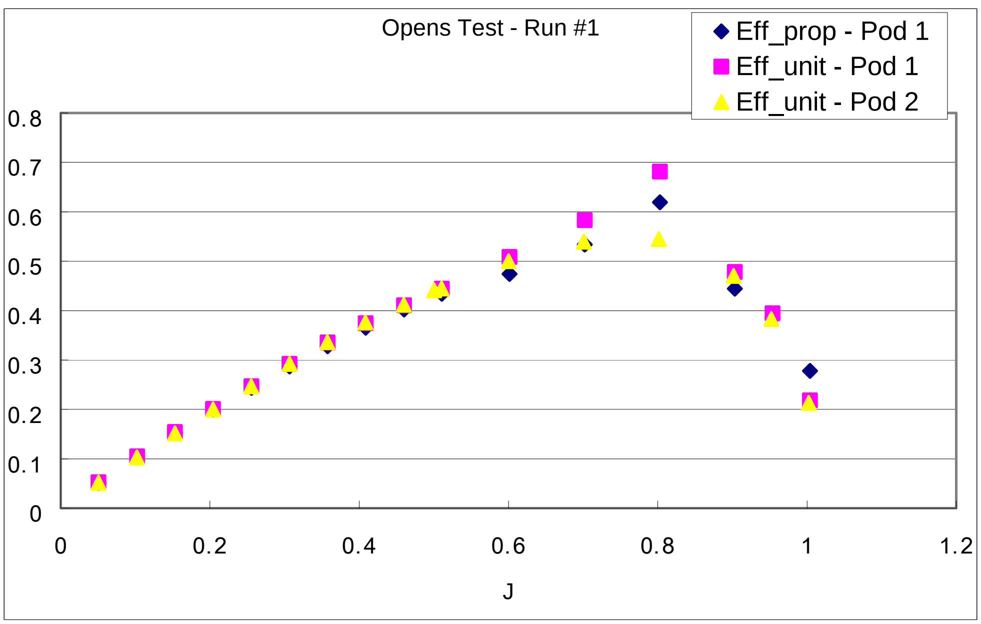

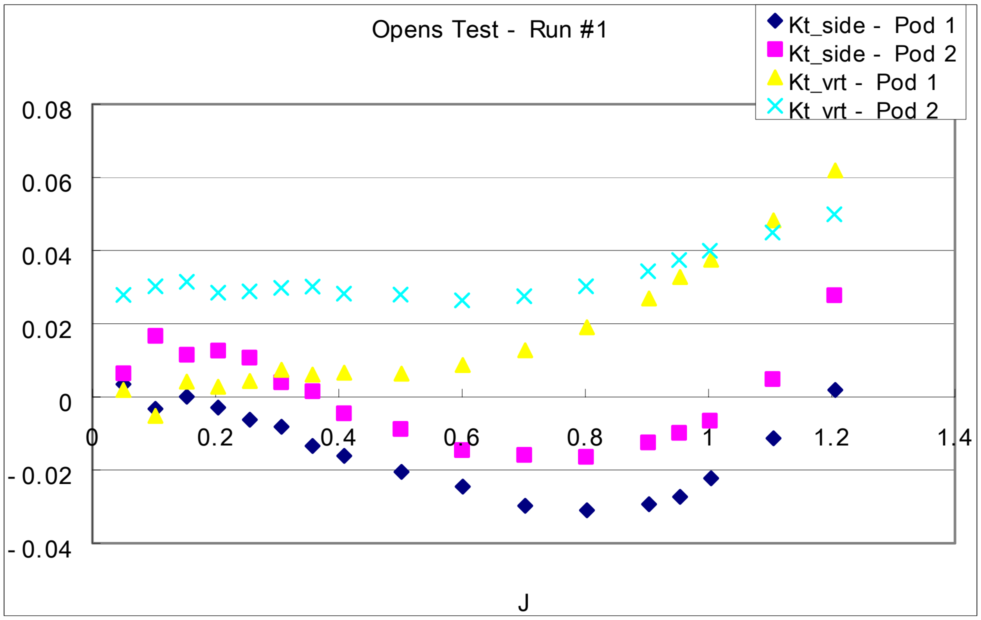
Opens Test - Run #1
Kt_side - Pod 1
Kt_side - Pod 2
Kt_vrt - Pod 1
Kt_vrt - Pod 2
0.08
0.06
0.04
0.02
0
- 0.02
- 0.04
0
0.2
0.4
0.6
0.8
1
1.2
1.4
J

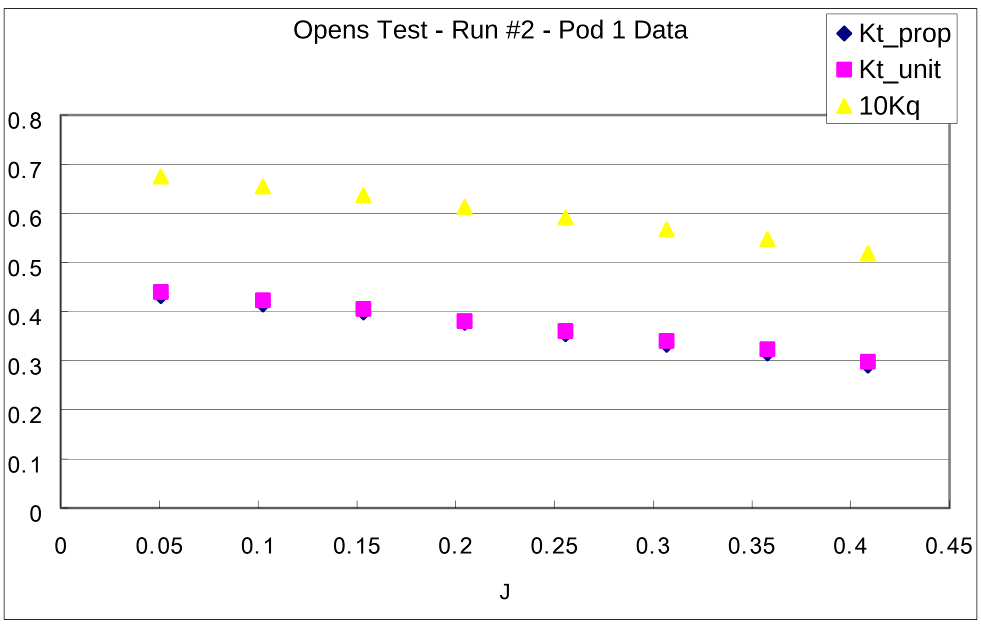
Opens Test - Run #2 - Pod 1 Data
Kt_prop
Kt_unit
10Kq
0.8
0.7
0.6
0.5
0.4
0.3
0.2
0.1
0
0
0.05
0.1
0.15
0.2
0.25
0.3
0.35
0.4
0.45
J

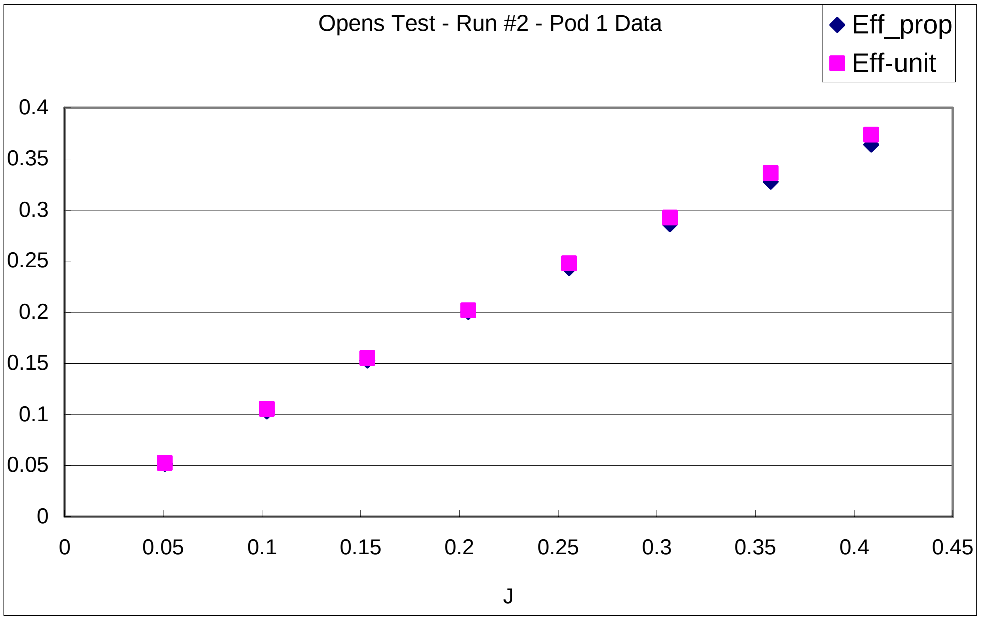
Opens Test - Run #2 - Pod 1 Data
Eff_prop
Eff-unit
0.4
0.35
0.3
0.25
0.2
0.15
0.1
0.05
0
0
0.05
0.1
0.15
0.2
0.25
0.3
0.35
0.4
0.45
J

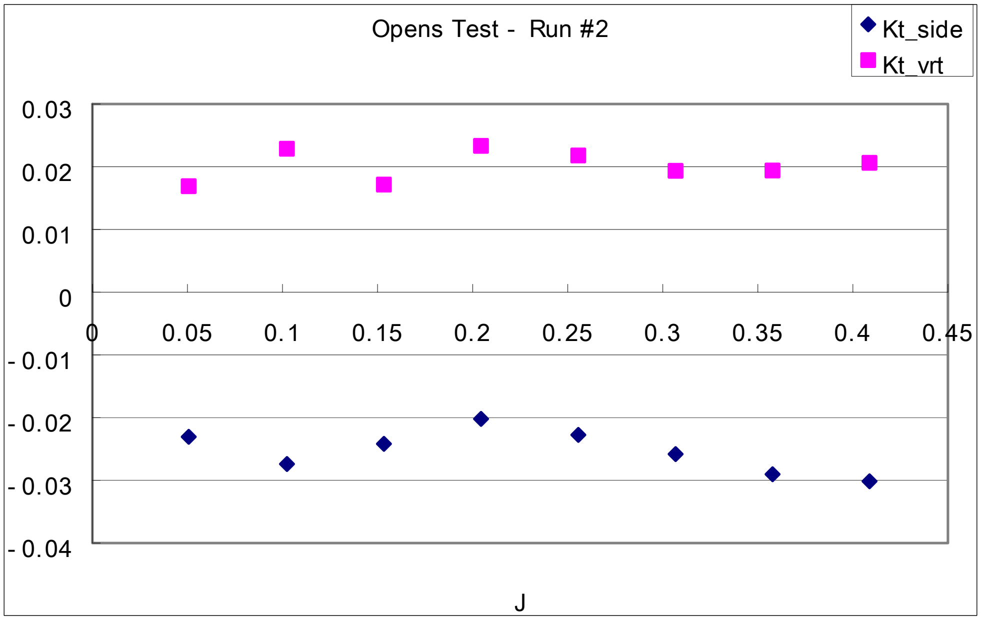
Opens Test - Run #2
Kt_side
Kt_vrt
0.03
0.02
0.01
0
- 0.01
- 0.02
- 0.03
- 0.04
0
0.05
0.1
0.15
0.2
0.25
0.3
0.35
0.4
0.45
J

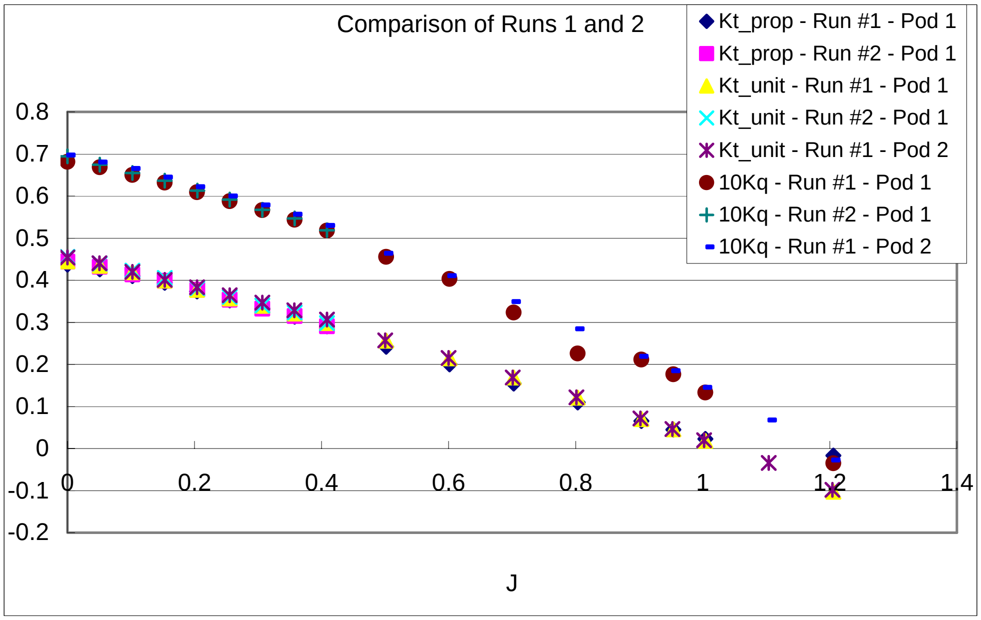
Comparison of Runs 1 and 2
Kt_prop - Run #1 - Pod 1
Kt_prop - Run #2 - Pod 1
Kt_unit - Run #1 - Pod 1
Kt_unit - Run #2 - Pod 1
Kt_unit - Run #1 - Pod 2
10Kq - Run #1 - Pod 1
10Kq - Run #2 - Pod 1
10Kq - Run #1 - Pod 2
0.8
0.7
0.6
0.5
0.4
0.3
0.2
0.1
0
-0.1
-0.2
0
0.2
0.4
0.6
0.8
1
1.2
1.4
J

G-4: Oblique Flow Tests

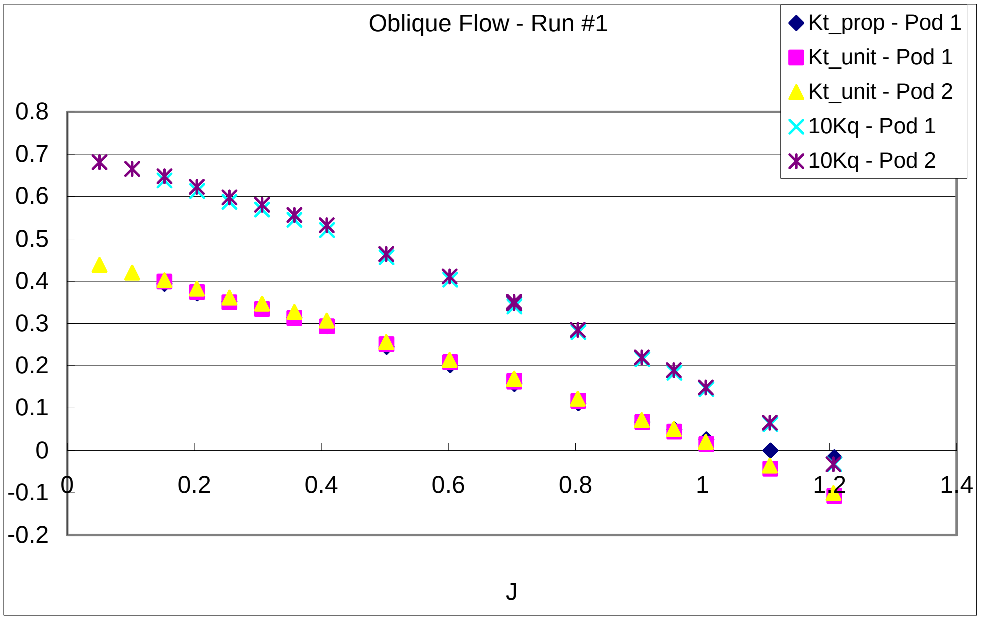

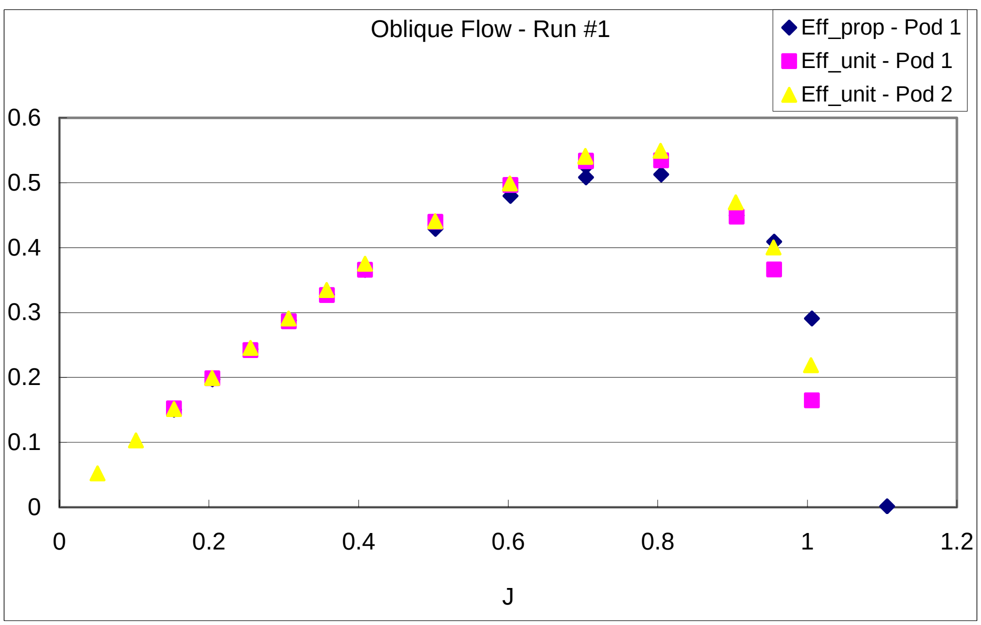

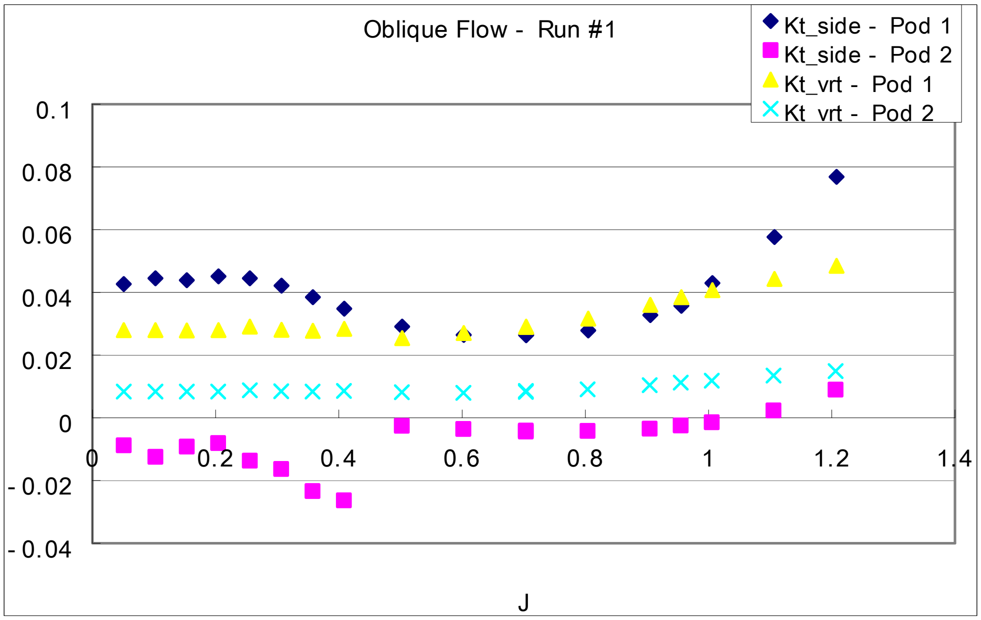
Oblique Flow - Run #1
Kt_side - Pod 1
Kt_side - Pod 2
Kt_vrt - Pod 1
Kt_vrt - Pod 2
0.1
0.08
0.06
0.04
0.02
0
- 0.02
- 0.04
0
0.2
0.4
0.6
0.8
1
1.2
1.4
J

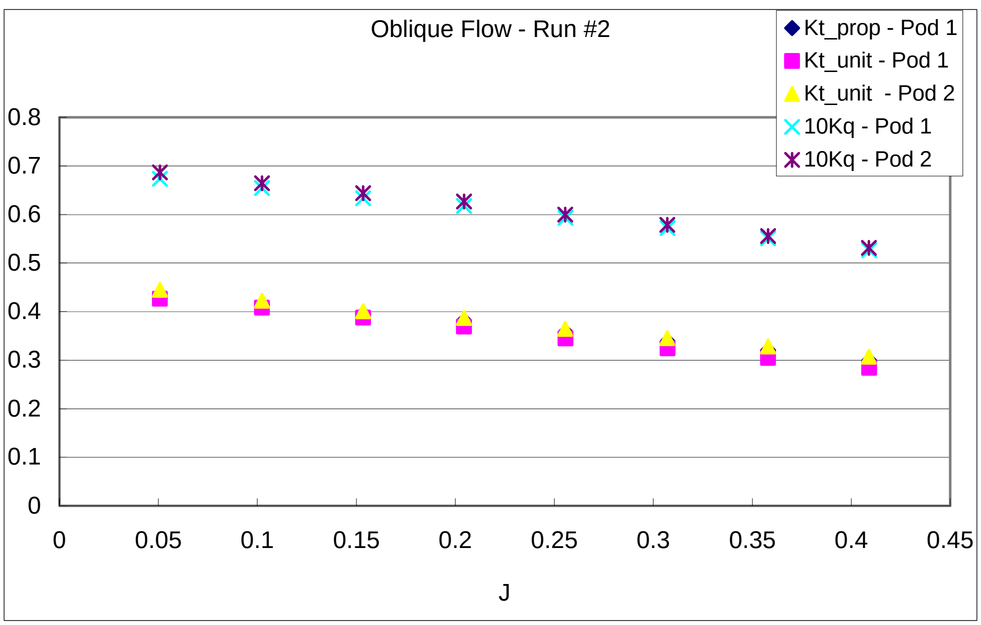
Oblique Flow - Run #2
Kt_prop - Pod 1
Kt_unit - Pod 1
Kt_unit - Pod 2
10Kq - Pod 1
10Kq - Pod 2
0.8
0.7
0.6
0.5
0.4
0.3
0.2
0.1
0
0
0.05
0.1
0.15
0.2
0.25
0.3
0.35
0.4
0.45
J

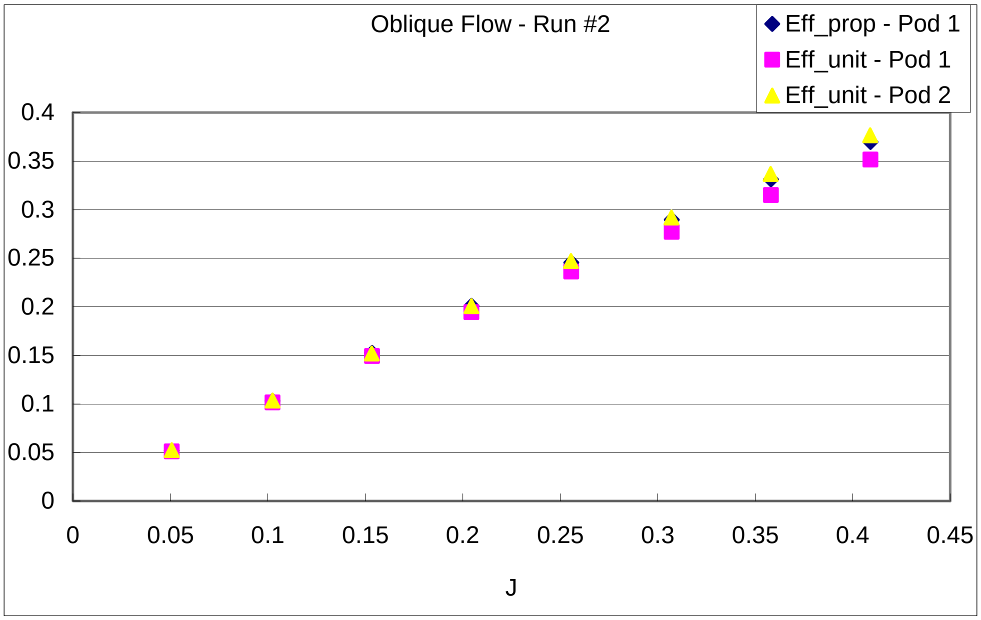
Oblique Flow - Run #2
Eff_prop - Pod 1
Eff_unit - Pod 1
Eff_unit - Pod 2
0.4
0.35
0.3
0.25
0.2
0.15
0.1
0.05
0
0
0.05
0.1
0.15
0.2
0.25
0.3
0.35
0.4
0.45
J

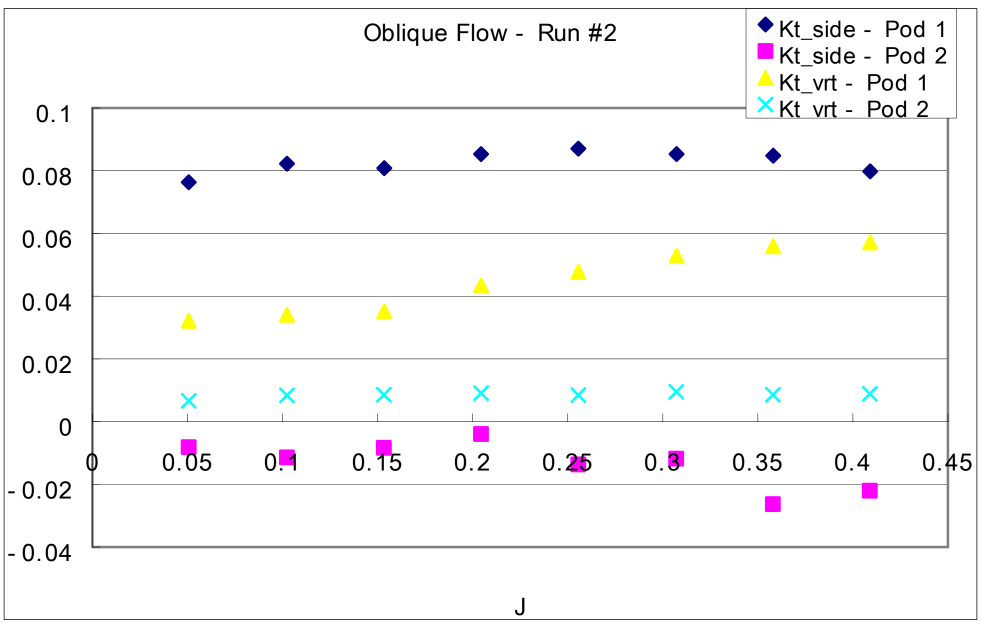
Oblique Flow - Run #2
Kt_side - Pod 1
Kt_side - Pod 2
Kt_vrt - Pod 1
Kt_vrt - Pod 2
0.1
0.08
0.06
0.04
0.02
0
- 0.02
- 0.04
0
0.05
0.1
0.15
0.2
0.25
0.3
0.35
0.4
0.45
J

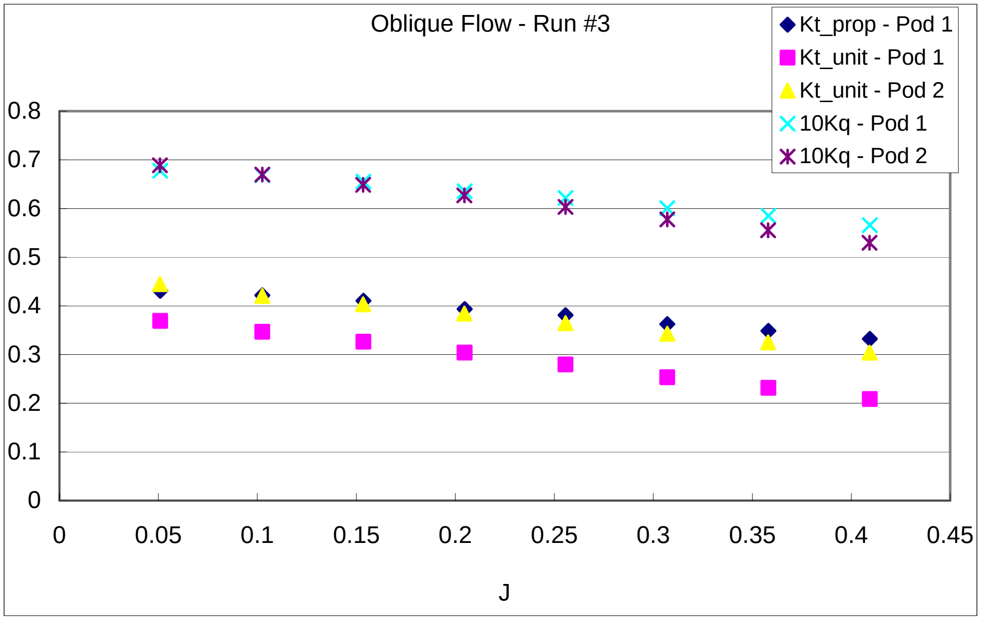
Oblique Flow - Run #3
Kt_prop - Pod 1
Kt_unit - Pod 1
Kt_unit - Pod 2
10Kq - Pod 1
10Kq - Pod 2
0.8
0.7
0.6
0.5
0.4
0.3
0.2
0.1
0
0
0.05
0.1
0.15
0.2
0.25
0.3
0.35
0.4
0.45
J

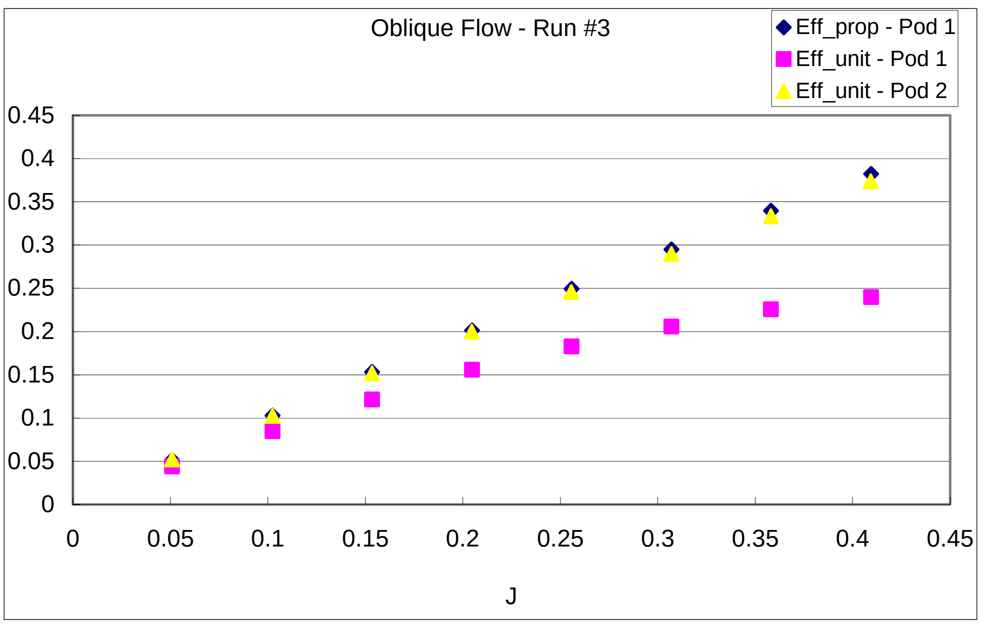
Oblique Flow - Run #3
Eff_prop - Pod 1
Eff_unit - Pod 1
Eff_unit - Pod 2
0.45
0.4
0.35
0.3
0.25
0.2
0.15
0.1
0.05
0
0
0.05
0.1
0.15
0.2
0.25
0.3
0.35
0.4
0.45
J

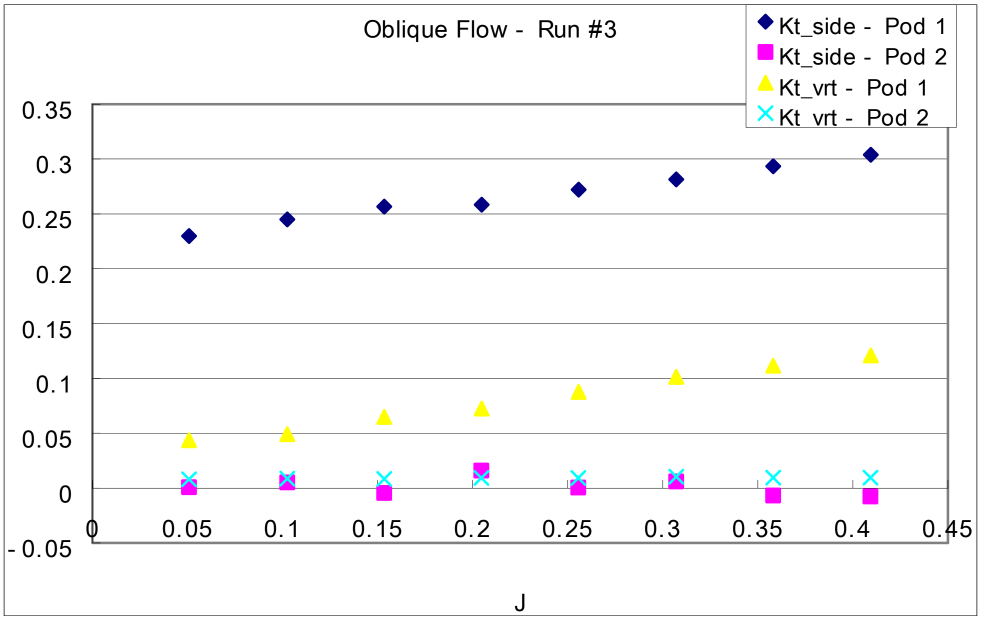
Oblique Flow - Run #3
Kt_side - Pod 1
Kt_side - Pod 2
Kt_vrt - Pod 1
Kt_vrt - Pod 2
0.35
0.3
0.25
0.2
0.15
0.1
0.05
0
- 0.05
0
0.05
0.1
0.15
0.2
0.25
0.3
0.35
0.4
0.45
J

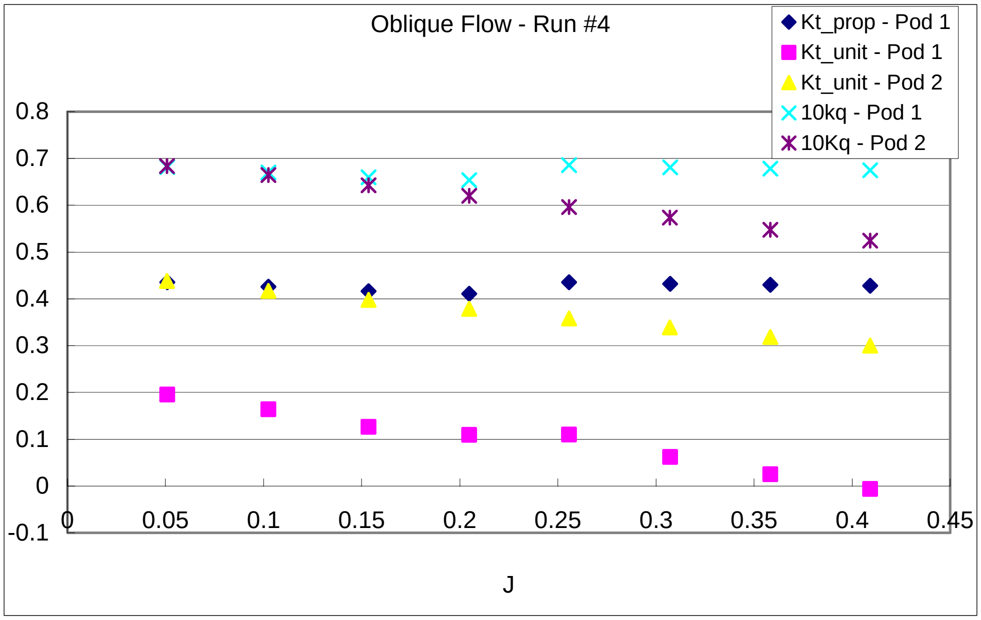
Oblique Flow - Run #4
Kt_prop - Pod 1
Kt_unit - Pod 1
Kt_unit - Pod 2
10kq - Pod 1
10Kq - Pod 2
0.8
0.7
0.6
0.5
0.4
0.3
0.2
0.1
0
-0.1
0
0.05
0.1
0.15
0.2
0.25
0.3
0.35
0.4
0.45
J

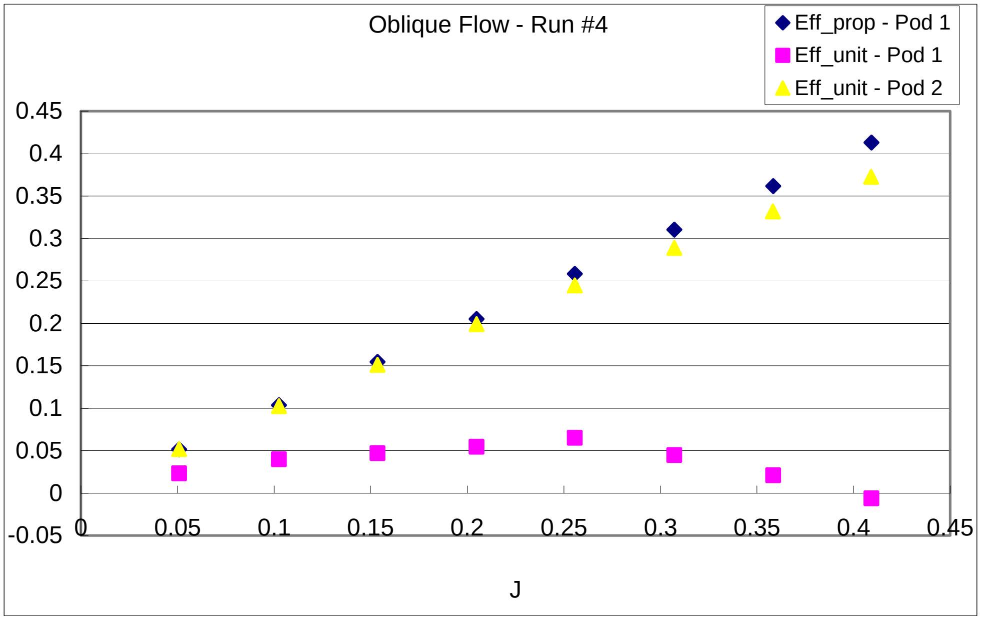
Oblique Flow - Run #4
Eff_prop - Pod 1
Eff_unit - Pod 1
Eff_unit - Pod 2
0.45
0.4
0.35
0.3
0.25
0.2
0.15
0.1
0.05
0
-0.05
0
0.05
0.1
0.15
0.2
0.25
0.3
0.35
0.4
0.45
J

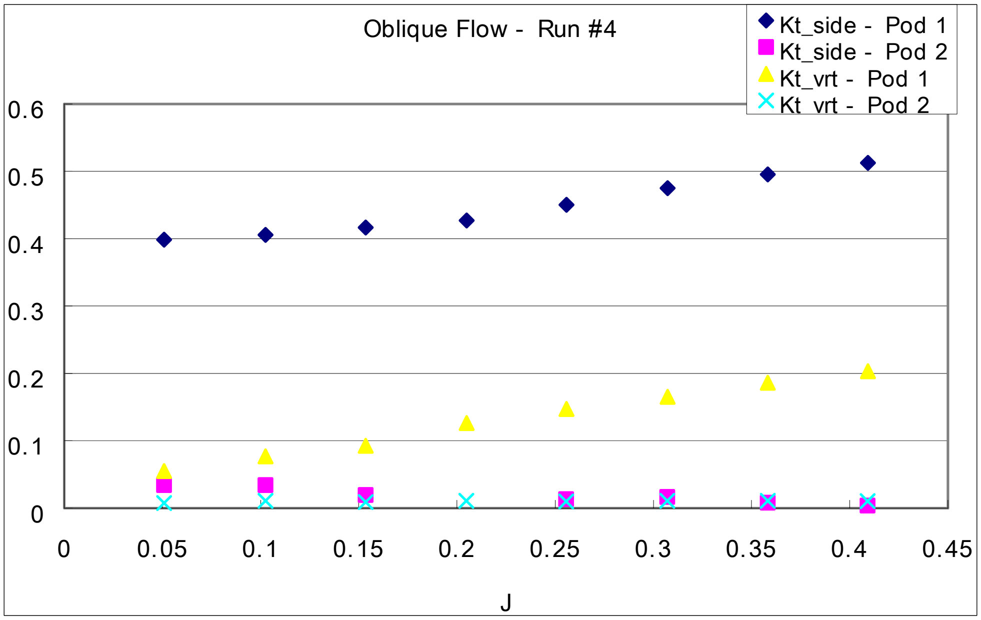
Oblique Flow - Run #4
Kt_side - Pod 1
Kt_side - Pod 2
Kt_vrt - Pod 1
Kt_vrt - Pod 2
0.6
0.5
0.4
0.3
0.2
0.1
0
0
0.05
0.1
0.15
0.2
0.25
0.3
0.35
0.4
0.45
J

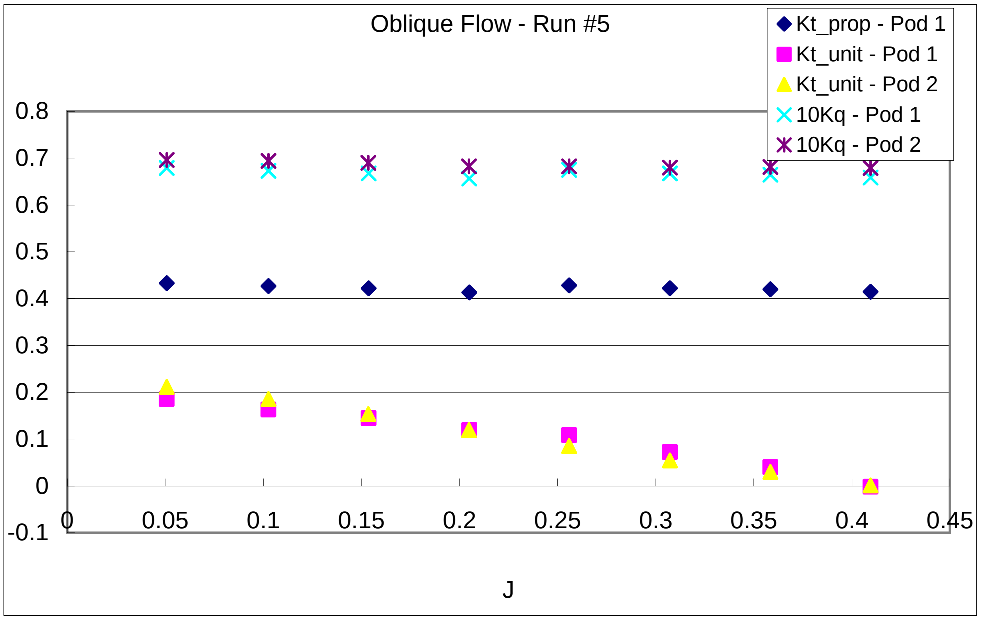
Oblique Flow - Run #5
Kt_prop - Pod 1
Kt_unit - Pod 1
Kt_unit - Pod 2
10Kq - Pod 1
10Kq - Pod 2
0.8
0.7
0.6
0.5
0.4
0.3
0.2
0.1
0
-0.1
0
0.05
0.1
0.15
0.2
0.25
0.3
0.35
0.4
0.45
J

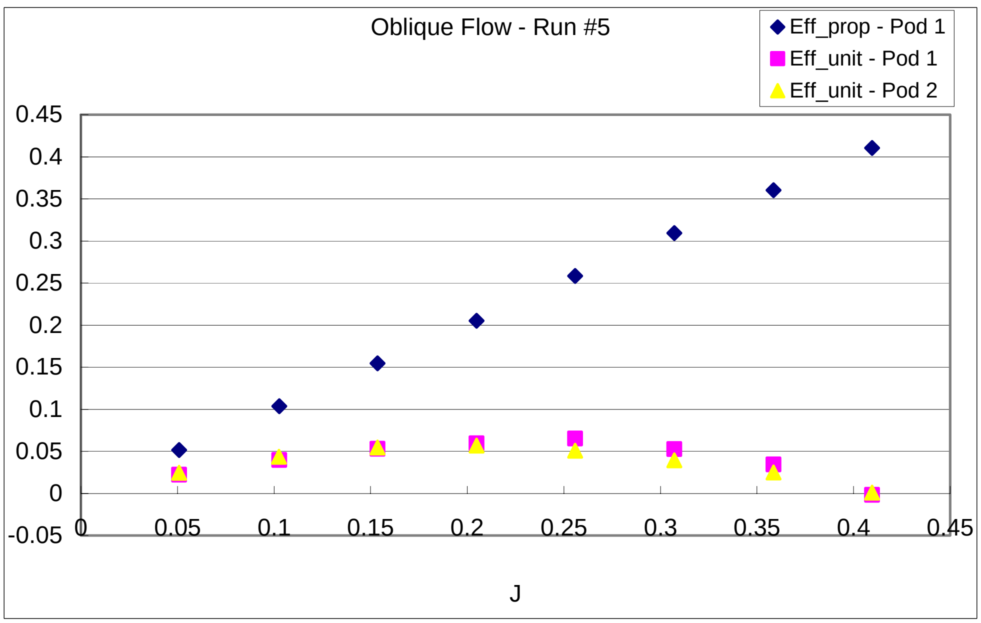
Oblique Flow - Run #5
Eff_prop - Pod 1
Eff_unit - Pod 1
Eff_unit - Pod 2
0.45
0.4
0.35
0.3
0.25
0.2
0.15
0.1
0.05
0
-0.05
0
0.05
0.1
0.15
0.2
0.25
0.3
0.35
0.4
0.45
J

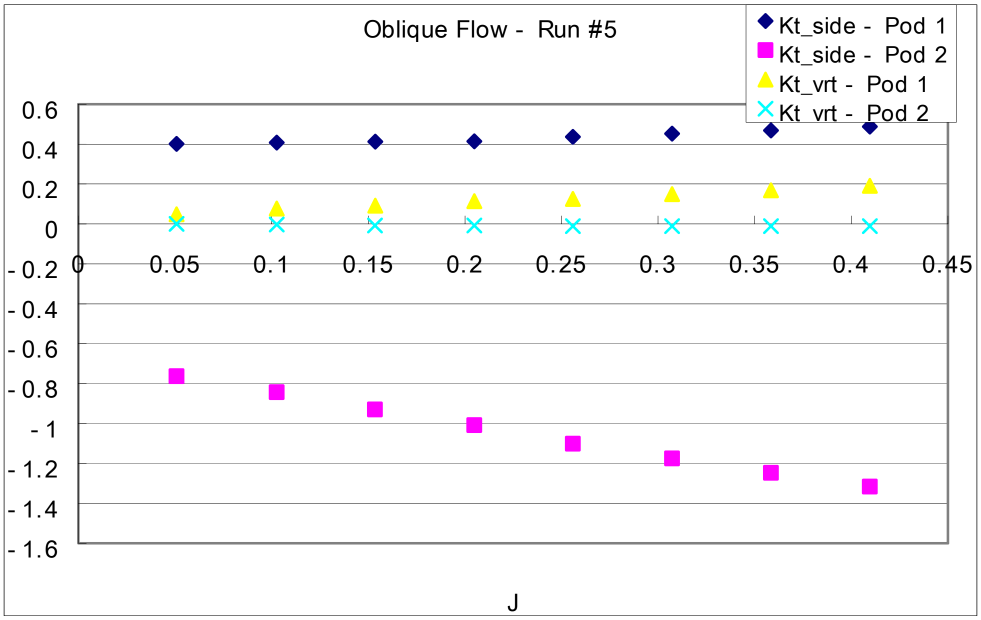
Oblique Flow - Run #5
Kt_side - Pod 1
Kt_side - Pod 2
Kt_vrt - Pod 1
Kt_vrt - Pod 2
0.6
0.4
0.2
0
- 0.2
- 0.4
- 0.6
- 0.8
- 1
- 1.2
- 1.4
- 1.6
0
0.05
0.1
0.15
0.2
0.25
0.3
0.35
0.4
0.45
J

APPENDIX H: Results for Case Seven

H-1: Bollard Runs

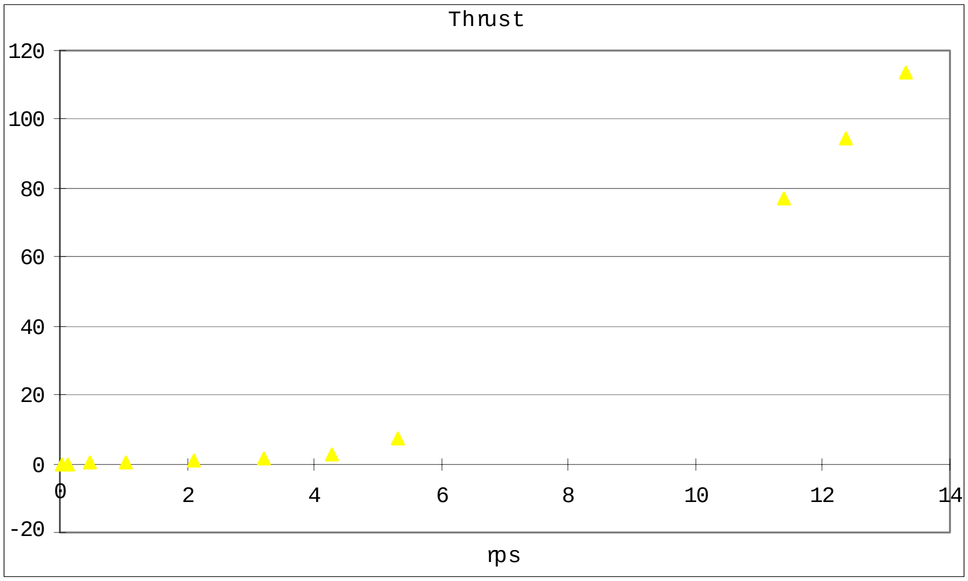

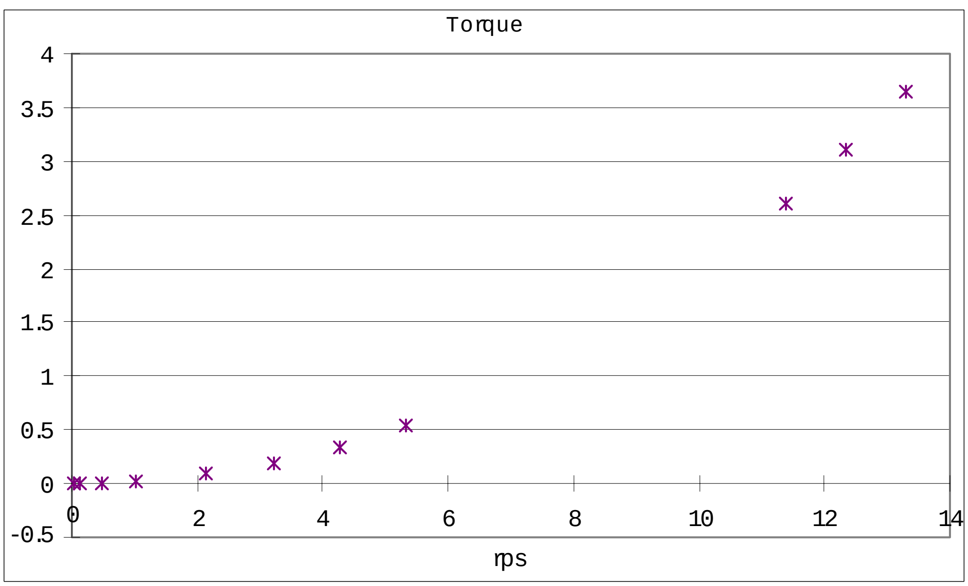

H-2: Opens Tests